DEVELOPING MICROWAVE-ASSISTED SYNTHESIS FOR HYBRID ZEOLITIC-IMIDAZOLATE FRAMEWORKS DERIVING FROM ZIF-8 FOR TUNABLE GAS SEPARATIONS

A Dissertation

by

FEBRIAN HILLMAN

Submitted to the Office of Graduate and Professional Studies of
Texas A&M University
in partial fulfillment of the requirements for the degree of

DOCTOR OF PHILOSOPHY

Chair of Committee,	Hae-Kwon Jeong
Co-Chair of Committee,	Benjamin A. Wilhite
Committee Members	Hongcai Zhou
	Mustafa Akbulut
Head of Department	M. Nazmul Karim

May 2019

Major Subject: Chemical Engineering

ABSTRACT

Around half of energy consumption in the US industrial sector comes from separation process, in which are commonly achieved through distillation. One drawback for distillation is its thermally driven process requiring phase change to achieve separation, making it thermodynamically inefficient. Alternatively, membrane-based separation is a partial pressure driven process allowing energy saving up to 90 % relative to distillation. Currently, the most common membrane material is made out of polymer. However, its performance is limited by polymeric upper bound, restricting them to be commercially attractive for light gases separation.

Zeolitic-imidazolate frameworks (ZIFs) recently gained popularity for membrane-based gas separations (i.e. ZIF-8 has shown impressive propylene/propane separation). ZIFs are porous crystalline structure consist of metal center bridged by imidazolate linker. Despite their potential for gas separation applications, ZIFs crystalline nature limits their available aperture sizes. One strategy to overcome this limitation is to tune their effective apertures through the hybrid approach. By mixing different metal centers and/or linkers (M/L), the molecular sieving properties of so called hybrid ZIFs can be finely tuned, which can potentially extend the separation applications of ZIF materials for many important gas mixtures.

In this dissertation, we investigated the tunable properties of various hybrid ZIFs deriving from ZIF-8, and adopt the microwave-assisted (MW) synthesis technique, which have been shown to be advantageous over the convective heating as it provides rapid and volumetric heating. The MW synthesis significantly reduces synthesis time, produces higher yield for various hybrid ZIFs, and enable one-step synthesis of hybrid ZIFs consisting both mixed metals and linkers. MW technique also facilitate the linker doping synthesis strategy, which was previously reported to be unsuccessful through conventional approach. The linker doping strategy expands the option of imidazolate linker that can be mixed to synthesize hybrid linker ZIFs while retaining their topology. Furthermore, the first example of high quality mixed metal ZIF membranes were fabricated using MW seeding technique and secondary growth. Finally, we developed novel rapid one-pot MW synthesis of mixed linker ZIF membranes—the fastest metal organic framework membranes fabrication. Through mixing M/L, all hybrid ZIFs investigated here showed tunable molecular sieving properties and/or "gate-opening" framework flexibilities.

ACKNOWLEDGEMENTS

I would like to thank my committee chair, Dr. Jeong, and my committee members, Dr. Wilhite, Dr. Zhou, and Dr. Akbulut, for their guidance and support throughout the course of this research.

Thanks also go to my friends and labmates and the department faculty and staff for making my time full of learning and discovering. Special thanks go to Keiko Kato for the support and discussion throughout my study.

Finally, thanks to my family for the their encouragement and support.

CONTRIBUTORS AND FUNDING SOURCES

This work was supervised by a dissertation committee consisting of Professor Jeong, Professor Wilhite, and Professor Akbulut of the Department of Chemical Engineering and Professor Zhou of the Department of Chemistry.

The thermal analysis data in chapter III and IV was provided by Zachary Perry and Angelo Kirchon from Professor Zhou's group. The X-ray absorption near edge structure (XANES) and the extended X-ray absorption fine structure (EXAFS) in chapter III were performed by Prof. Seung-Min Paek and Prof. Woo Taik Lim. Some of the FT-IR and nitrogen physisorption in chapter III were collected by Mohamad Rezi, and some 1H-NMR data in chapter VI were collected by Moonjoo Lee. All other work conducted for the dissertation was completed by the student independently.

Graduate study was supported in part by a fellowship from Texas A&M College of Engineering, National Science Foundation (CMMI-1600263, CBET-150530, CMMI-1561897), the Qatar National Research Fund (NPRP 7-042-2-021 and NPRP 8-001-2-001), R&D Convergence Program of MSIP (Ministry of Science, ICT and Future Planning), NST (National Research Council of Science & Technology) of the Republic of Korea (CRC-14-1-KRICT), the National Research Foundation of Korea (NRF: 2015R1D1A3A01016279), the 2015 Overseas Research Professor Program of the LG Yonam Foundation. The FE-SEM acquisition was supported by the National Science

Foundation under Grant DBI-0116835, the VP for Research Office, and the Texas A&M Engineering Experimental Station.

TABLE OF CONTENTS

Page

LIST OF FIGURES

Page

LIST OF TABLES

Page

CHAPTER I

INTRODUCTION

Separation and purification processes are of critical importance in chemical/petrochemical industries, which are commonly achieved through energy-intensive distillation.[1-3] The rising demand for separation, in particular for the light olefins (i.e. ethylene and propylene), expect an increase in energy consumption. In US alone, ~ 15 % of total energy consumption originates from chemical separations.[4-5] The high demand in energy not only increases the cost, but also elevates the production of greenhouse gases through combustion of fossil fuel, which can affect climate change[6-7] and impact future societies.[8] Replacement of thermally driven traditional distillation process with more energy efficient partial-pressure driven membrane-based separation is expected to reduce up to 90% energy consumption.[3]

At the moment, polymeric membranes are dominant for gas separations[9] primarily due to their processability into scalable hollow fibers with sub-micron thick selective skin layers and their low membrane cost. One major limitation of current polymeric membranes is the trade-off between permeabilities and selectivities,[10-11] two important membrane performance metric. This restrains the performance of polymeric membranes, which frequently fall outside the commercially attractive region as reported by Robeson illustrated in Figure I-1.[10-12] Moreover, the polymer membranes suffer from plasticization

and swelling issues at elevated pressure which may reduce the selectivity in gas separation performance.[13-15]

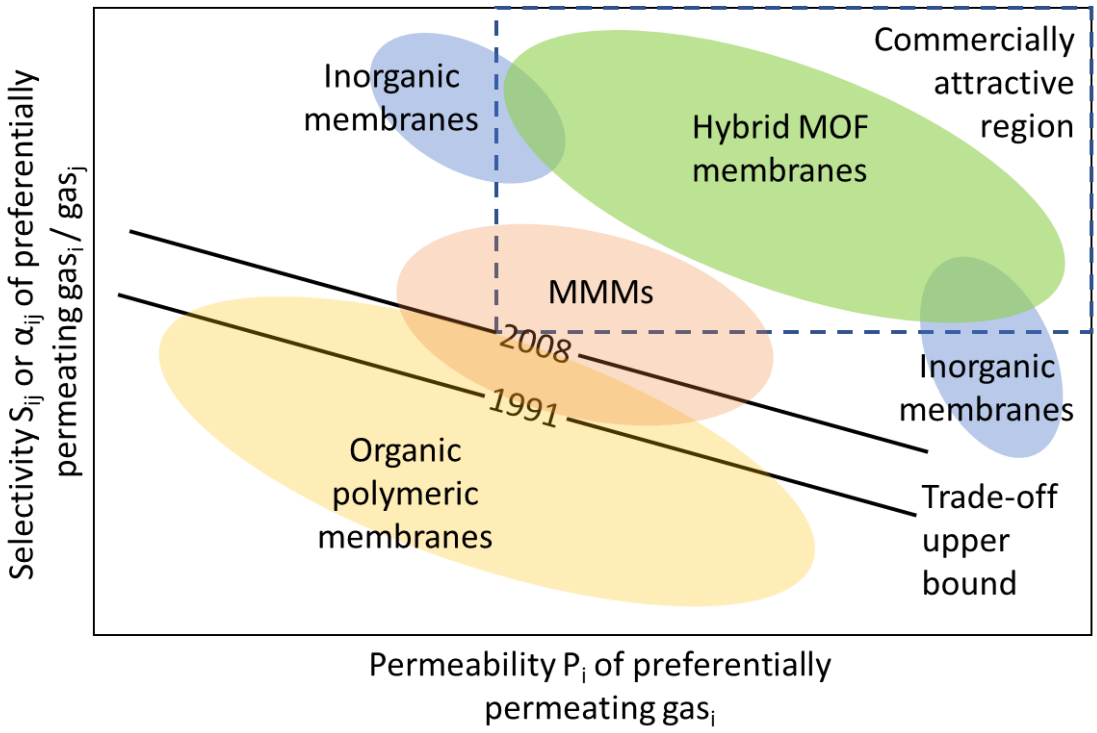

Figure I-1. Schematic representation of the relationship between permeability and selectivity, with Robeson upper bounds from 1991 and 2008.[10-11] The distance or position of the commercially interesting area relative to the upper bound can vary depending on the separation problem. Reproduced and modified with permission.[12] Copyright 2017, Wiley.

New membrane material consisting inorganic crystalline compound such as zeolites[16] and metal organic frameworks (MOFs)[17] have been studied to overcome the polymeric membrane upper bound limit. However, these crystalline materials suffer from fundamental limitation where their available pore apertures are discrete. As a result, often

times their apertures are too large, which makes them not selective while highly permeable, and vice versa as illustrated in Figure I-1**.** Two approaches can be taken to challenge the polymer upper bound limit and crystalline nature of inorganic membranes: 1) mixed matrix membranes (MMMs), which are composite membranes made by combining an inorganic or inorganic-organic hybrid material in the form of micro- or nanoparticles (as a filler) and a polymer matrix;[12, 18] and 2) hybrid metal organic framework membranes consisting of mixed metals and linkers.[19-20]

Mixed matrix membranes (MMMs) have gained interests because it combine synergistically the easy processability of polymers and the superior gas-separation performance of porous filler materials.[12] Koros[18] mentioned that MMMs can be considered as evolutionary advancement bridging the gap between polymer and inorganic membranes. Many have also shown the potential of MMMs for gas separation as reviewed in several excellent articles.[12, 21-27] However, as composite-like material, MMMs face multiple fabrication challenges such as interfacial defects, agglomeration, and sedimentation as discussed by Chen et al.[28] Additionally, to further push the boundary limit of permeability and selectivity, development of hybrid MOF membranes are necessary (Figure I-1).

Metal organic frameworks or MOFs are inorganic-organic crystalline structure consisting of metal nodes bridged by organic linkers. One of the unique features of MOFs is the flexibility in their design and synthesis, which allows the preparation of MOFs containing more than one metal (mixed-metal) or more than one linker (mixed-linker),

termed hybrid MOFs.[20] Introduction of new metal or linker within the framework of MOFs can change its structure topology, pore window and cage, and surface properties (e.g. polarity, hydrophobicity, etc.) as illustrated in Figure I-2. In case of gas separation, tuning of pore apertures for molecular sieving is critical to target the sieving size of various component mixture, thus, expanding the available apertures option for crystalline MOFs.

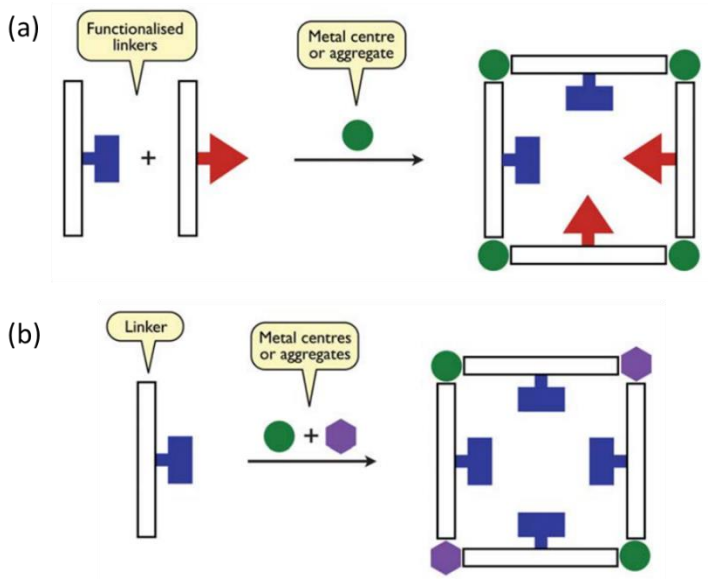

Figure I-2. Schematic representation of the formation of (a) a mixed linker MOFs with different functionalized organic linker and (b) a mixed metal MOFs through use of different metal centers in the synthesis. Reproduced with permission.[19] Copyright 2011, The Royal Society of Chemistry.

Among MOFs, zeolitic imidazolate frameworks (ZIFs) have recently gained interests for gas separation due to their ultra- microporosities (pores less than 5 Å) and relatively high chemical/thermal stabilities.[29] ZIF-8, in particular, is a prototypical ZIFs that has attracted most of research interests mainly due to its impressive propylene (~ 4.0

Å) and propane (~ 4.2 Å) separation performance, which is one of the most difficult chemical separations because of their very similar properties (i.e. relative volatilities and molecular sizes).[30-36] Despite its impressive separation performance,[30, 33-37] ZIF-8, like other crystalline material, has very narrow region (i.e. ~ 4.0 - 4.2 Å) for achieving efficient separation performance.[31] In other words, ZIF-8 is not as selective for smaller guest molecules than 4.0 Å, and hardly permeable for larger guests than 4.2 Å.

Being a subclass of metal organic frameworks (MOFs),[38-40] ZIFs inhere the flexibility in their design and synthesis, which allows the crystal formation containing more than one metal (mixed metal) or more than one linker (mixed linker).[20] This mixing strategy allows continuous tuning of its framework properties, which can be a solution to overcome the fundamental crystalline limitation.[20, 41-44] Because the potential of ZIF-8 for gas separation is promising, it is not surprising to pursue the hybrid approach deriving from ZIF-8 as the parent structure. However, to date, there are only a handful of reports investigating this matter. To name a few, Nair and co-worker[43] have shown that gas transport diffusivity, hydrophobicity, and through mixed linker derived from ZIF-8 can be tuned continuously by varying linker ratio in the framework. Jeong and co-worker[36] reported that metal substitution of ZIF-8 can also alter the bond "stiffness" of the framework tailoring the effective pore apertures.

In general, the common synthesis of hybrid ZIFs has been through slow diffusion techniques,[45-47] conventional hydrothermal,[48-50] and solvothermal methods,[43, 51-57] requiring several hours up to days of synthesis time. Furthermore, in some cases, two-step

post-synthesis modification is required to obtain certain hybrid ZIFs, adding more complications to the synthesis process. In addition, the yields of those synthesis protocols are often low, an economical issue for hybrid ZIFs to be used in a large industrial scale. Microwave-assisted synthesis has recently become popular in MOFs synthesis as facile, rapid, inexpensive, and commercially viable routes toward the production of these compounds.[58]

By recognizing the fundamental crystalline issue and slow synthesis of ZIFs and realizing the potential of mixing metals and/or linkers approach (termed hybrid ZIFs) deriving from ZIF-8, this dissertation is principally dedicated to investigate and develop microwave-assisted synthesis for hybrid ZIFs deriving from ZIF-8 with tunable gas separation properties. The dissertation comprises of 7 chapters. The following chapter II provides general backgrounds on (1) ZIF-8 with SOD structure for efficient gas separation, (2) the reported synthesis for mixed linkers ZIFs, (3) mixed metals ZIFs, (4) mixed linkers and metals ZIFs, and (5) potential of hybrid ZIFs for gas separations.

The research results are presented in Chapter III to VI in which the developed synthesis method for hybrid ZIFs crystals and polycrystalline membranes with microwave-assisted techniques are elucidated. Specifically, Chapter III describes about the rapid microwave-assisted synthesis of hybrid ZIFs with mixed metals and mixed linkers. The microwave-based method significantly shortens synthesis time, produces a higher yield, substantially reduces the amounts of linkers, and eliminates the use of deprotonating agents. Chapter IV shows novel mixed linker ZIF synthesis through linker

doping approach. This strategy expands the option of imidazolate linker that can be incorporated to synthesize hybrid ZIFs. Chapter V discusses the synthesis of mixed metal hybrid ZIF membranes by adopting microwave-seeding technique and secondary growth method. The gas separation performance were shown to be improved through mixing metal approach. In chapter VI, we report a novel rapid one-pot microwave synthesis of mixed linker hybrid ZIF membranes, which is the fastest polycrystalline MOF membrane synthesis within 90 seconds. Furthermore, this is the first example of hybrid ZIF membranes showing tunable gas separation performance. The conclusions and future perspectives are presented in the final chapter VII.

CHAPTER II

BACKGROUND

II.1. **ZIF-8 with SOD topology for gas separation**

ZIF-8 is a prototypical ZIF with Zn^{2+} metal centers bridged by 2-methylimidazolate (2-mIm) linker with SOD topology consisting eight 6-membered ring with defined window aperture of 3.4 Å[29] and six 4-membered ring with the size ~ 0.8 Å,[59] and cage size of 11.6 Å as illustrated in Figure II-1a.[29] It is worth noting that the 4-membered ring of ZIF-8 is too small for even the smallest gas (i.e. helium with kinetic diameter of 2.6 Å) to diffuse through. Therefore, only the 6-membered of ZIF-8 is considered as pore aperture for gas separation. ZIF-8 became one of the most studied ZIFs due to its robust synthesis, which can be obtained in various methods (e.g. solvothermal, microwave, sono-chemical, mechanol-chemical)[60] and conditions (i.e. organic[29] and aqueous[61]). Furthermore, it has shown exceptional gas separation for propylene and propane mixture.[30-36] The SOD topology provides multiple benefit for the separation through ZIF-8 porous structure. First, there are eight available effective pore apertures (6-membered ring) around the cage, maximizing the diffusion of guest molecules through the cages of ZIF-8. Second, the large SOD cage allows the smaller guest molecule to bypass the larger ones that may entrapped inside the framework as illustrated in Figure II-1b, which is a common limitation for many molecular sieving material with unidimensional channel allowing only single file type diffusion.

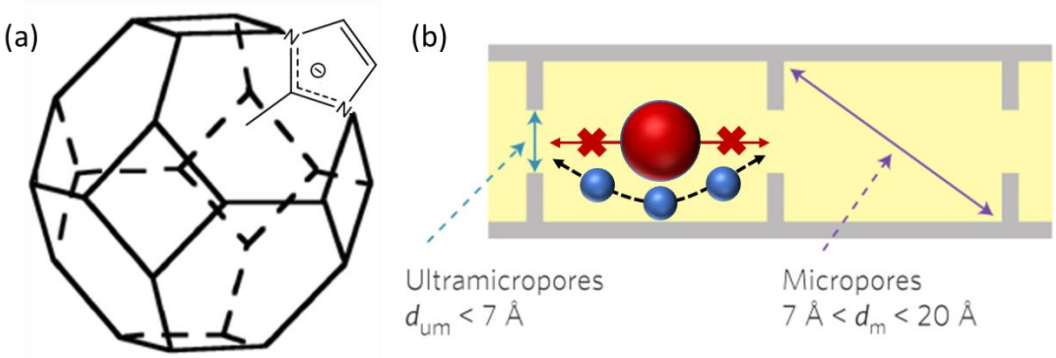

Figure II-1. a) illustration of SOD topology of ZIF-8, and b) molecular sieving diffusion through ZIF-8 cages. Reproduced with permission.[62] Copyright 2017, Springer Nature.

Li et al.[32] were the first to realize the potential of ZIF-8 for kinetic separation of propylene and propane, which is one of the most difficult chemical separations due to their very close relative volatilities and molecular sizes. Although ZIF-8 adsorption capacity of both propylene and propane at 30 °C and 600 Torr were identical, the rates of adsorption are markedly different. The diffusion rate coefficient of propylene is ~ 125 times higher than propane, making it much more selective through the ZIF-8 structure. Later, Koros et al.[31] showed that the effective aperture of ZIF-8 at 35 °C are larger than the determined defined pore aperture of 3.4 Å. The framework has flexibility where the 6-membered ring can go through linker flip-flopping motion enlarging its pore opening to ~ 4.0 Å.[31] This flip-flopping behavior can be illustrated as swinging motion of "saloon door" shown in Figure II-2.

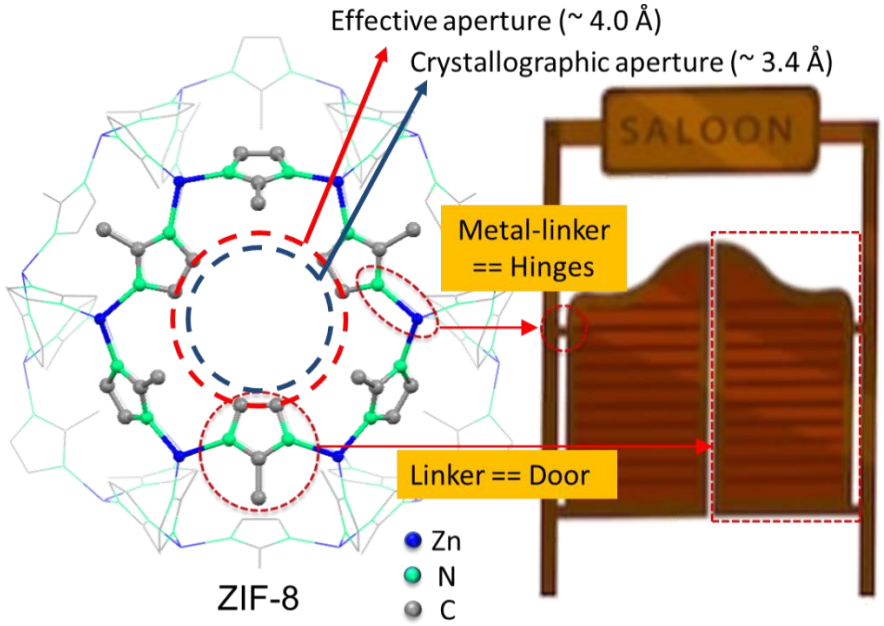

Figure II-2. Schematic illustration of how the flip-flopping motion of the linkers in ZIF-8 affects its effective aperture size.

Despite its potential, ZIF-8 can only separate propylene and propane mixtures and is ineffective for other gas mixtures. Tuning the ZIF-8 by replacing the 2-mIm linker with different bulkiness, such as benzimidazole (bIm) and imidazole-2-carboxaldehyde (2-Ica), have been previously investigated. However, the change in the ZIFs structure (i.e. the molecular sieving properties) through this strategy is too drastic, prohibiting continuous tuning to target gas mixtures. In other words, ZIFs as crystalline materials suffer from fundamental materials limitations where the available aperture sizes are discrete as shown in Figure II-3. For example, ethylene (~ 3.9 Å)/ethane (~ 4.0 Å) separation, ZIFs with an effective aperture size of ~ 3.9 Å are desirable, yet no such reported ZIFs available.

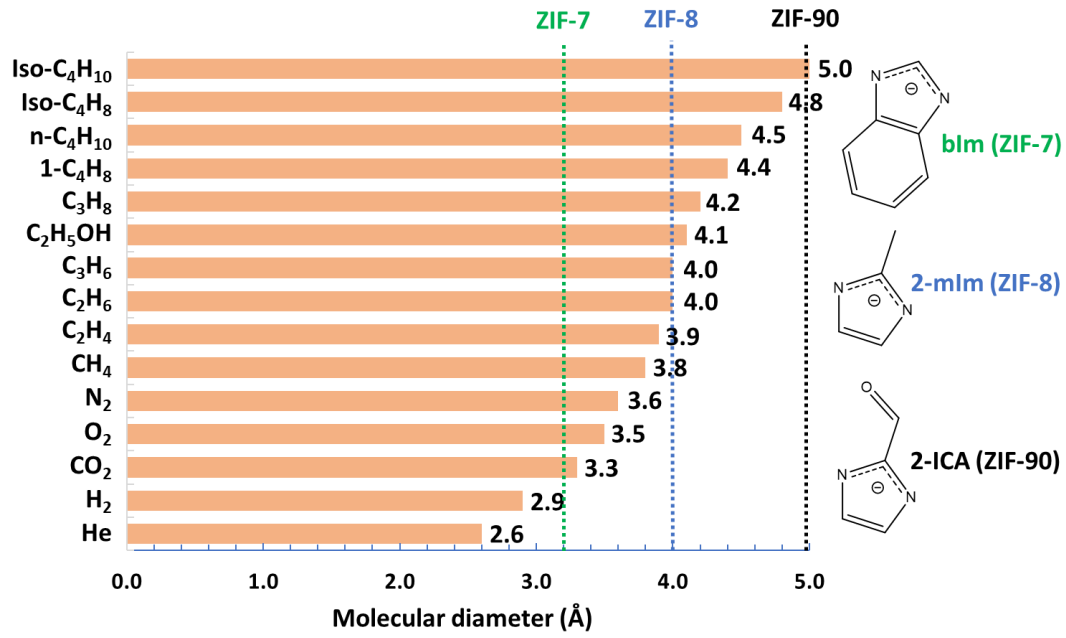

Figure II-3. Size of common gas molecules with the effective aperture sizes of typical SOD-ZIFs showing the apertures are available in a discrete manner.

To overcome this materials challenge, researchers have introduced different metal nodes and linkers, termed hybrid ZIFs.[42, 53, 63] The bonding between metal and linkers (M—N bond) can be illustrated as the hinge of a "saloon door", while the imidazolate linkers represent the door as shown in Figure II-3. Similar to swinging motion of door, which affected by stiffness of hinge and size and weight of the door, the effective apertures of ZIFs (e.g. flip-flopping motion of linkers) and internal surface properties (e.g. polarity and hydrophobicity) can be tuned by mixing different metals and linkers. Thus, hybrid ZIFs can be a potential solution in overcoming the crystalline limitation while maintaining high separation performance to target any gas mixtures.

II.2. **Conventional synthesis of mixed linkers zeolitic-imidazolate frameworks**

The mixing of linkers within the same framework of ZIFs can alter the properties of the ZIF parents: structure change, framework functionality, and stability. Various linkers have been investigated for the formation of mixed linker ZIFs as shown in Figure II-4. In general, the direct in-situ synthesis[42, 45-46, 53, 64] is more prone to allow structure change from the ZIF parent. The presence of secondary linkers in the precursor solution allows crystal formation with a new structure that is more stable than retaining the same topology as the ZIF parent.[64] On the other hand, post-synthetic linker modification tends to retain the structure topology.[65-67] Therefore, it would create distortion to change crystal topology during linker modification, which at times is not favored. Furthermore, some linker modification methods[65-66, 68-69] (e.g. linker substitution) would require the diffusion of secondary linker through the ZIF parent crystals. Large secondary linkers that cannot diffuse through the small pore of a ZIF parent can only modify at the outer shell of the ZIF, which would not affect much on the overall structure of the crystals. Here, we discuss synthesis parameters affecting structure change of mixed linker ZIFs synthesized through direct in-situ approach, and various post-synthetic modification approaches to obtain mixed linker ZIFs.

Table II-1 provides list of mixed linker ZIFs synthesized with different metal salt and solvent. The mixed linker ZIFs synthesized through post-synthetic modification show the parent ZIF.

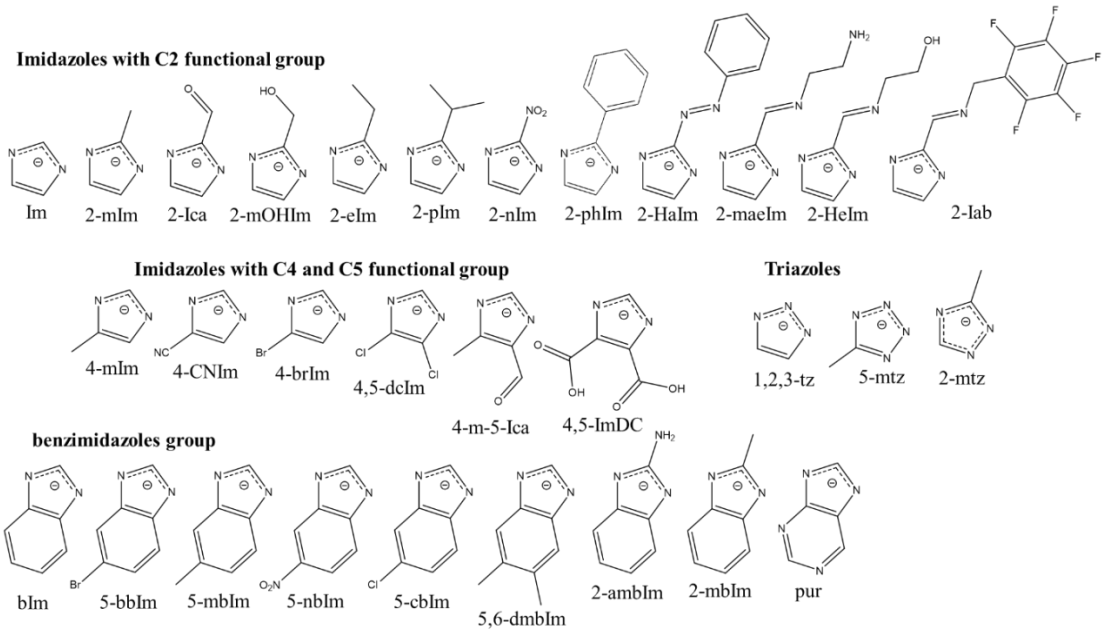

Figure II-4. Schematic of various functionalized imidazolate linkers.

Table II-1. List of various mixed-linker ZIFs with their corresponding topology. The parent of the ZIF are listed for the mixed linker ZIFs synthesized through post-synthetic modification.

ZIF Type	1st Linker	2nd Linker	Metal	Zeolite code	Parent ZIF	Ref
ZIF-7-8	2-mIm	bIm	Zn	SOD	-	42, 53
ZIF-8-90	2-mIm	2-Ica	Zn	SOD	-	53
ZIF-8-ambz	2-mIm	2-ambIm	Zn	SOD	-	54
MAF-47	2-mIm	2-mtz	Zn	SOD	-	44
ZIF-en	2-mIm	2-maeIm	Zn	SOD	ZIF-8-90	54
ZIF-8-DMBIM	2-mIm	5,6-dmbIm	Zn	SOD	ZIF-8	68
SALEM-2	2-mIm	Im	Zn	SOD	ZIF-8	66-67
ZIF-108-mim	2-mIm	2-nIm	Zn	SOD	ZIF-108	70
ZIF-91	2-Ica	2-mOHIm	Zn	SOD	ZIF-90	71
ZIF-92	2-Ica	2-heIm	Zn	SOD	ZIF-90	71
-	2-Ica	2-Iab	Zn	SOD	ZIF-90	72
ZIF-108-eim	2-nIm	2-eIm	Zn	SOD	ZIF-108	70
-	2-HaIm	Im	Zn	SOD	-	73
ZTIF-1	2-eIm	5-mtz	Zn	SOD	-	74
ZIF-68	2-nIm	bIm	Zn	GME	-	45
ZIF-69	2-nIm	5-cbIm	Zn	GME	-	45

ZIF-70	2-nIm	Im	Zn	GME	-	45, 70
ZIF-78	2-nIm	5-nbIm	Zn	GME	-	45, 70
ZIF-79	2-nIm	5-mbIm	Zn	GME	-	45
ZIF-80	2-nIm	4,5-dcIm	Zn	GME	-	45
ZIF-81	2-nIm	5-bbIm	Zn	GME	-	45
ZIF-82	2-nIm	4-CNIm	Zn	GME	-	45
-	2-nIm	Pur	Zn	GME	-	52
CdIF-9	2-eIm	2-nIm	Cd	RHO	CdIF-4	65
SALEM-1	2-eIm	2-mIm	Cd	RHO	CdIF-4	65
MAF-6	2-eIm	2-mIm	Zn	RHO	-	64
-	2-nIm	Pur	Zn	RHO	-	52
ZTIF-2	2-pIm	5-mtz	Zn	RHO	-	74
ZIF-74	5,6-dmbIm	2-nIm	Zn	GIS	-	46, 70
ZIF-75	5,6-dmbIm	Im	Zn	GIS	-	46
TIF-5Zn	5,6-dmbIm	Im	Zn	GIS	-	51
TIF-5Co	5,6-dmbIm	Im	Co	GIS	-	51
JUC-160	2-mbIm	bIm	Zn	GIS	-	55
ZIF-300	2-mIm	5-bbIm	Zn	CHA	-	75
ZIF-301	2-mIm	5-cbIm	Zn	CHA	-	75
ZIF-302	2-mIm	5-mbIm	Zn	CHA	-	75
TIF-3	Im	5-mbIm	Zn	ACO	-	51
ZIF-76	Im	5-cbIm	Zn	LTA	-	46
ZIF-60	Im	2-mIm	Zn	MER	-	46
HZIF-1Mo	2-mIm	H_2MoO_4	Zn	-	-	76
HZIF-1W	2-mIm	H_2WO_4	Zn	-	-	76
ZIF-8-TZ	2-mIm	1,2,3-tz	Zn	-	ZIF-8	77
ZIF-67-TZ	2-mIm	1,2,3-tz	Co	-	ZIF-67	77
ZIF-62	Im	bIm	Zn	-	-	46
TIF-4	Im	5-mbIm	Zn	-	-	51
ZIF-61	Im	2-mIm	Zn	-	-	46
TIF-2	Im	5-mbIm	Zn	-	-	51
ZIF-73	2-nIm	5,6-dmbIm	Zn	-	-	46
ZIF-7-90	bIm	2-ICA	Zn	-	-	57

II.2.1. ***Mixed linker ZIFs by direct in-situ synthesis***

One of the first hybrid ZIFs was synthesized by Huang et al.[64] through direct in-situ approach termed MAF-6 consisting transition metal Zn^{2+} bridged by mixture of 2-

methylimidazole (2-mIm) and 2-ethylimidazole (2-eIm) linkers. Unlike the ZIF parent with monolinker of 2-mIm (ZIF-8[29]) or 2-eIm (ZIF-14[47]) which have SOD and ANA topology, respectively, the MAF-6 has a crystal topology of RHO.[64] Different type of linkers can have different effects on the orientations of adjacent metal coordination polyhedral. Therefore, it is not surprising that ZIF-8, ZIF-14, and MAF-6 each possesses different topology although each consist of imidazolate-based linker with substituent at 2-position.[64]

The structures of mixed linker ZIFs were also affected by various synthesis parameters. For example, dual-linker ZIFs with 2-nitroimidazolate and purine linker synthesized with zinc oxide as a metal source yielded crystals with GME topology, whereas replacing the metal salt with zinc nitrate formed crystals with RHO topology.[52] The effect of different metal salt on the crystallization (e.g. nucleation, growth, crystal size distribution) of ZIFs have also been previously reported.[35, 78-79] Different counter-ions may affect the interaction for coordination bonding between Zn^{2+} with the imidazolate linkers, which can alter crystallization and even final topology of the crystals.

Use of co-solvents can also affect the formation of mixed linker ZIFs.[51, 75] For example, TIF-2 and TIF-3 have different topology although they were synthesized from the same dual linkers (5-methylbenzimidazole, 5-mbim; and imidazole, Im) and metal salt (zinc acetate).[51] It was pointed out that the amount of co-solvent used for the synthesis lead to different crystal formation of TIF-2 and TIF-3. Furthermore, variation of linker ratio and type of solvent can affect the crystal topology as well. By lowering the ratio of

5-mbIm to Im, and changing the primary solvent (from 2-amino-1-butanol to 3-amino-1-propanol), they were able to obtain TIF-4 with a different topology of cag. Yaghi's group also pointed out the importance of co-solvent for crystallization of series of mixed linker ZIFs (ZIF-300, -301, -302) possessing the CHA zeolite topology.[75] It is noted that often co-solvent can direct the structure of resulting mixed linker ZIFs due to 1) occupying spaces and 2) interaction with linkers.

Huang et al.[55] showed that the structure formation of hybrid ZIFs is also temperature sensitive. For example, the zinc based mixed linker ZIFs consisting of benzimidazole (bIm) and 2-methylbenzimidazole (2-mbIm) possessing GIS topology (termed JUC-160[55, 80]) can only be obtained at 180 °C. When the reaction is performed at 100 °C or 140 °C, pure phase ZIF-7 (a SOD zinc based ZIF with monolinker of benzimidazole) or a mixture of JUC-160 and ZIF-7 was yielded, respectively. However, they pointed out the pure phase ZIF-7 crystal could be turned into JUC-160 through post-linker modification if reacted with 2-mbIm at 180 °C.

Adding secondary linker have been shown to improve the framework stability. ZIFs consisting of tetrazolate linker were shown to have poor chemical stability relative to other ZIFs despite their high CO_2 uptake owing to its uncoordinated N-heteroatom sites.[81] Adding non-tetrazolate imidazolate linker can improve its stability against common solvent such as ethanol, methanol, DMF, water, etc.[74] Furthermore, these non-tetrazolate imidazolate linker may act as structure directing agent. For example, the crystals formed with 5-methyltetrazolate (5-mtz) linker and Zn ion leads to structure with

lon topology, whereas adding 2-ethylimidazole or 2-propylimidazole would lead to crystal with SOD or RHO topology, respectively.

Bernt et al.[73] reported mixed linker ZIFs consisting of 2-phenylazoimidazole (2-HaIm) and imidazole (Im) linkers obtained through conventional heating, microwave-assisted heating, and ultrasound-assisted synthesis, in which all techniques yield phase-pure products with main difference in duration of synthesis time. One interesting observation about the dual-linker ZIFs is the functional azo group from 2-HaIm linker is sensitive toward energy from ultraviolet and visible light. The azo group can switch from trans to cis configuration when exposed to UV irradiation; the configuration can also be reversed back to trans by exposing it to visible light.

Wang et al.[76] reported new approach toward mixing linker of ZIFs by integrating zeolite typical 4-connected open framework TO_4 (T = Si^{4+}, Al^{3+}, etc.) as the secondary linker into the ZIFs network as shown in Figure II-5. In order to achieve this, the overall charge balance of TO_4 must be the same as the typical imidazolate linker (Im^{2-}). Therefore, T has to be atom with charge of 6+ to form TO_4^{2-}, in which Mo^{6+} and W^{6+} were used in the reported work. Two mixed linker ZIFs were synthesized through this strategy, HZIF-1Mo (Zn^{2+} with mixed linker of MoO_4^{2-} and 2-mIm) and HZIF-1W (Zn^{2+} with mixed linker of WO_4^{2-} and 2-mIm) possessing a unique sdt topology, which is still unknown in both zeolites and ZIFs. HZIF-1W in particular has a high thermal stability (up to 550 °C), which is significantly greater than many other ZIFs and MOFs. Both HZIF-1 also showed catalytic activity for oxidation of alcohols, and photocatalytic activity toward degradation

of methyl orange. Its capability as both heterogeneous catalyst and photocatalyst made it unique compared to pure zeolite or ZIFs.

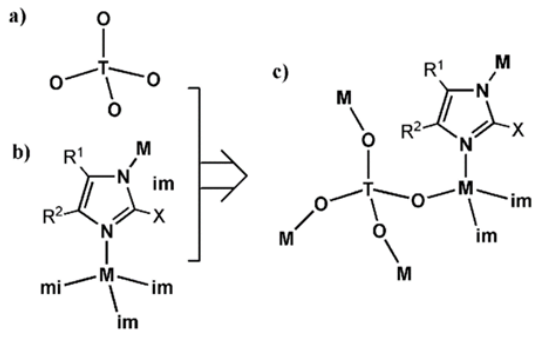

Figure II-5. Bridging linker of a) TO_4 where T has to be atom with charge of 6+ (such as Mo^{6+} and W^{6+}) and O is oxygen; b) imidazolate linker; c) ZIFs structure with TO_4 and imidazolate linker. Reproduced with permission.[76] Copyright 2011, Wiley.

Nair and co-worker[43, 53-54, 57, 82] reported multiple dual-linkers ZIFs with varying linker ratios. For dual-linkers ZIFs with the parent ZIF possessing similar structure such as ZIF-8-90, the structure change from linker ratio variation would be small and difficult to identify through XRD pattern comparison as shown in Figure II-6a. On the other hand, linker ratio variation of ZIF-7-8 significantly affects crystal structure as shown through XRD pattern in Figure II-6b. This is because the parent ZIF-7 and ZIF-8 have different space group of rhombohedral $R\bar{3}$ and cubic $I\bar{4}3m$. Furthermore, they reported that the mixed linker incorporation to the framework is not linear to the starting precursor solution. For example, ZIF-7-8 (dual linker 2-mIm and bIm) and ZIF-8-90 (dual linker of 2-mIm and imidazole-2-carboxaldehyde, 2-ICA) have preferential incorporation of its secondary

linker over 2-mIm synthesized through nonsolvent-induced crystallization (NSIC)[83] method. The difference in solubility of various linkers with the nonsolvent can affect the incorporation of the linker ratio to the framework: the linker with lower solubility will be incorporated in precursors to a larger extent than the other linker. Different synthesis conditions also affect the linker incorporation of hybrid ZIF-7-90 (dual linker of bIm and 2-ICA). Linear incorporation was reported for the condition producing large crystals (>50μm); whereas synthesis condition producing small crystals (<10μm) yield ZIF-7-90 crystals with 2-ICA preferred inclusion.[57]

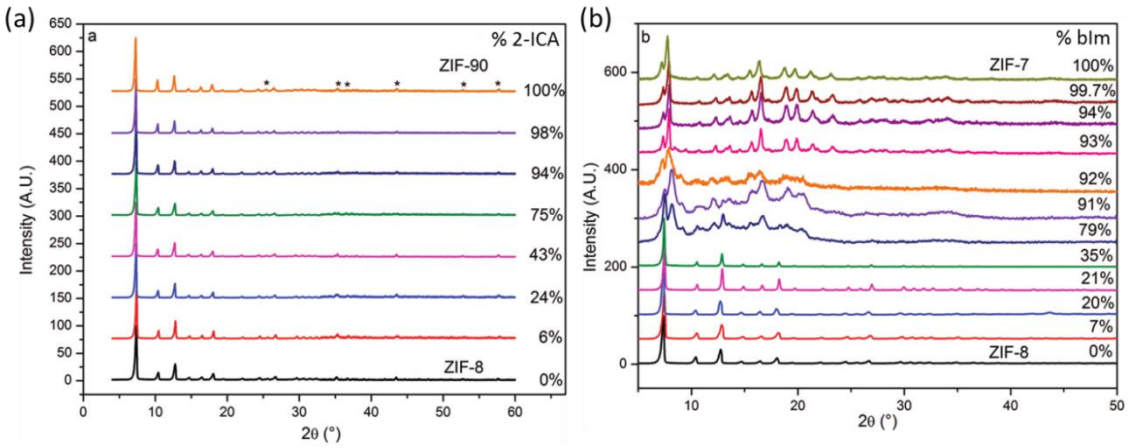

Figure II-6. Powder XRD patterns of (a) ZIF-8-90 hybrids, because of their identical space groups and very small differences in the unit cell dimensions between ZIF-8 and ZIF-90, the patterns appear almost identical but have subtle changes in peak positions and peak intensities; (b) ZIF-7-8 hybrids, there is a distinct shift from $\boldsymbol{I\bar{4}3m}$ to $\boldsymbol{R\bar{3}}$ space group after 35% bIm loading. Asterisks represent positions of α-Al_2O_3 diffraction peaks. Reproduced with permission.[53] Copyright 2012, American Chemical Society.

II.2.2. ***Mixed linker ZIFs by post-synthetic modification methods***

The post-synthetic modification methods for the synthesis of mixed linker ZIFs can be divided into three approaches: 1) post-synthetic linker exchange, 2) post-synthetic chemical modification, 3) post-synthetic thermal modification.

II.2.2.1. *Post-synthetic linker exchange*

Burnett et al.[84] first demonstrated that the pore of MOFs can be engineered through post-synthetic modification by solvent assisted linker exchange, commonly known as SALE. This strategy has been adopted to solve common problem of MOF materials with small porosity, which limits them for application due to difficulty of any molecule to diffuse through the structure. SALE can be easily adopted for ZIFs structure as well. For example, the steric hindrance in CdIF-4 (a RHO cadmium-based ZIF bridged with 2-ethylimidazole, or 2-eIm linkers) from the linker suppresses its micropore volume. A substitution on CdIF-4 with smaller linker size may help open up its pore. Hupp and co-worker[65] modified the linker of CdIF-4 with less bulky 2-nitroimidazole (2-nIm) through SALE approach. A complete linker substitution can be accomplished, exchanging all the 2-eIm with 2-nIm, and forming new structure known as CdIF-9. Although CdIF-9 can be synthesized through direct in-situ approach, it suffers from low yield of ~14 %. Knowing the facile synthesis of CdIF-4 with high yield of ~63 %, the linker substitution of CdIF-4 may present a new approach of obtaining high yield of CdIF-9.

The SALE technique also allowed synthesis of ZIFs that had proven inaccessible via conventional MOF assembly method. For example, Cd-based ZIFs with 2-mIm linker

possessing RHO topology and Zn-based ZIFs with unsubstituted imidazole linker (Im) possessing SOD topology cannot be synthesized through in-situ method.[65-66] This is because the difficulty of forming large RHO and SOD cage with relatively small imidazolate linker making the structure unstable and thermodynamically unsynthesizeable through in-situ synthesis. However, SALE allows linker exchange of CdIF-4 with 2-mIm while maintaining its RHO topology, forming SALEM-1, and ZIF-8 with Im (up to 85% linker exchange) while retaining its SOD topology, termed SALEM-2. Furthermore, Hupp and co-worker[65] pointed out the importance of the ZIF parent for successful SALE. While SALEM-1 can be obtained from linker substitution of CdIF-4 with 2-mIm, it cannot be obtained through SALE of CdIF-9.

The success of SALE may be associated with the pka value of the linker. The targeted linker to be substituted (the linker in the framework) needs to have a higher pka value than the new secondary linker to promote the linker exchange reaction.[77] Furthermore, the size of substituting linker can be an important parameter to consider for linker exchange as well. Caro and co-worker[68] attempted to incorporate bulky 5,6-dimethylbenzimidazole (5,6-dmbIm) linker into the ZIF-8 framework. However, they observed the exchange of 2-mIm with 5,6-dmbIm only takes place mainly in the outermost layer of ZIF-8 crystal, in which they called the modification process a shell-linker-exchange reaction (SLER) as shown in Figure II-7; the shell modified ZIF-8 with 5,6-dmbIm was then termed as ZIF-8-DMBIM. This shell-limited modification might be due to the bulky 5,6-dmbIm is too big to pass through the narrow windows of ZIF-8 due to

molecular sieving effect, therefore the linker exchange reaction only takes place in the outershell of ZIF-8 crystal.

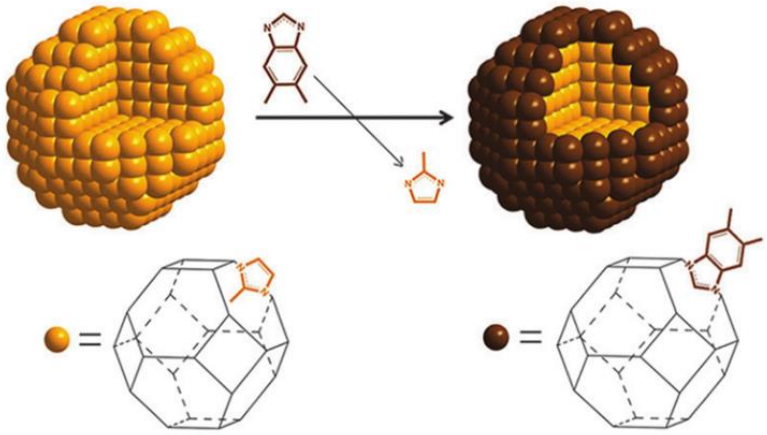

Figure II-7. schematic representation of the shell-linker-exchange-reaction (SLER) process of ZIF-8 with 5,6-dimethylbenzimidazole. Reproduced with permission.[68] Copyright 2013, The Royal Society of Chemistry.

This linker exchange at outershell was also observed in the ZIF-8 linker exchange with 2-ICA, termed ZIF-8-90 SALE.[85] Using fluorescent confocal imaging technique, they were able to identify the concentration gradient of the 2-mIm and 2-ICA linkers throughout the ZIF-8-90 SALE due to the differences in their fluorescence behavior as shown in Figure II-8. Nair and co-worker[85] performed a detailed mechanistic study of this linker exchange process at various temperature. The rate of linker exchange increases with temperature, indicating the correlation of linker exchange rate with diffusivity of the linkers. The amount of secondary linker incorporation is relatively linear with square root of time, indicating a diffusion-limited process. They also pointed out that linker exchange

at high temperature can exhibit linker etching—pitching phenomena which can create morphological defects on the crystals.

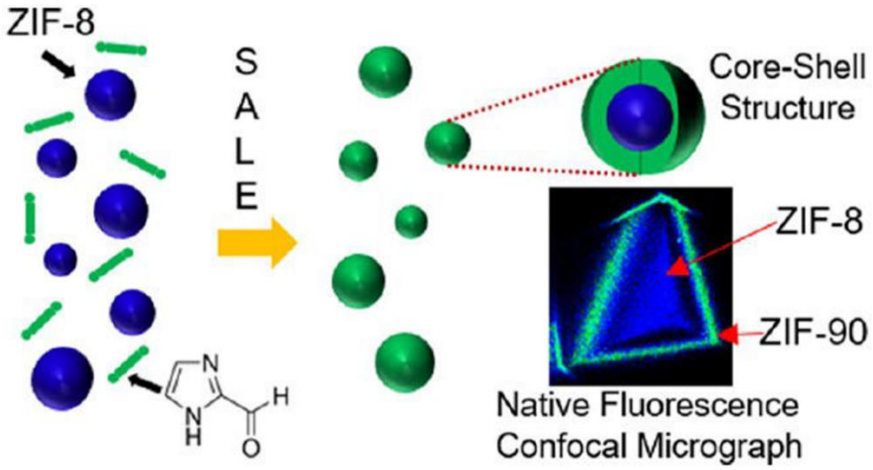

Figure II-8. Illustration of shell-linker exchange of ZIF-8 with 2-ICA, and fluorescence confocal micrograph confirming the linker exchange occurring at the outershell of the crystals. Reproduced with permission.[85] Copyright 2017, American Chemical Society.

In some cases, linker exchange modification can also lead to structure change of the parent ZIF. For example, linker exchange on ZIF-108 (a zinc-based ZIF of SOD topology possessing 2-nIm linkers) with Im, 5-nbIm, and 5,6-dmbIm leads to formation of ZIF-70 with GME, ZIF-78 with GME, and ZIF-74 with GIS topologies, respectively.[70] The structure transformation suggests that linker exchange process is a dissolution-heterogeneous nucleation process rather than conventional single crystal to single crystal transformation.[65, 86-87] This dissolution process in the linker exchange of ZIF-108 may occur because of the metastability of Zn—N coordination bonds due to the electron-withdrawing effect of nitro-group.[88] In the case of SLER of ZIF-8,[68, 85] the absence of nitro

group make Zn—N to be more stable, which allows linker exchange without dissolution of crystals.

Erkartal et al.[77] also employed PSM to convert SOD structure ZIF-8 and ZIF-67 to DIA topology with 1,2,3-triazole linker, termed ZIF-8-TZ and ZIF-67-TZ, respectively. They claimed that one main reason for this change of crystal structure is due to the change of number of coordination sites of the inserted and the replaced linkers, and difference of pka values of the linkers. The significantly lower pka of the substituting linker (protonated 1,2,3-triazole, pka ~ 9.3) than the substituted linker (protonated 2-methylimidazole, pka ~ 14.4) promotes the linker exchange reaction. In addition, the coordination number of each metal center (Zn^{2+} for ZIF-8, and Co^{2+} for ZIF-67) increase from 4 to 6 during this exchange. The structure change reduces the pore volume of the structure measured through N_2 gas sorption as shown in Figure II-9.

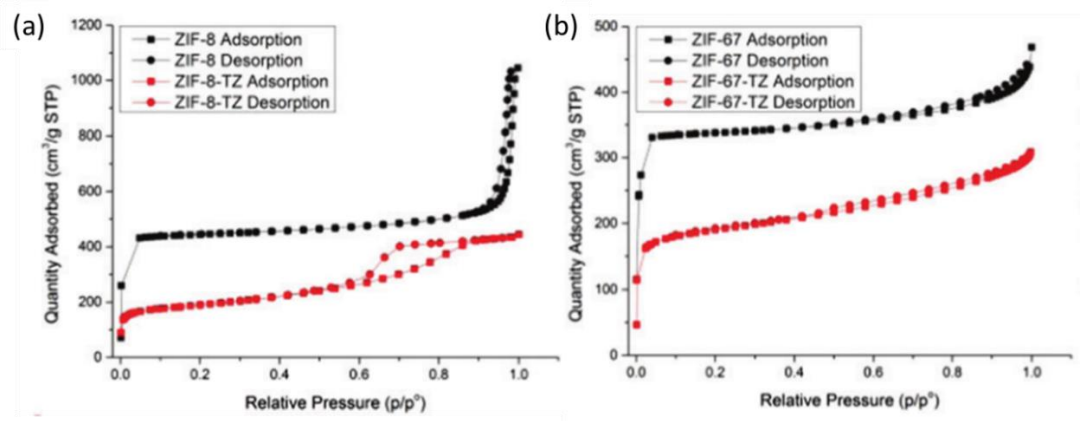

Figure II-9. N2 gas sorption isotherms of (a) ZIF-8 and ZIF-8-TZ, and (b) ZIF-67 and ZIF-67-TZ. Reproduced with permission.[77] Copyright 2017, The Royal Society of Chemistry.

II.2.2.2. *Post-synthetic chemical modification*

Other than linker exchange, modification of linker through reaction can also affect the ZIFs properties. For example, Morris et al.[71] modified the reactive aldehyde group of ZIF-90 (Zn^{2+} bridged by imidazolate-2-carboxaldehyde, 2-ICA linkers) through reduction and imine functionalization. The aldehyde group from ZIF-90 can be reduced easily to alcohol functionality to obtain ZIF-91, or modified with bulky ethanolamine forming ZIF-92 as illustrated in **Figure II-10**a. Only small changes in the porosity of the crystals were observed after the reduction from ZIF-90 to -91 because of the small size difference between aldehyde and alcohol. On the other hand, the imine functionalization of aldehyde to bulky ethanolamine group caused a constriction in the pore aperture of the new framework ZIF-92 as shown through nitrogen physisorption isotherm (**Figure II-10**b).

This can hinder diffusion of molecules through ZIF-92 structure, making it unattractive for applications.

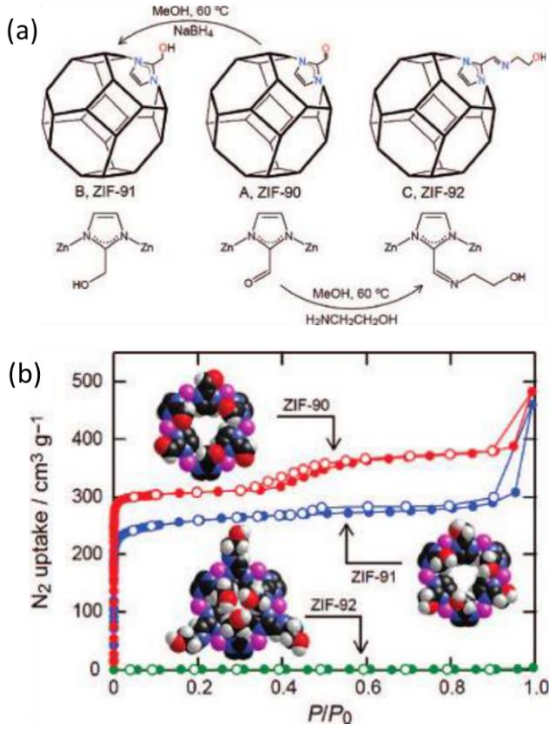

Figure II-10. (a) Transformation of ZIF-90 by reduction to give ZIF-91, and reaction with ethanolamine to give ZIF-92. (b) Nitrogen isotherms of ZIF-90 (red), ZIF-91 (blue), and ZIF-92 (green) measured at 77 K. Reproduced with permission.[71] Copyright 2008, American Chemical Society.

One way to avoid total closure of pore from the chemical modification is by controlling the functionalization process. Nair and co-workers[54] utilized dual-linkers ZIFs as a mean to control the post-synthetic chemical modification method by using different linkers with one being inert and the other reactive to modification. The desired amount of linkers to be modified can be directly controlled through linker ratio variation. Dual-

linkers ZIF-8-90, which can be synthesized through direct synthesis with varying linker ratio, consist of relatively stable 2-mIm linkers and 2-Ica linker with reactive carbonyl moiety. Post-synthetic imine functionalization of ZIF-8-90 restrict reaction only at the 2-Ica linker allowing a control of linker modification.

II.2.2.3. *Post-synthetic thermal modification*

Other interesting approach in modification of ZIFs is through thermal modification reported by Zhang and Koros.[67] An attempt on linker substitution of ZIF-8 with unfunctionalized imidazolate linker (Im) to enlarge the pore of the SOD structure have been reported up to 85% linker substitution. Other than SALE, this mixed linker ZIFs can also be obtained through the thermal modification of ZIF-8. It is known that ZIF-8 has thermal stability up to 500 °C.[29] By exposing ZIF-8 with controlled thermal treatment, methyl group from the 2-mIm linker may dissociate transforming it into Im linker, which "open-up" the ZIF's aperture as illustrated in Figure II-11. The amount of dissociated methyl group depends on the temperature of thermal treatment. The thermal treatment below 300 °C does not show any dissociation of the methyl group. Methyl group dissociation started to occur when ZIF-8 are exposed to temperature above 400 °C. The crystallinity of the ZIF's structure is jeopardized with thermal treatment above 500 °C as PXRD peaks weakened at higher 2θ angles, which suggested existence of locally disordered pores that may reduce its BET surface area and micropore volume. The thermal modification can dissociate up to ~17% of the framework methyl groups before impairing the crystallinity of the structure.

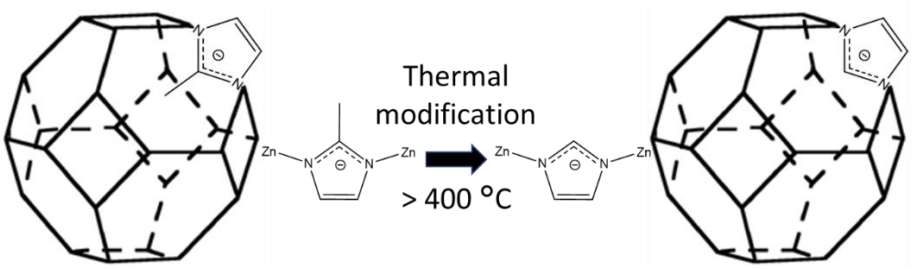

Figure II-11. Illustration of methyl group dissociation from 2-mIm through thermal modification on ZIF-8.

II.3. **Conventional synthesis of mixed metals zeolitic-imidazolate frameworks**

The effect of varying metals in metal organic frameworks are often regarded as inert when compared to the change from modification of linker with functional group.[89] This drives the majority of study on MOFs modification toward linker group over the metal nodes. Furthermore, the incorporation of new metal nodes into the porous framework is less predictable and has many limitations due to the various geometrically preferred orientation for different metal ions. Hupp and Farha et al.[89] argue that changing metal node in MOFs can improve catalytic behavior, or improve the gas sorption properties of the framework. Here we discuss the various strategy to successfully synthesize mixed metal ZIFs through direct in-situ synthesis and post-synthesis modification, and explain the effect of incorporating new metal nodes on the properties of the hybrid ZIFs beneficial for various application. Table II-2 provides list of mixed metal ZIFs with the corresponding linker. The mixed metal ZIFs synthesized through post-synthetic modification show the parent ZIF.

Table II-2. List of mixed-metal ZIFs with their corresponding topology. The parent of the ZIF are listed for the mixed metal ZIFs synthesized through post-synthetic modification.

ZIF Type	1st Metal	2nd Metal	Linker	Zeolite code	Parent ZIF	Ref
CoZn-ZIF-8	Zn	Co	2-mIm	SOD	-	42, 48-50, 90
CdZn-ZIF-8	Zn	Cd	2-mIm	SOD	-	91-92
Cu/ZIF-8	Zn	Cu	2-mIm	SOD	-	93
ZIF-8(Zn/Mn)	Zn	Mn	2-mIm	SOD	ZIF-8	69, 90, 94
Co-Zn(nIm)2	Zn	Co	2-nIm	SOD	ZIF-108	94
Ni-Zn(nIm)2	Zn	Ni	2-nIm	SOD	ZIF-108	94
-	Zn	Fe	2-nIm	SOD	ZIF-108	94
-	Zn	Cr	2-nIm	SOD	ZIF-108	94
-	Zn	Mg	2-nIm	SOD	ZIF-108	94
Cu/ZIF-67	Co	Cu	2-mIm	SOD	-	95
BIF-3-Li	B	Li	2-mIm	SOD	-	96
BIF-3-Cu	B	Cu	2-mIm	SOD	-	96
BIF-9-Li	B	Li	4-mIm	RHO	-	97
BIF-9-Cu	B	Cu	4-mIm	RHO	-	97
Cu-Zn(nIm)2	Zn	Cu	2-nIm	RHO	ZIF-108	94
ZIF-71(Zn/Mn)	Zn	Mn	4,5-dcIm	RHO	ZIF-71	69
BIF-1-Li	B	Li	Im	-	-	96
BIF-1-Cu	B	Cu	Im	-	-	96
BIF-2-Li	B	Li	2-mIm	-	-	96
BIF-2-Cu	B	Cu	2-mIm	-	-	96
ZIF-202	Zn	Cu	Im	-	-	98
ZIF-203	Zn	Cu	Im	-	-	98
ZIF-204	Zn	Cu	Im	-	-	98
-	Zn	Cu	2-mIm	-	ZIF-8	90
-	Zn	Cu	2-mIm	-	ZIF-8	90
BIF-4	B	Cu	bIm	-	-	96
BIF-5	B	Cu	bIm	-	-	96
BIF-6	B	Cu	Im	-	-	96
BIF-7	B	Cu	2-mIm	-	-	96
BIF-8	B	Cu	2-eIm	-	-	96
-	B	Li	bIm	-	-	97
-	B	Cu	bIm	-	-	97

II.3.1. ***Mixed metals by direct in-situ synthesis***

One of the first mixed metals ZIFs were reported by Feng and co-worker[96-97] where they replaced two Zn^{2+} sites in a $[Zn(Im)_2]$ framework with monovalent (Li^+ or Cu^+) and trivalent non-metallic cations (B^{3+}) as illustrated in **Figure II-12**: BIF-1 to BIF-9. With this strategy, they were able to obtain ZIFs with the lightest possible tetrahedral nodes in the Periodic Table, lithium and boron. Presynthesize four-connected $B(Im)_4^-$ and three-connected $HB(Im)_3^-$ were used to form BIFs with four-connected (BIF-1, -2, -3, -9), three-connected (BIF-6, -7, -8), and mixed (3,4)-connected (BIF-4, -5) framework topologies. They observed that changing the monovalent cations from Li^+ to Cu^+ gives isostructural BIF.[96]

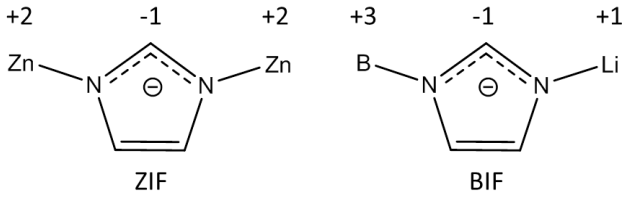

Figure II-12. Schematic of charge distribution in ZIF and BIF. Reproduced with permission.[97] Copyright 2009, American Chemical Society.

One shortcomings on the BIFs are the short B-N distance (~1.5 Å) between boron and the imidazolyl group (when compared to other metal-linker distances in MOFs, usually 2.0 Å or larger), which tends to narrow the pore aperture and places limitation on the accessibility of internal pore surfaces.[97] As a result, the BET surface area for BIF-3-Li

with sod topology is reduced to ~ 40% of the corresponding ZIF-8 with the same topology. By replacing 2-mIm from BIF-3 with 4-mIm as the linker, they were able to create new framework (BIF-9)[97] with RHO topology which has inherently larger pore (8 membered ring) than the SOD topology (6 membered ring windows), increasing the structure surface area relative to the parent BIF-3.

Many reports on mixed metal ZIFs associate the mixing of ZIF-8 and ZIF-67, termed CoZn-ZIF-8,[48-50, 99-101] due to its robust synthesis and similarities in properties between Co^{2+} and Zn^{2+} (e.g. ionic radii and preferred tetrahedral coordination). This allows the synthesis of CoZn-ZIF-8 at mild condition of room temperature,[48-50, 99-101] and even aqueous environment[48] as illustrated in Figure II-13. The mixed metal CoZn-ZIF-8 showed better catalytic properties in converting epoxides and cycloaddition reaction than its monometallic parent framework.[50, 101] The higher catalytic property of CoZn-ZIF-8 may owe to its higher basicity compared to ZIF-8 and ZIF-67 parent.[101] As an electrocatalyst, the graphitized CoZn-ZIF-8 exhibit excellent oxygen-reduction reaction activity approaching the value of Pt/C.[49]

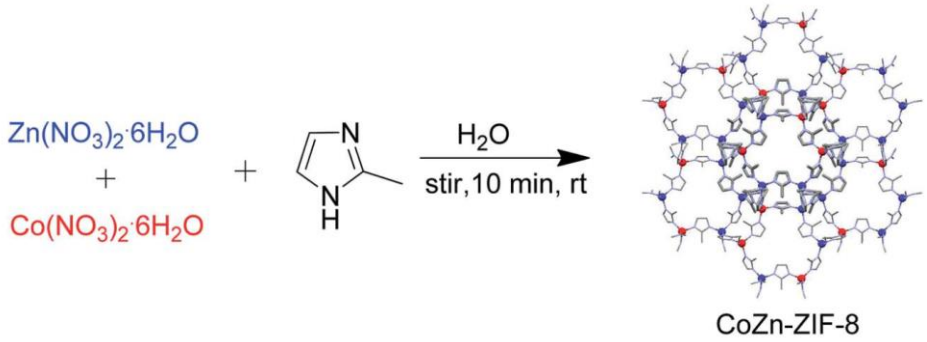

Figure II-13. Schematic representation of the preparation of mixed metal CoZn-ZIF-8 in aqueous and room temperature environment. Reproduced with permission.[48] Copyright 2016, The Royal Society of Chemistry.

Other mixed metal studies related with ZIF-8 and ZIF-67 are incorporation of Cu ions, termed Cu/ZIF-8 and Cu/ZIF-67, respectively.[93, 95] Interestingly, the concentration of Cu in the final framework is much less than the starting precursor solution. For example, synthesis of Cu/ZIF-8 with 1, 5, 10, 25% of Cu in the synthesis solution would only lead to Cu incorporation of 0.6, 2, 4, 9% in the framework.[93] Furthermore, Cu can only be incorporated at small concentration to the framework possibly due to the instability of Cu^{2+} easily being reduced to Cu^{+} compromising the stability of the ZIF structure. As a result, higher doping concentration of copper to ZIF-8 (> 50% in the synthesis solution) would lead to a collapse of the framework. Interestingly, based on electron paramagnetic test (EPR) result suggests the absence of Cu^{2+} signal, indicating the copper in Cu/ZIF-67 are Cu^{+}. However, the study could not define the structure of Cu/ZIF-67 with certainty.[95]

Both Cu/ZIF-8 and Cu/ZIF-67 showed an improved catalytic activity relative to the parent ZIF-8 and ZIF-67, respectively.[93, 95] The Cu/ZIF-8 was shown to be efficient

and reusable catalysts for the Friedländer and Combes condensations and Huisgen's dipolar cycloaddition reaction, in which it increases the yield and reduces synthesis time.[93] The Cu/ZIF-67 was tested as photocatalyst for methyl orange photodegradation under visible-light illumination. With the presence of Cu/ZIF-67, methyl orange degrades faster when compared to monometallic ZIF-67.[95]

II.3.2. *Mixed-metals ZIFs by post-synthetic exchange (transmetalation)*

Unlike the linker substitution, the post-synthesis exchange on the metal of ZIFs present more daunting task: the center-node exchange requires breaking of 4 bonds from the tetrahedral arrangement with the linker as opposed to 2 bonds breaking on each nitrogen end of the imidazolate linker during the linker exchange. Schoenmakers provides a study on the cation exchange on ZIF-8 in the Master Thesis.[90] The success of exchanging metal in ZIFs may depend on the stability of the metal with the nitrogen of the imidazolate linker. This framework stability follows the trend of the Irving-Williams series for transition metal complexes:[89, 102]

$$Ba^{2+} < Sr^{2+} < Ca^{2+} < Mg^{2+} < Mn^{2+} < Fe^{2+} < Co^{2+} < Ni^{2+} < Cu^{2+} > Zn^{2+}$$

Furthermore, the different number valent of cations also has impact on the interaction with the imidazolate linker. The energy change for cation substitution was determined to be higher (less thermodynamically favored) for lower valent cations,[103] indicating higher valent cation to have stronger and preferred interaction with the nitrogen from the imidazolate linker.

Other than stability of cation with the imidazolate linker, the preferred geometry of the cation also plays important role in exchange process. For example, the ZIFs structure requires a tetrahedral geometry of the metal to be 4-connected with the imidazolate linker. Cation with non-tetrahedral preferred geometry may not even be possible to be synthesized directly such as ZIF-8 like structure with manganese (with preferred geometry of octahedral).[90] Metal substitution of ZIFs with cation having non-tetrahedral preferred geometry can reduce the crystallinity or even change on the overall structure of the ZIFs.[90] For example, a change of XRD peak patterns was observed when the Zn^{2+} of ZIF-8 is substituted with Cu^{2+}, in which has preferred octahedral geometry.[104-105] However, exchanging with other divalent cation with tetrahedral preferred geometry such as cobalt may retain the crystallinity.[90] It is worth mentioning that the breaking of bond between metal with imidazolate linker may occur from protonation reaction. Therefore, the pH condition of the exchange reaction can be a crucial key for the succession of cation exchange in ZIFs.[90]

Ban et al.[94] employed the PSM method to obtain mix metal from the parent ZIF-108 with seven different cations: Cr^{2+}, Fe^{2+}, Mn^{2+}, Co^{2+}, Ni^{2+}, Cu^{2+}, Mg^{2+}. The electron-withdrawing of nitro group in ZIF-108 alters its Zn-N bond to be longer than some other ZIFs (ZIF-8, ZIF-7).[29] This makes ZIF-108 less stable than other ZIFs, which makes it suitable as a parent material for substitution. All seven dual-metal ZIF-108 were isostructural to the parent ZIF-108 (SOD topology) except for copper substituted ZIF-108 (or termed as Cu-Zn(nIm)$_2$) with RHO topology. They pointed out that the concentration

of metal ions in the solution for metal substitution should be lower than a critical value (critical ion concentration) to avoid complete dissolution of the parent material. The substitution ratio of Cu^{2+} was much higher than those of the other metal ions, in accordance with the Irving-Williams series.[102] Because both isostructural and heterostructural ZIFs were derived from the parent material ZIF-108, this indicates that the metal substitution involves a heterogeneous nucleation process accompanied by partial dissolution of the parent material.

Through controlled experiment, a comparison was performed on the formation of dual-metal ZIF-108 from one-step synthesis (direct route) vs. two-step synthesis (post-modification or metal substitution).[94] The activation energy in two-step process was found to be lower than that of a one-step route. In the metal exchange process, the parent ZIF-108 may provide numerous active sites for coordination with foreign metal ions, and act as suitable secondary building blocks for regrowth of other structures (e.g. four- and six-membered rings exist as common building blocks in both SOD and RHO structures). This made some of the dual-metal ZIFs are difficult to obtain through one-step route such as the cobalt substituted ZIF-108, in which is obtainable with two-step strategy.

II.4. **Conventional synthesis of mixed metals and linkers zeolitic-imidazolate frameworks**

Finally, the utmost tuning of hybrid ZIFs properties can be achieved through mixing both multiple metals and linkers within the same framework. Table II-3 summarizes a short list of the reported mixed-linker and mixed-metal ZIFs with their

corresponding topology. Ban et al.[70] reported the hybrid mixed metal and linker ZIFs through multiple steps synthesis. First, dual metal of ZIF-108 (with Co, Ni, and Cu) were synthesized through in-situ method, termed Co-Zn(nIm)$_2$, Ni-Zn(nIm)$_2$, and Cu-Zn(nIm)$_2$, respectively. The dual metal ZIF-108 were then modified through linker exchange reaction to yield a dual-metal-dual-linker ZIF-108. Three different linkers (Im, 5-nbIm, and 5,6-dmbIm) were used for the linker exchange modification, forming 9 dual-metal-dual-linker ZIFs.

Table II-3. List of mixed-linkers and -metals ZIFs with their corresponding topology. The parent of the ZIF are listed for the mixed-linkers and -metals ZIFs synthesized through post-synthetic modification.

ZIF Type	1st Metal	2nd Metal	1st Linker	2nd linker	Zeolite Code	Parent ZIF	Ref
CoZn-ZIF-7-8	Zn	Co	2-mIm	bIm	SOD	-	42
-	Zn	Co	2-nIm	5,6-dmbIm	SOD	Co-Zn(nIm)2	70
-	Zn	Ni	2-nIm	5,6-dmbIm	SOD	Ni-Zn(nIm)2	70
-	Zn	Mn	2-mIm	2-eIm	SOD	ZIF-8(Zn/Mn)	69
-	Zn	Co	2-nIm	Im	GME	Co-Zn(nIm)2	70
-	Zn	Co	2-nIm	5-nbIm	GME	Co-Zn(nIm)2	70
-	Zn	Ni	2-nIm	Im	GME	Ni-Zn(nIm)2	70
-	Zn	Ni	2-nIm	5-nbIm	GME	Ni-Zn(nIm)2	70
-	Zn	Cu	2-nIm	Im	RHO	Cu-Zn(nIm)2	70
-	Zn	Cu	2-nIm	5-nbIm	RHO	Cu-Zn(nIm)2	70
-	Zn	Cu	2-nIm	5,6-dmbIm	RHO	Cu-Zn(nIm)2	70
-	Zn	Mn	4,5-dcIm	4-brIm	RHO	ZIF-71(Zn/Mn)	69

One effect can be expected from mixing metal or linker on ZIFs is the realignment of structure, which essentially can lead to collapse of the structure or unattainable porous frameworks. The structure of ZIFs may be challenged more with the existence of dual

metal and dual linker within the same framework. For example, the linker exchange on dual-metal Cu-Zn(nIm)$_2$ can only be obtained at low ratio, or even no exchange for the linker modification with 5-nbIm.[70] The dual-metal Cu-Zn(nIm)$_2$ may not tolerate the exchange of its linker, in which otherwise may lead to collapse of the structure. Furthermore, the outcome of the double exchange modification may not be the same if the exchange process was initiated with linker exchange follow by metal exchange, or vice versa.

Other dual-metal ZIFs may be more tolerable to structure realignment such that dual-metal Co-Zn(nIm)2 and Ni-Zn(nIm)2 allow a topology change from SOD to GME during the linker exchange.[70] The type of substituting linker and metal may also play significant role in the exchange process. For example, the dual-metal-dual-linker ZIF-71(Zn/Mn)-(Cl2/Br) and ZIF-8(Zn/Mn)-(mIm/eIm) does not undergo much structure alignment during the linker and metal exchange, in which each retain the topology of their parent of RHO and SOD, respectively.[69] Therefore, both of them are attainable regardless the steps taken for the modification process: linker exchange follow by metal exchange, or vice versa as illustrated in Figure II-14.

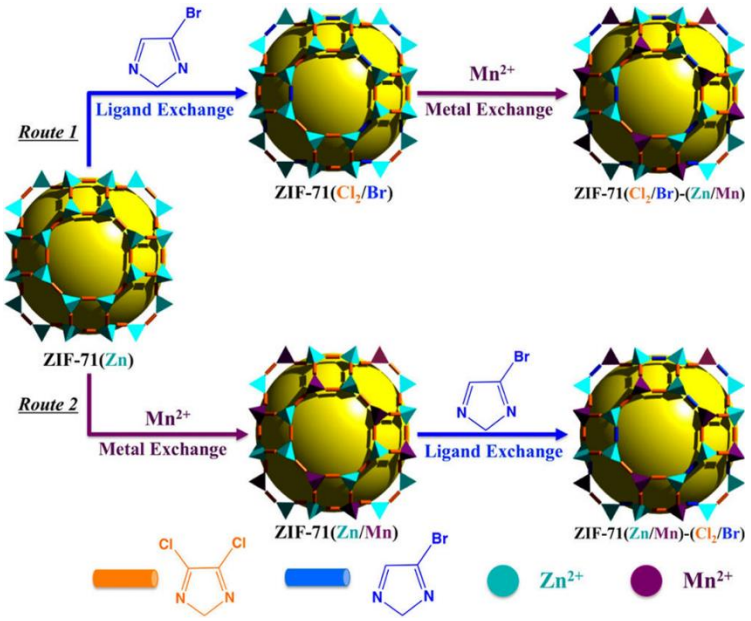

Figure II-14. Stepwise post-synthesis metal and linker exchange on ZIF-71. Reproduced with permission.[69] Copyright 2013, American Chemical Society.

II.5. **Potential of hybrid zeolitic-imidazolate frameworks for gas separations**

The main motivation that attracts many studies on the hybrid MOFs and ZIFs with mixed linkers and metals is the possibility of tuning the structure and internal properties, which can be substantial for optimization of many applications including separations, catalysis, etc.. Here we will focus toward gas separations; and readers interested in other applications such as catalysis may refer to other review.[20] By incorporating multiple linkers to the framework, hybrid ZIFs obtain multiple characteristics from the combination of the diverse functionality of different linkers. Varying the ratio of mixed metal ions with different ionic radii and electronegativity can tune the bond properties (e.g. length,

chemical and thermal strength, mechanical stiffness) between metal to imidazole linker. Therefore, engineering ZIFs structure to optimize the gas separations performance can be achieved through mixing various imidazole linkers and metal ions within the same framework.

II.5.1. *Computational studies on the mixed metals and linkers ZIFs*

Several groups have performed computational studies on the effect of the properties of ZIFs from modification of linkers[106] and metals.[63] Through density functional theory (DFT), Zheng et al.[106] investigated the effect of post-modification of ZIF-8 on its "gate" size and opening by analyzing the geometric (steric hindrance) and electrostatic effects of the methyl group. They found that the existence and position of methyl groups on the imidazolate linker affect the equilibrium of "gate-opening" size. Furthermore, substituting the methyl group of ZIF-8 with more electron donating functional group (e.g. amino) can reduce the "gate-opening" size, and vice versa for electron withdrawing group. This effect is contributed to the electrostatic attractive/repulsive force that can alter the opening of the gate. This strategy on choosing and positioning functional group on the linker can essentially tune the effective aperture size of the ZIF structure, critical for gas separations.

On the other hand, Krokidas et al.[63] have investigated the effect of metal substitution on ZIFs, in particular the cobalt substitution of ZIF-8 (Zn^{2+} to Co^{2+}, ZIF-67) through computational studies. While both ZIF-8 and ZIF-67 shares the same SOD structure with similar frames, the ZIF-67 aperture (3.31 Å) is slightly smaller than ZIF-8

(3.42 Å).[29, 46, 63] Furthermore, the "flip-flopping" motion of the 6-membered ring on the ZIF-67 exhibits a sharper distribution when compared to ZIF-8 as shown in **Figure II-15**. Our group pointed out that the cobalt-to-nitrogen bonding (Co—N) is stiffer than zinc-to-nitrogen bonding (Zn—N) making ZIF-67 structure to be less flexible. The pore constriction along with stiffer pore movement makes ZIF-67 to be a more selective structure than ZIF-8. When compared for the propylene/propane simulation studies, the diffusive selectivities of propylene molecule on ZIF-67 can be improved to ~ 190 from ~ 45 for ZIF-8.

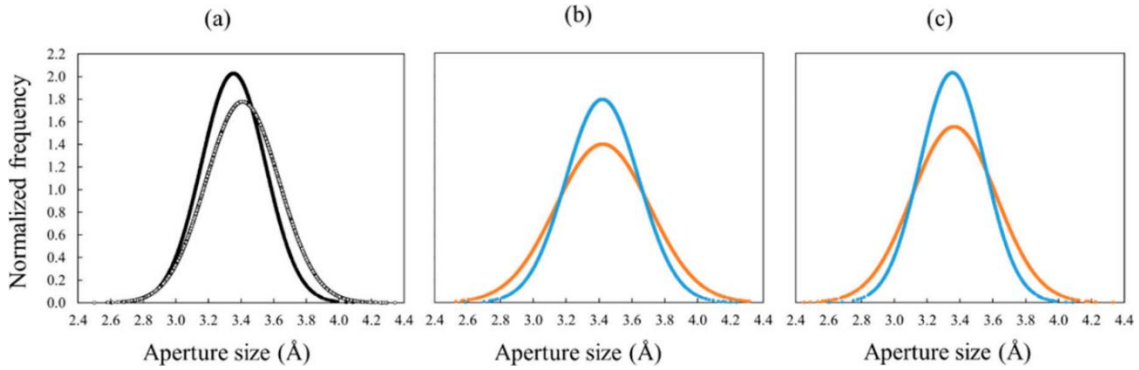

Figure II-15. Distribution of the aperture sizes observed in MD runs of 10 ns. The vertical axis is normalized and corresponds to an area of unity: (a) ZIF-67 (filled black line) and ZIF-8 (open-spaced line at 295 K), (b) ZIF-8 aperture, and (c) ZIF-67 aperture response upon heating (blue line, 295 K; orange line, 530 K). Reproduced with permission.[63] Copyright 2016, American Chemical Society.

II.5.2. *Hybrid ZIF adsorbents for gas separations*

Multiple hybrid ZIF crystals have been investigated as adsorbents for gas separations described in more detail in the following sections.

II.5.2.1. *Mixed linker ZIF adsorbents*

Yaghi's group was among the first to study the change of properties of ZIFs by mixing two imidazolate linkers while keeping the same GME topology.[45-46] By keeping one of the linker as 2-nitroimidazole (2-nIm), they were able to show the effect of changing the second linker with different type of imidazole based linker. The bulkiness of second linker affects the size of the kno cage of the GME hybrid ZIF crystals, in which tuning the crystallographically defined pore size, pore volume, and calculated BET surface area as shown in Figure II-16a.[45-46] The dual-linker ZIFs attraction toward CO_2 uptake can also be tuned with different polar functional groups as shown in Figure II-16b.[45-46]

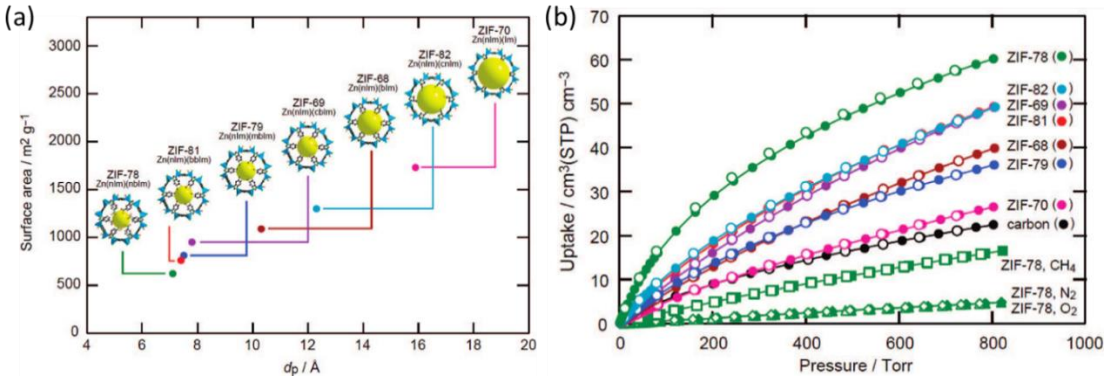

Figure II-16. (a) Plot of defined pore size and surface area for the GME dual-linker ZIFs with varying secondary linker. (b) CO2 isotherm on dual-linker ZIFs and commercial BPL carbon. Different polar functional groups in the secondary linker (--NO2, --CN, --Br, --Cl, --C6H6, --CH3, --H) of ZIFs affect attraction toward CO2. Reproduced with permission.[45] Copyright 2009, American Chemical Society.

While varying secondary linker can tune the structure of the ZIFs, at times, these changes are too drastic. Nair and co-worker[43, 53-54, 57] were among the first to investigate

the effect of varying the ratio of two linkers to tune the pore aperture of dual-linkers ZIFs (e.g. ZIF-8-90[43] and ZIF-7-90[57]) through diffusivity measurement of n-butane and i-butane. They found that the transport diffusivities of both butane isomers can be tuned continuously through linker ratio variation. Figure II-17 shows the diffusivity measurement of ZIF-8-90. A decreasing 2-mIm/2-ICA linker ratios leads to an increase in the effective pore size and allows faster hopping of both n-butane and i-butane through the pore windows. Through molecular sieving effect, pore constriction from replacement of 2-ICA with 2-mIm linkers increases diffusive selectivity of n-butane over i-butane.

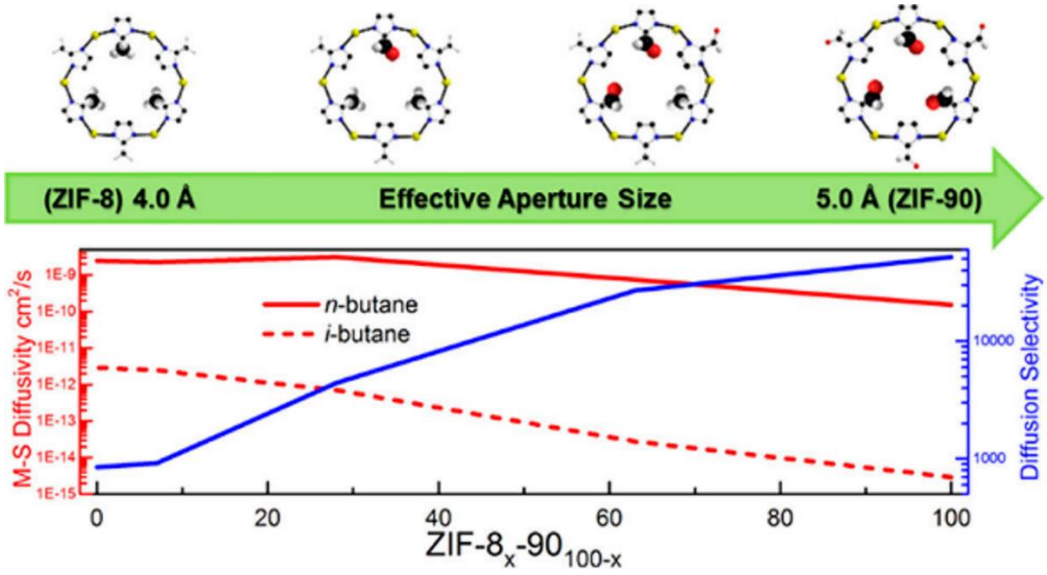

Figure II-17. Corrected Maxwell-Stefan (M-S) diffusivities of n-butane and i-butane (left axis), and the corresponding n-butane/i-butane selectivities (right axis) of ZIF-8-90 with varying ZIF-8 (2-mIm) to ZIF-90 (2-ICA) linkers. Reproduced with permission.[43] Copyright 2015, American Chemical Society.

Guest adsorption can also be tuned through linker ratio variation. For example, nitrogen physisorption isotherm on ZIF-7-8 (dual linker 2-mIm and bIm) showed the decrease on adsorbed quantity as more bulky bIm was incorporated into the framework, reducing the microporosity of the ZIF-7-8. Furthermore, the bulky bIm linkers are much less amenable to rotational displacement than 2-mIm linkers, reducing the gate-opening[107-112] phenomena. Therefore, at full linker replacement of 2-mIm with bIm (ZIF-8 to ZIF-7), pore constriction of ZIF-7 (with defined pore of ~ 2.9 Å[113]) restrain diffusion of N_2 gas with kinetic diameter of ~ 3.64 Å. Water adsorption behavior can also be tuned by varying linker ratio with hydrophobic characteristics. For example, the mixed linker ZIF-8-90 (dual linker 2-mIm and 2-ICA) water adsorptivity can be increased by incorporating more 2-ICA linkers with hydrophilic carbonyl groups..[43]

One interesting modification on mixed linker ZIFs is the shell-linker-exchange-reaction (SLER).[68, 85] The outershell modification of ZIFs can be important in creating shield in the outer section of the ZIFs while maintaining the important properties at the core of the crystals. For example, the SLER modified ZIF-8-DMBIM (refer to "post-synthetic linker exchange" section) has high hydrophobic characteristic while still possessing high surface area and pore volume at the inner core of crystals. The hydrophobic 5,6-dmbIm increases the contact angle of water for the modified ZIF-8-DMBIM to 121° when compared to original ZIF-8 (60°), and only a negligible decrease in BET surface area and pore volume was observed after SLER. Furthermore, the modification affects the "gate-opening" behavior in the adsorption of isobutanol, where

elimination of “gate-opening” effect was observed after the SLER treatment for ZIF-8-DMBIM. Intuitively, one can expect that the bulky 5,6-dmbIm linker will constrict the pores of ZIF-8-DMBIM hence reducing transport diffusivity. However, ZIF-8-DMBIM was observed to have higher isobutanol transport diffusivity when compared to pure ZIF-8. These phenomena might be a result of stronger framework–guest interaction of ZIF-8-DMBIM with the alcohol than ZIF-8.

Another modification on the pore aperture of ZIFs is through thermal modification. Zhang and Koros[67] reported that the dissociation of methyl group on ZIF-8 “open up” the ZIF’s aperture, which can increase guest molecule diffusivity and permeability. Variation on temperatures of the thermal treatment was studied on the amount of dissociated methyl group, and thus the guest molecule diffusivity as shown in Figure II-18. Methyl dissociation was observed starting around 400 °C, in which slightly increases the guest molecules diffusivity over unmodified ZIF-8. The diffusivities were increased rapidly (increased by 432, 28, and 400 times for SF6, n-C4H10, and iso-C4H10, respectively) as the thermal treatment is further increased to 500 °C (Figure II-18). However, thermal modification at 500 °C showed weakened PXRD peaks at higher 2θ angles, which suggested existence of locally disordered pores that may reduce its BET surface area and micropore volume.

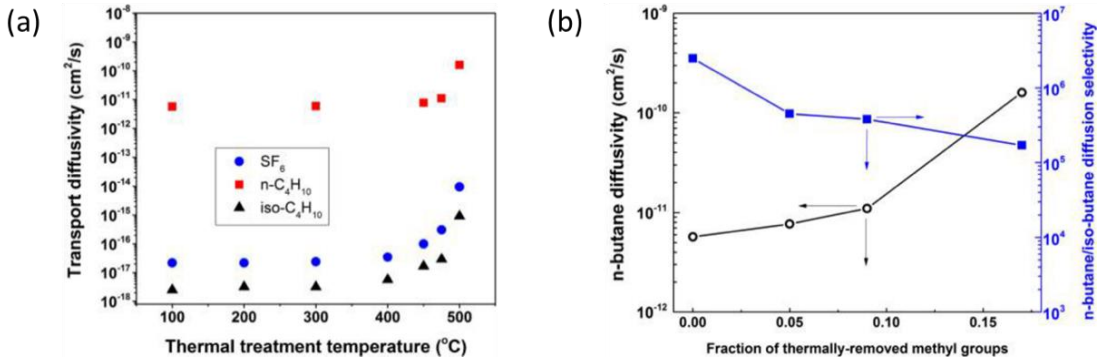

Figure II-18. (a) Guest molecule (SF6, n-C4H10, and iso-C4H10) transport diffusivity data in the ZIF-8 precursor (activated at 100 C) and ZIFs thermally modified at 200, 300, 400, 450, 475, and 500 C. (b) Effect of thermally induced methyl group removal on ZIF-8's n-butane/i-butane diffusion selectivity. Reproduced with permission.[67] Copyright 2015, American Chemical Society.

Zhang et al.[44] observes a significant improvement of various guest molecule adsorption when the C-H moiety in ZIF-8 (or called MAF-4) is replaced with N atom to form MAF-7 with 2-methyl-1,2,3-triazole (2-mtz) linker. The isoelectronic N atom can provide a Lewis base active site for guest binding.[114] This leads to substantial improvement of CO_2 and C_2H_2 adsorption in MAF-7 at room temperature as shown in Figure II-19a & b, despite the similarities in pore volume and surface area with the parent ZIF-8 (determined through N_2 sorption measurements). Furthermore, water uptake on MAF-7 increases by over 100 times than ZIF-8, in which can be tune by mixing ZIF-8 and MAF-7 (creating MAF-47) shown in Figure II-19c.

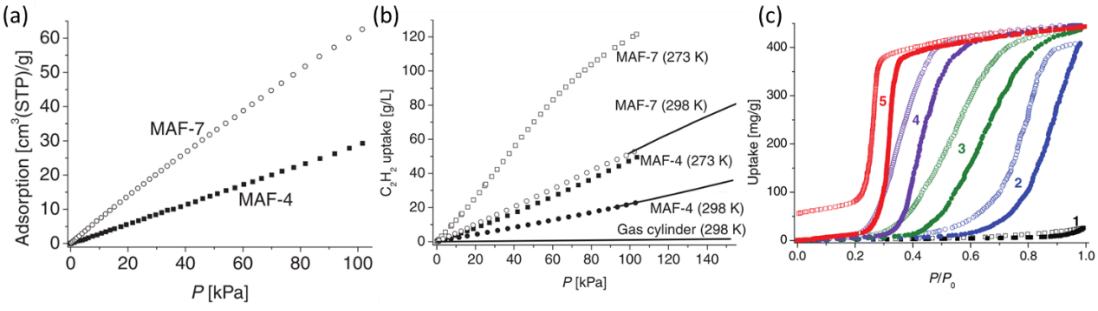

Figure II-19. Adsorption isotherm of (a) CO2 at 273 K and (b) C2H2 at 273 and 298 K on MAF-4 and MAF-7. (c) Water vapor sorption isotherms of MAF-4, MAF-47, and MAF-7, where 1-5 corresponds to MAF-47 with 2-mIm linker concentration of 1 (MAF-4), 0.76, 0.49, 0.23, 0 (MAF-7), respectively. Reproduced with permission.[44] Copyright 2011, Wiley.

II.5.2.2. *Mixed-metals ZIFs adsorbents*

The first reported mixed metal ZIFs, termed boron imidazolate frameworks (BIFs, refer to "mixed-metal zeolitic-imidazolate frameworks" section) consisted mixture of boron and monovalent cations (Li^+ and Cu^+) bridged by imidazolate linkers.[96-97] When the monovalent cations in BIF-9 were changed from Li^+ to Cu^+, the bond lengths (boron-to-nitrogen and copper-to-nitrogen) elongate creating larger pore volume for BIF-9-Cu than BIF-9-Li.[97] However, the streak difference in molecular weight of Cu and Li made BIF-9-Li has lighter framework density. When tested on various gas sorption measurement, BIF-9-Li were able to adsorbed more N2 and H2 molecules as shown in Figure II-20.

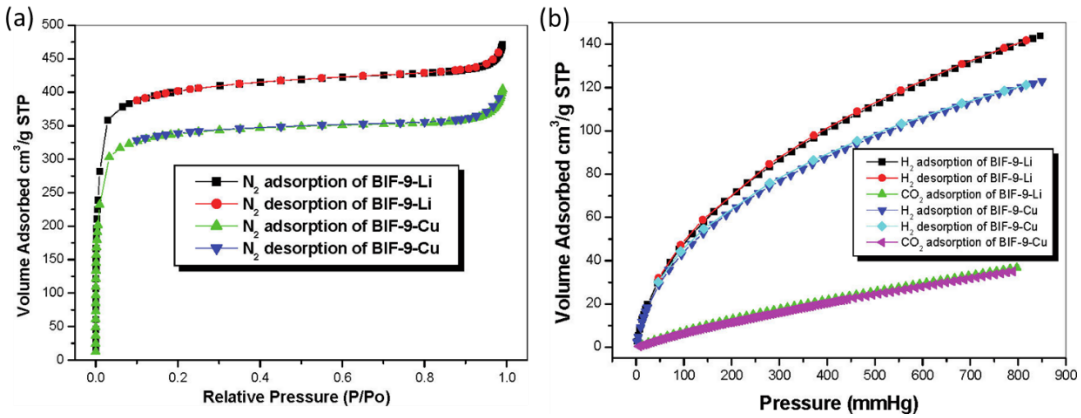

Figure II-20. Gas sorption isotherm of BIF-9-Li and BIF-9-Cu for (a) N2 at 77 K and (b) H2 at 77 K and CO2 at 273 K. Reproduced with permission.[97] Copyright 2009, American Chemical Society.

When the change in the ZIFs structure is very small from mixing metal ions, the effect on the guest adsorption can be negligible. For example, nitrogen physisorption were tested on CoZn-ZIF-8 with various Co/Zn ratios, where all the dual-metal ZIFs exhibit similar isotherm type I curve with comparable BET surface area.[42] On the other hand, structure change from mixing metals is not the only parameter affecting guest sorption. Yang et al.[95] observed improvement of CO_2 and H_2 solubility (larger Henry's constant) for copper doped ZIF-67 structure (termed Cu/ZIF-67) while showing similar N_2 sorption behavior when compared to ZIF-67 as shown in Figure II-21. Ban et al.[94] have also tested various gas sorption measurements on multiple dual-metals ZIFs consisting of pair of Zn, Ni, Co, or Cu using ZIF-108 as the parent. They pointed out that the metal substitution process can form crystal defects leading to increase in BET surface area and HK (Horvath-Kawazoe) pore size distribution.

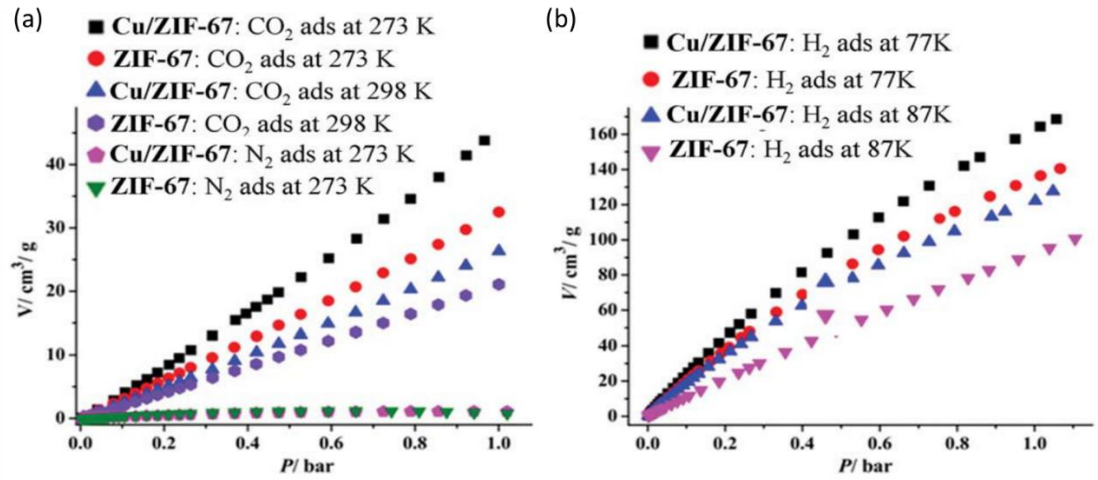

Figure II-21. Gas sorption isotherm of ZIF-67 and Cu/ZIF-67 for (a) N2 at 273 K, and CO2 at 273 and 298 K, (b) H2 at 77 and 87 K. Reproduced with permission.[95] Copyright 2012, The Royal Society of Chemistry.

II.5.3. ***Hybrid ZIF membranes for gas separation***

Multiple hybrid ZIFs have been investigated as membrane for gas separation. While majority of the hybrid ZIF membranes were in a form of mixed matrix membranes (MMMs), a few of polycrystalline post-synthetically modified ZIF membranes have been reported.

II.5.3.1. *Mixed linker ZIF membranes*

With various reports on the tuning of guest adsorption and diffusivity through mixing linkers strategy, some groups have further investigated the use of these mixed linker ZIFs as the inorganic filler of mixed matrix membranes (MMMs). For example, Nair and co-worker[82] compared the gas separation performance of CO_2/CH_4 using MMMs setup with Matrimid® 5128 polymers and various dual linker ZIFs as shown in Figure

II-22. The MMMs with hybrid ZIFs showed improved selectivity of CO_2 at the expense of reduced permeability when compared to their parent ZIF-8. This can be associated with the inclusion of bulky benzene group for the mixed linker ZIFs. Furthermore, the amino moiety in ZIF-8-ambz (dual linkers of 2-mIm and 2-aminobenzimidazole, 2-ambz) may have substantial intermolecular interaction with each other (such as hydrogen bonding) that could change the flexibility or even structure of the ZIF-8-ambz. This restriction of flexibility may alter the diffusion pathway through the mixed linker ZIFs. Other reports on MMMs with amine functionalized ZIFs also affected the CO_2/CH_4 permeation characteristics,[115-116] likely due to this structural change from intramolecular interaction rather than the affinity of polar amine group toward CO_2.[82]

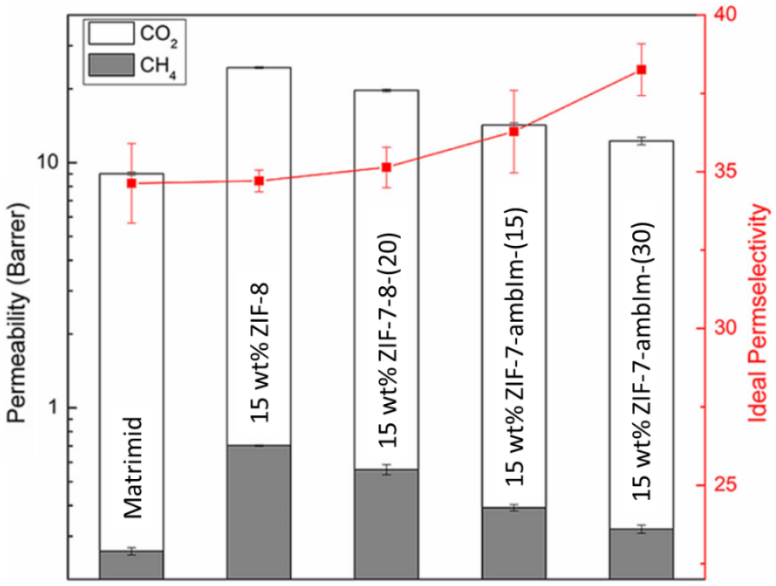

Figure II-22. Single gas permeation results of mixed matrix membranes with ZIF-8 and dual-linkers ZIFs fillers at 3.45 bar and 35 °C. Value in parentheses correspond to the % amount of secondary linker in the framework of the dual-linkers ZIFs. Secondary linkers

for ZIF-7-8 and ZIF-8-ambIm are bIm and 2-ambIm, respectively. Reproduced with permission.[54] Copyright 2013, American Chemical Society.

Caro and co-workers[68] have also studied the SLER modified ZIF-8-DMBIM as inorganic filler of MMMs consisting of silicone rubber polymer (e.g. polymethylphenylsiloxane, PMPS), termed ZIF-8-DMBIM-PMPS. The MMMs were tested for pervaporation recovery of isobutanol from water and comparing them with ZIF-8 filled MMMs (ZIF-8-PMPS). The ZIF-8-DMBIM-PMPS membrane improved the permeate concentration of isobutanol than the values obtained via evaporation by the vapor-liquid equilibrium. When compared to ZIF-8–PMPS membrane, the ZIF-8-DMBIM-PMPS membrane exhibited improved selectivity towards isobutanol while keeping the isobutanol flux (productivity) constant. The improved selectivity results from the increased hydrophobicity, the decreased threshold pressure for isobutanol adsorption and the enhanced transport diffusivity after SLER treatment of ZIF-8.

Caro and co-workers[117-118] also investigated on the tuning of gas separation performance through linker modification of polycrystalline ZIF-90 membranes. It is worth noting that preparing well-intergrown ZIF-90 membranes is important prior to linker modification, in which they functionalized the ceramic alumina support with APTES (3-aminopropyltriethoxysilane) prior to ZIF-90 growth.[119] The functionalization of ceramic support has been adopted for preparation of other polycrystalline ZIF membranes as well.[120-121] Functionalization on the carbonyl group of ZIF-90 through imine condensation with bulky ethanolamine or APTES can improve their separation factor performance at

the expense of reduction in permeance as shown in Figure II-23. Longer modification reaction can also further increase the separation factor performance.

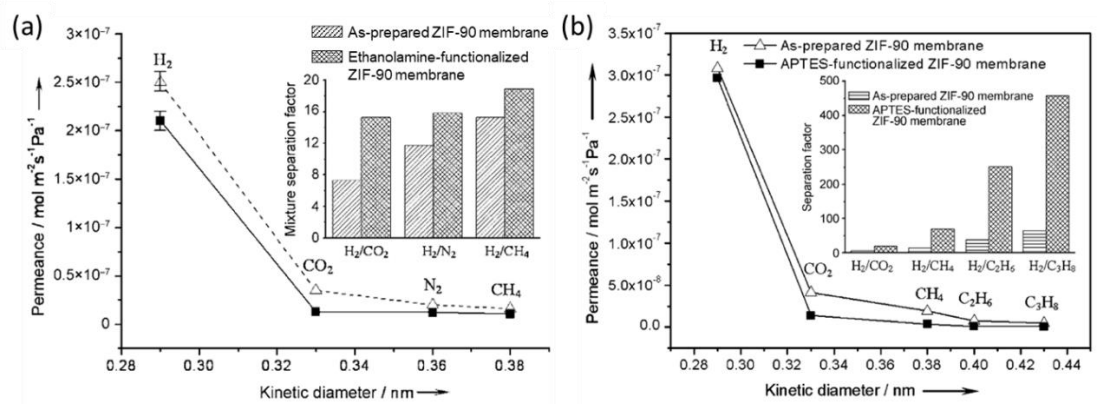

Figure II-23. Single-gas permeances on the as-prepared (triangle) and imine-functionalized (square) ZIF-90 membrane with (a) ethanolamine and (b) APTES at 200 °C and 1 bar as a function of the kinetic diameter. The inset shows the mixture separation factors for H2 over other gases from equimolar mixture. Reproduced with permission.[117-118] Copyright 2011 and 2012, Wiley.

Following reports from Yaghi's group[45] on the excellent CO_2 sorption behavior on dual linkers ZIF-78, Lin's group[122] investigated the preparation of ZIF-78 polycrystalline membranes to study its performance for CO_2 gas separation application. The polycrystalline ZIF-78 membrane was prepared on zinc oxide porous support, where the zinc oxide itself acted as a metal source for seed layer of ZIF-78. The work emphasized on the importance of activation process of the ZIF-78 membrane. Due to the use of bulky dimethylformamide (DMF) solvent for the synthesis protocols, it is important to remove DMF at a slow rate. In which otherwise may lead to formation of cracks causing the

membrane to be non-selective. The slow activated ZIF-78 membrane shows molecular sieving behavior for binary mixed-gas H_2/CO_2 separation with H_2 permeability of 7.2×10^3 Barrer and a H_2/CO_2 separation factor of 9.5. Yang et al.[123] claimed that the membrane performance in gas separation of ZIF-78 can be further improved if the morphology is controlled to certain orientation, which can be achieved by varying the concentration nutrients, linker concentration, and linker ratio of 2-nIm to 5-nbIm.

II.5.3.2. *Mixed metal ZIF membranes*

ZIF-8 is one of the most studied ZIFs since its discovery in separating industrially important propylene/propane gas mixtures.[30, 33-37, 124-125] This drives many researchers to investigate the hybrid ZIF structure deriving from ZIF-8. Computational study showed substantial improvement of cobalt substituted ZIF-8 (namely ZIF-67) for the propylene/propane diffusive selectivity.[63, 126] However, up to date no well-intergrown ZIF-67 polycrystalline membrane has been prepared with selective gas separation, possibly due to its difficulty in preparing ZIF-67 polycrystalline membranes. For example, Wang et al.[127] attempted to prepare polycrystalline dual-metals ZIF-8 membranes with cobalt and zinc ions, termed CoZn-ZIF-8. However, the dual-metals ZIF membranes gas separation performance on the propylene/propane permeation testing contradict with the computational studies[63] possibly due to the poor membrane quality.

An et al.[128] recently compared ZIF-8 and ZIF-67 as inorganic fillers for MMMs with 6FDA-DAM polymer (PI). They observed that the MMMs with ZIF-67 fillers (PZ67) showed improvement in permselectivity for propylene/propane gas separations over ZIF-

8 fillers (PZ8) with the expense of reduction in permeability as shown in Figure II-24. While the solubility selectivity for both PZ67 and PZ8 were comparable, the diffusive selectivity of PZ67 were determined to be higher than PZ8, which yields the higher permselectivity. The similarities in ZIF-8 and ZIF-67 possibly leads to their similar strength in interfacial adhesion with PI polymers, leading to the similarities in the solubility selectivity.

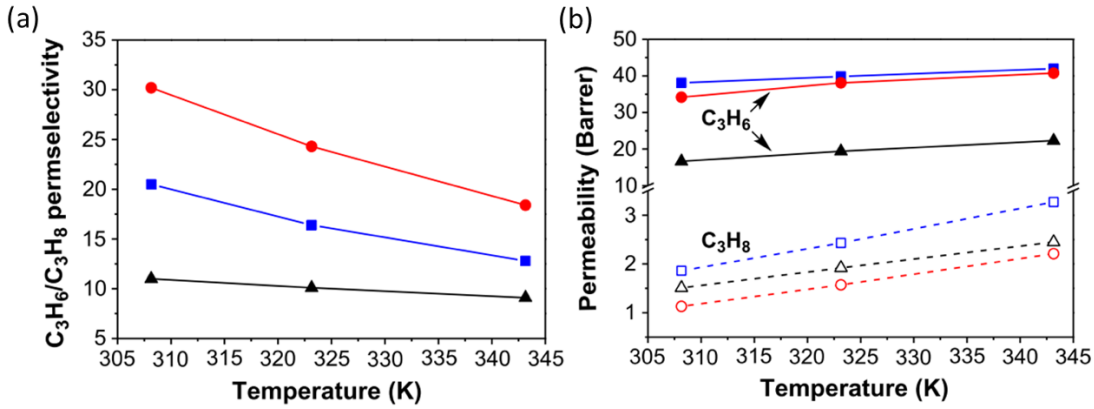

Figure II-24. Comparison of propylene/propane separation performance for PZ67 (circle) and PZ8 (square) MMMs and PI polymer (triangle) at various temperature. (a) For permselectivity and (b) for permeability. Reproduced with permission.[128] Copyright 2017, Elsevier.

Ban et al.[94] have also investigated the dual-metal ZIFs from ZIF-108 parent for their gas separation performance as inorganic fillers for MMMs of polysulfone (PSF) polymer. The MMMs consisting the dual-metals ZIFs filler showed improved separation factor for CO_2/N_2 and CO_2/CH_4 binary gas separation than PSF membrane and pure ZIF-108 MMMs. They attribute the improvement in gas separation performance of the MMMs

containing dual-metals ZIFs filler to the enlarged pore size after metal substitution from the ZIF-108 parent and specific affinity of certain gas molecules for the substituting metal ions.

CHAPTER III

RAPID MICROWAVE-ASSISTED SYNTHESIS OF HYBRID ZEOLITIC-IMIDAZOLATE FRAMEWORKS WITH MIXED METALS AND MIXED LINKERS*

III.1. **Introduction**

Separation applications using porous solid materials such as zeolites and metal-organic frameworks (MOFs) have been extensively studied.[19-20, 38-39, 129-136] Zeolitic-imidazolate frameworks (ZIFs),[29] a subclass of MOFs, in particular have attracted many attentions due to their chemical/thermal stabilities, ultra-microporosities, and high surface areas when compared to other MOFs materials.[29] ZIFs possess zeolite-like topologies in which the tetrahedral Si or Al and the bridging O in zeolite structure are replaced by transition metals (such as Zn,[29] Co,[46] and Cd[65, 137]) and imidazolate-derived ligands. Among many ZIFs, ZIF-8 with a sodalite (SOD) zeolitic topology consisting of Zn and 2-methylimidazolate has been extensively studied mainly due to its robust synthesis and potential for gas separations.[31, 33-37, 61, 108, 125, 138-140] Despite their potentials for gas separation applications, ZIFs, like any other crystalline materials, suffer from one fundamental issue: their available aperture sizes are discrete due to their crystalline nature. For example, there are no ZIFs materials effective for ethylene/ethane separation.

**This chapter was adapted with permission from Febrian Hillman, John M. Zimmerman, Seung-Min Paek, Mohamed R. A. Hamid, Woo T. Lim, Hae-Kwon Jeong, J. Mater. Chem. A, 2017, 5, 6090-6099 and modified. Copyright 2017, The Royal Society of Chemistry.*

In general, the gas separation performance of porous solids is determined by their diffusion and adsorption properties.[141] Studies have shown that these properties can be continuously tuned by mixing metals[48, 93, 127, 142-144] and/or linkers[43-44, 53-57, 145] to form hybrid MOFs/ZIFs (also called multi-component MOFs[19]). For example, Nair and co-workers[53-54] were able to continuously tune the framework functionality or microporosity of a ZIF through the mixed linker strategy. Kaur et al.[48] reported mixed metal CoZn-ZIF-8 (ZIF-8 like crystals with SOD topology possessing mixed metal centres of Co and Zn) and showed an increase of pore volume and BET surface area when compared to monometallic Zn-ZIF-8. The common synthesis of hybrid ZIFs has generally been through slow diffusion techniques,[45-47] conventional hydrothermal,[48-50] and solvothermal methods,[43, 51-57] requiring several hours up to days of synthesis time. In addition, the yields of those synthesis protocols are often low, an economical issue for hybrid ZIFs to be used in a large industrial scale. Microwave-assisted synthesis has recently become popular in MOF synthesis as facile, rapid, inexpensive, and commercially viable routes toward the production of these compounds.[58] However, to the best of our knowledge there has not been any mixed metal or mixed linker ZIFs synthesized through microwave-based methods. Furthermore, there has been no report on *in-situ* synthesis of hybrid ZIFs with both mixed metal centres and mixed linkers.

Here, we report the rapid synthesis of a series of hybrid ZIFs with an SOD zeolitic topology using microwave irradiation: mixed metal ZIFs with Co and Zn metal centres, refer as CoZn-ZIF-8,[48, 50, 127] and mixed linker ZIFs with benzimidazole (ZIF-7 linker) and

2-methylimidazole (ZIF-8 linker), refer as ZIF-7-8.[53] The synthesis of ZIFs with both mixed metal and mixed linker has been reported previously.[69] However, it requires multiple steps of post-synthetic metal ion and linker exchange in the ZIFs. In this work, we report the first example of one-step synthesis of both mixed metal and linker ZIFs (with Co/Zn and 2-methylimidazole/benzimidazole, refer as CoZn-ZIF-7-8) through the microwave method. Hybrid ZIFs were synthesized in ~1.5 minutes under microwave power of ~ 100 W. A series of characterization tools were employed to confirm that hybrid ZIFs are phase-pure with the SOD ZIF-8 structure. In addition to drastically reduced synthesis time, the use of microwave irradiation produces higher yield and uniform crystal size,[146] reduces the use of expensive organic linker (for the mixed metal CoZn-ZIF-8 synthesis[48, 50]), and eliminates the use of deprotonators (i.e. sodium formate for the mixed linker ZIF-7-8 synthesis[53]) when compared to conventional method.

III.2. **Experimental**

III.2.1. ***Materials***

Zinc nitrate hexahydrate ($Zn(NO_3)_2 \cdot 6H_2O$, 98%, Sigma-Aldrich, hereafter ZnN) and cobalt nitrate hexahydrate ($Co(NO_3)_2 \cdot 6H_2O$, 98%, Sigma-Aldrich, hereafter CoN) were used as metal sources. 2-methylimidazole ($C_4H_5N_2$, 97%, Sigma-Aldrich, hereafter 2-mIm) and benzimidazole ($C_7H_6N_2$, 98%, Sigma-Aldrich, hereafter bIm) were used as linker sources. Methanol (99.8%, Alfa Aesar) and dimethylformamide (99.8%, Alfa Aesar, hereafter DMF) were used as solvents. All chemicals were used as purchased without further purification.

III.2.2. ***Microwave synthesis of mixed metal CoZn-ZIF-8***

A solution of (4.45 - x) mmol of ZnN and x mmol of CoN in 15 mL of methanol was prepared as a mixed metal solution. The value of x was varied from 0 to 4.45 to alter the ratio of Co/Zn in the metal solution. A separate solution of 17.8 mmol of 2-mIm in 15 mL of methanol was prepared as a linker solution. The metal solution was then poured to the linker solution while continuously stirring the solution for 1 min. The mixed solution was then transferred to a microwave-transparent glass tube and immediately followed by the microwave radiation with the power of 100 W for 1.5 min. The solution was then allowed to cool to room temperature by sitting on ambient for 30 min followed by centrifugation at 8000 RPM for 30 min. The precipitate was collected and dispersed in 30 mL of methanol and washed three times. The resulting powder was then dried in an oven at 120 °C for 12 hour prior to characterization.

III.2.3. ***Microwave synthesis of mixed linker ZIF-7-8***

A solution of 2.23 mmol of ZnN in 15 mL of DMF was prepared as a metal solution. A separate solution of (8.90 - x) mmol of 2-mIm and x mmol of bIm in 15 mL of methanol was prepared as a linker solution. The value of x was varied from 0 to 0.62 mmol. Similar to the synthesis of CoZn-ZIF-8, the metal solution was poured to the linker solution while continuously stirring the solution for 1 min. The mixed solution was then transferred to a microwave-transparent glass tube and immediately followed by the microwave radiation with the power of 100 W for 1.5 min. The solution was then allowed to cool naturally to room temperature for 30 min. To obtain the nanocrystal, the solution

was centrifuged at 8000 RPM for 30 min, the precipitate was dispersed in 30 mL of methanol and washed three times. The resulting powder was then dried in an oven at 220 °C for 12 hour prior to characterization.

III.2.4. ***Microwave synthesis of mixed metal and linker CoZn-ZIF-7-8***

A solution of 2.22 mmol of ZnN and 2.22 mmol of CoN in 15 mL of DMF were prepared as a metal solution. A separate solution of 16.7 mmol of 2-mIm and 1.07 mmol of bIm in 15 mL of methanol were prepared as a linker solution. The metal solution was then poured to the linker solution while continuously stirring the solution for 1 min. The mixed solution was then transferred to microwave-transparent glass tube and immediately followed by the microwave radiation with the power of 100 W for 1.5 min. The solution was then allowed to cool to room temperature by sitting on ambient for 30 min. To obtain the nanocrystal, the solution was centrifuged at 8000 RPM for 30 min, the precipitate was dispersed in 30 mL of methanol and washed three times. The resulting powder was then dried in an oven at 220 °C for 12 h prior to characterization.

III.2.5. ***Characterizations***

Powder X-ray diffraction (PXRD) was performed at room temperature on a Rigaku Miniflex II powder X-ray diffractometer using Cu-Kα radiation (λ = 1.5406 Å) which was scanned with a step size of 0.02°. Scanning electron micrographs were collected using a JEOL JSM-7500F operating at 5 keV acceleration voltage and 15 mm working distance. Elemental analyses were performed through Neutron Activation Analysis (NAA). The subsequent gamma-ray spectrometry was performed sequentially using a high-purity Ge

(HPGe) gamma-ray detector (Canberra Industries), and the data reduction was done using NAA software from Canberra Industries. Infra-red spectra were collected using a NICOLET IR100 FT-IR spectrometer. Pulverized Zn-ZIF-8, Co-ZIF-8, and CoZn-ZIF-8 particles were homogeneously mixed with KBr and pelletized for measurements. Nitrogen adsorption measurements were conducted using an ASAP 2000 (Micrometrics). The X-ray absorption spectroscopy (XAS) measurements such as the X-ray absorption near edge structure (XANES) and the extended X-ray absorption fine structure (EXAFS) at both Co K-edge and Zn K-edge were conducted by using the beamline 8C of Pohang Accelerator Lab in Korea. All samples were finely ground and densely packed onto Kapton tape for XAS data acquisition. The monochromatized X-ray from a double crystal monochromator with Si(111) crystals was used for the energy scan. The XAS spectra of samples were obtained at room temperature in transmission mode using an Ar/He ionization detector. Higher harmonic oscillation was removed by detuning the monochromator crystal by ~ 90%. To find an exact threshold energy for calibration, the XAS spectra were collected simultaneously with reference metal foils such as Co (7708.9 eV) and Zn (9658.6 eV) along with the samples. The data analysis was carried out by the standard procedure. The inherent backgrounds of XAS spectra were removed by fitting the polynomial to the entire region. The Fourier transforms (FTs) from the k^3-weighted EXAFS spectra were obtained by applying Hanning window in the range from 2.6 to 15.2 $Å^{-1}$. The thermal analyses were performed on a Mettler-Toledo TGA-DSC-1 with heating rate of 5 °C/min under continuous flow of argon at atmosphere.

III.3. **Results and analysis**

III.3.1. ***Mixed metal CoZn-ZIF-8***

Co_xZn_{1-x}-ZIF-8 was obtained rapidly through microwave synthesis, where x indicates the Co fraction with respect to total metal content in the synthesis solution. The incorporation of Co and Zn in the framework can be observed through direct optical observation on the color difference shown in Figure III-1a. ZIF with pure Zn (Zn-ZIF-8) exhibits white color while ZIF with pure Co (Co-ZIF-8, formally known as ZIF-67[46]) exhibits purple color, consequently making the mixed metal CoZn-ZIF-8 to reflect color in between these two colors.[48, 127] Neutron Activation Analysis (NAA) showed the mol% Co incorporated to the framework to be 18%, 30%, 45%, 64%, and 79% for $Co_{0.20}Zn_{0.80}$-ZIF-8, $Co_{0.33}Zn_{0.67}$-ZIF-8, $Co_{0.50}Zn_{0.50}$-ZIF-8, $Co_{0.67}Zn_{0.33}$-ZIF-8, and $Co_{0.80}Zn_{0.20}$-ZIF-8, respectively. This result agrees well with those reported previously using the conventional solvothermal method[48, 127] where the metal ratio in the synthesis solution resembles closely to the actual ratio in the framework. It is worth mentioning that the amount of linker used for the synthesis solution can be reduced significantly through microwave synthesis route (linker to metal ratio of ~ 4 for microwave irradiation compared to ~ 71.4 for conventional method[48]). The substantially reduced usage of expensive organic linker makes the microwave synthesis to be more economically viable.

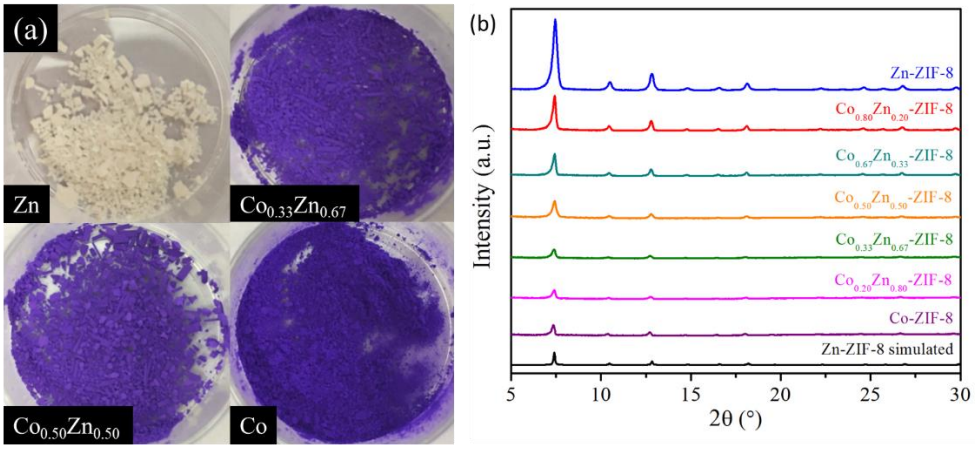

Figure III-1. (a) Photographs of Zn-ZIF-8, Co0.33Zn0.67-ZIF-8, Co0.50Zn0.50-ZIF-8, Co-ZIF-8; (b) Powder x-ray diffraction (PXRD) patterns of CoZnZIF-8 particles with various ratios of Co to Zn.

Figure III-1b shows the powder X-ray diffraction (PXRD) patterns of mixed metal CoZn-ZIF-8, in which several observations can be made. First, the mixed metal CoZn-ZIF-8 show the same XRD peaks of both Zn-ZIF-8 and Co-ZIF-8 confirming that they have a cubic unit cell in the I-43m space group which agrees to that reported previously.[48, 50, 100] Because Zn-ZIF-8 and Co-ZIF-8 are isostructural with a negligible difference in the unit cell dimension,[36] the Bragg angles of the peaks are more or less identical. Second, the XRD peak intensities of Co-ZIF-8 are notably lower than those of Zn-ZIF-8, even though the sample amounts and the crystallinity (judging from SEM/FT-IR/N_2 adsorption results presented in the following paragraphs) were more or less the same for both powders. This can be explained based on the fact that Co is fluorescent with Cu radiation, leading to the effective loss in the number of X-ray photons, thereby lowering the diffraction intensities, which leads to the systematic decrease of intensity peak with increasing Co/Zn ratio. The

decreasing trend of XRD peak intensities with increasing Co content could be used as a calibration tool for preliminary estimate on the Co content in the framework. The broad diffraction peaks of hybrid CoZn-ZIF-8 suggest that they are nano-sized crystals.

The size of these crystals was further confirmed by the electron micrographs as shown in Figure III-2(a-d). The nano-sized crystals and the uniformity of the crystal size owe likely to the homogenous volumetric heating in combination with rapid temperature rise under microwave irradiation.[146] Interestingly, Co-ZIF-8 crystals are significantly larger compared to Zn-ZIF-8 and mixed metal CoZn-ZIF-8. This may indicate that the nucleation of Co-ZIF-8 is less favorable under microwave irradiation when compared to Zn-ZIF-8.[147-148] To confirm the incorporation of both Co and Zn within the same framework of mixed metal CoZn-ZIF-8, elemental mapping through SEM coupled with energy dispersive X-ray spectroscopy (SEM-EDS) was taken and presented in Figure III-2e. The mapping on the crystal shows uniform distribution of Co and Zn throughout the CoZn-ZIF-8 framework.

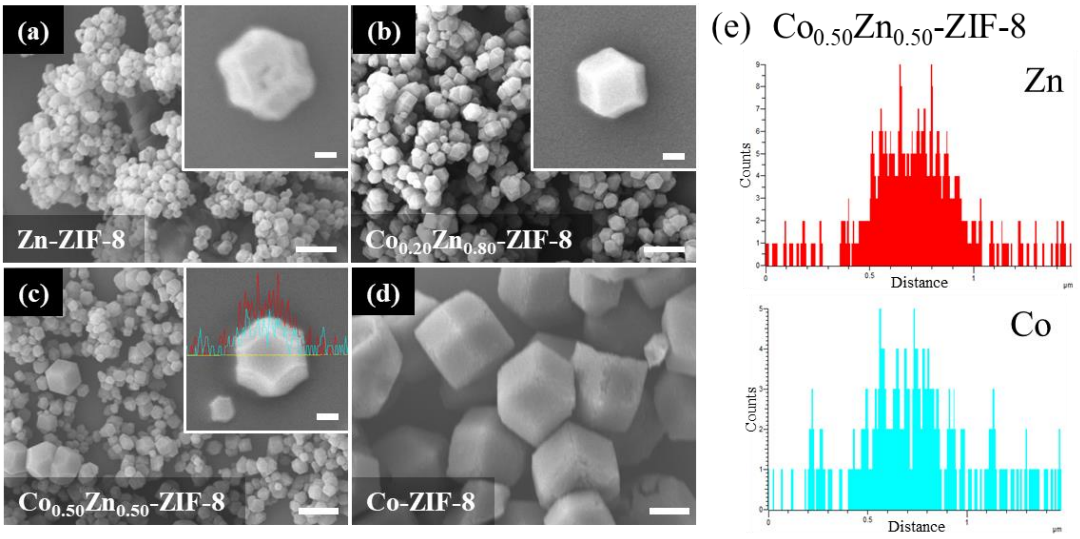

Figure III-2. Scanning electron microscopy (SEM) images of (a) Zn-ZIF-8, (b) $Co_{0.33}Zn_{0.67}$ZIF-8, (c) $Co_{0.50}Zn_{0.50}$ZIF-8, (d) Co-ZIF-8. All scale inside the white box is 100 nm, and outside white box is 1 μm. (e) SEM-EDS profile for $Co_{0.50}Zn_{0.50}$ZIF-8 crystal using line scanning method where yellow line in the inset of SEM image from (c) indicate the EDS analysis area.

As shown in Figure III-3, the FT-IR spectra show distinguishable and systematic shifts on M-N (metal-to-nitrogen) stretching frequencies with various Co/Zn contents. The stretching vibrations of Zn-N in pure Zn-ZIF-8 and Co-N in pure Co-ZIF-8 appear on IR band at ~421 cm^{-1} and ~425 cm^{-1}, respectively, consistent with the previous report.[36] As more Co incorporated to the hybrid CoZn-ZIF-8 system, M-N stretching frequencies are continuously blue-shifted as shown in Figure III-3. This implies that the stiffness of the M-N bonding can be tuned continuously by varying the ratio of Co to Zn. This ability to control the bond stiffness upon systematic incorporation of framework hetero-metal centers could potentially lead to tunable aperture sizes for the separations of gas mixtures of various size disparities. In addition, this systematic blue shift can provide another

preliminary means to estimate the content of Co incorporated to the framework. The M-N stretching frequency from the hybrid CoZn-ZIF-8 was compared to the physical mixture of Co-ZIF-8 and Zn-ZIF-8 with the same metal ratio. Interestingly, the physical mixture exhibits less symmetrical M-N stretching frequency than the hybrid one, which may arise from the superposed signal of Co-N and Zn-N vibrations as opposed to the true hybrid M-N vibrations.

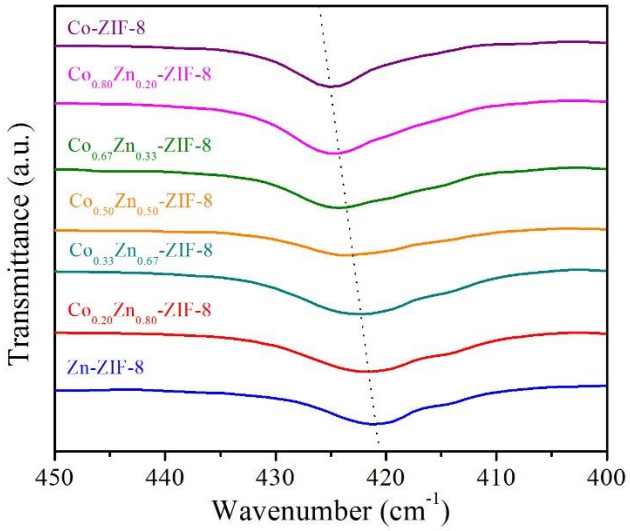

Figure III-3. FT-IR spectra showing stretching vibrations of metal to nitrogen on CoZn-ZIF-8 with various ratios of Co to Zn.

Nitrogen physisorption analysis showed type I isotherms for the hybrid CoZn-ZIF-8, which is similar to the Zn-ZIF-8 and Co-ZIF-8 as shown on Figure III-4. The micropore volume and estimated Brunauer-Emmet-Teller (BET) surface area were determined as presented in

Table **III-1**. The BET surface area for the Zn-ZIF-8 (1202 m^2/g) is within the range of the reported values.[149] Interestingly, the BET surface area for the mixed metal ZIF samples is similar to the ZIF parent. This observation is different from the previously reported result[48] where the $Co_{0.50}Zn_{0.50}$-ZIF-8 shows noticeably higher surface area. However, our finding in the similarity of surface area among the mixed metal samples can be reasoned as follows. Co-ZIF-8 and Zn-ZIF-8 are isostructural and the difference of Co^{2+} and Zn^{2+} ionic radii is small (~ 0.02 Å). Therefore, the pore volume and surface area of mixed metal CoZn-ZIF-8 may not vary much from their ZIF parents, Zn-ZIF-8 and Co-ZIF-8.

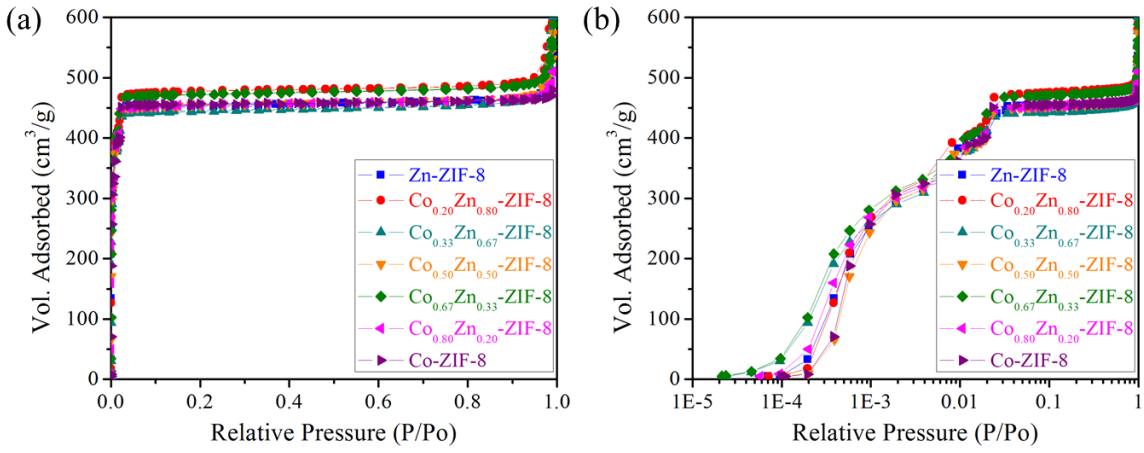

Figure III-4. Nitrogen physisorption isotherm of CoZnZIF-8 with various Co/Zn content at 77 K (a) with the linear scale x-axis, and (b) with the log scale x-axis.

Table III-1. Comparison of micropore volume and BET surface area of mixed metal CoZn-ZIF-8

	Micropore Volume (cm^3/g)	Surface Area (m^2/g)*
Zn-ZIF-8	0.688	1202.3
Co0.20Zn0.80-ZIF-8	0.716	1295.2
Co0.33Zn0.67-ZIF-8	0.667	1207.8
Co0.50Zn0.50-ZIF-8	0.681	1232.6
Co0.67Zn0.33-ZIF-8	0.711	1281.3
Co0.80Zn0.20-ZIF-8	0.684	1231.1
Co-ZIF-8	0.694	1235.0

*BET surface area

The thermal stability of the mixed metal CoZn-ZIF-8 was analyzed using thermogravimetric analysis (TGA) under inert argon gas up to 800 °C (see Figure III-5). Zn-ZIF-8 was shown to be stable up to 500 °C, which is more stable than Co-ZIF-8 that only withheld up to 350 °C. These values agree within the range of the reported values.[29, 150] Due to these differences, the thermal stability of the mixed metal CoZn-ZIF-8 can be anticipated to fall between the two ZIF parents. The stability of CoZn-ZIF-8 can be improved continuously by incorporating more Zn into the framework.

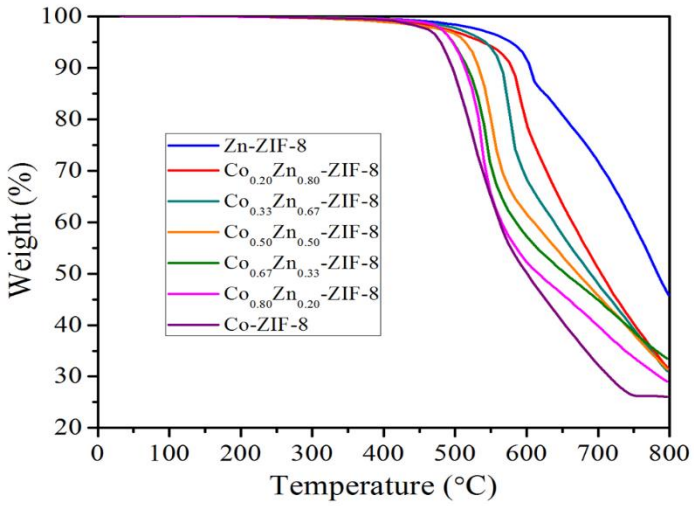

Figure III-5. Thermogravimetric analysis on mixed metal CoZn-ZIF-8 with various ratios of Co to Zn.

III.3.2. ***Mixed linker ZIF-7-8***

The microwave synthesis was also applicable for the synthesis of mixed linker ZIF-7-8 (mixture of 2-methylimidazole and benzimidazole). From the results previously reported,[53] it is noted that the relative amount of linker mixture incorporated in the framework is not the same as the synthesis solution. It was assumed that the linker incorporation to the framework using microwave synthesis is similar to the one reported using conventional solvothermal method.[53] One apparent advantage of using microwave irradiation is the rapid synthesis of ZIF-7-8 in ~1.5 minute compared to the long 48 hour synthesis for the conventional method.[53] Furthermore, the yield obtained using the microwave method is increased by ten-fold (the yields for conventional and microwave methods are 0.5% and 5% with respect to the zinc salt, respectively). Interestingly, the use of a deprotonator is unnecessary for the microwave synthesis, which was an important

parameter for the conventional method.[53] Our hypothesis is that the microwave irradiation results in localized hot spots where the local temperature is much higher than bulk temperature, enhancing deprotonation of linkers and thereby improving the formation of crystals.

Due to the difference in the structures of ZIF-7[29] (a rhombohedral R-3 space group) and ZIF-8[29] (a cubic I-43m space group), the PXRD pattern of hybrid ZIF-7-8 can be distinguishable from the ZIF parent. However, these differences only exist at the incorporation of a significant amount of the benzimidazole linker in the framework. Figure III-6a shows the PXRD patterns of the ZIF-7-8 with various ratios of 2-mIm to bIm. The ZIF-7-8 with bIm incorporation up to 20% in the framework retains most of its structure with the cubic unit cell in the I-43m space group of ZIF-8, which agrees with that reported previously.[53] SEM images in Figure III-6b-c showed that the mixed linker ZIF-7-8 crystals are micro-sized, much larger than the ones reported using conventional method.[53] This indicates that the microwave synthesis route for mixed linker ZIF-7-8 leads to faster crystal growth when compared to the conventional method. Faster crystal nucleation and crystal growth has also been previously observed for the synthesis of Zn-ZIF-8 with microwave irradiation when compared to conventional hydrothermal synthesis.[151]

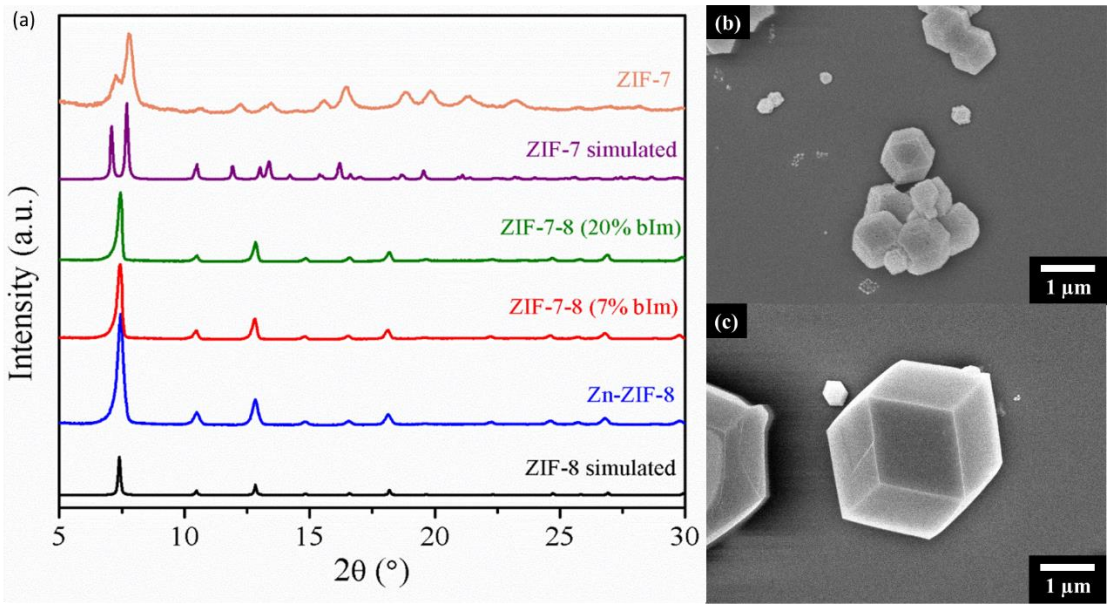

Figure III-6. (a) Powder x-ray diffraction (PXRD) pattern of ZIF-7-8 with various amount of benzimidazole incorporation. SEM images of ZIF-7-8 with (b) 7% bIm incorporation and (c) 20% bIm incorporation.

The N_2 isotherms presented in Figure III-7 show that replacing 2-mIm linker with bIm linker led to the reduction in pore volume, agreeing with that reported.[53] This can be explained by the bulkier bIm linker when compared to 2-mIm blocking some of the pore for the mixed linker ZIF-7-8 to be adsorbed by nitrogen. The BET surface area for the ZIF-7-8 with 7% bIm and 20% bIm incorporation were determined to be 1150.1 m^2/g and 771.8 m^2/g, respectively.

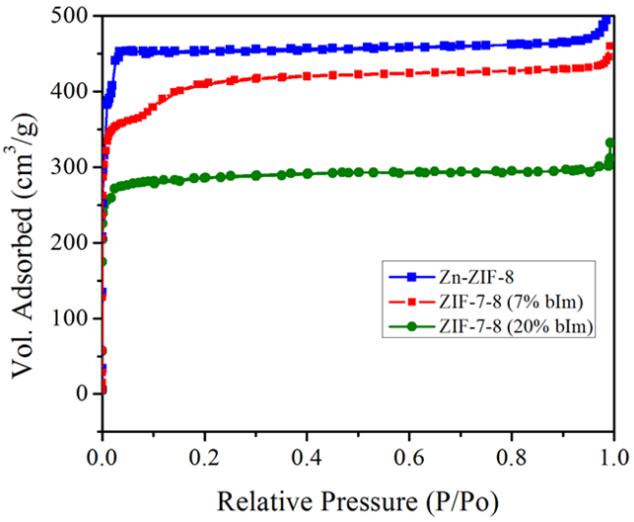

Figure III-7. Nitrogen physisorption isotherm of ZIF-7-8 with various bIm content at 77 K

III.3.3. ***Mixed metal and mixed linker CoZn-ZIF-7-8***

The microwave synthesis applicability can be extended to produce hybrid ZIF with both mixed metal and mixed linker. Here, we synthesized hybrid ZIF with mixed metal consisting of Co and Zn with ratio of 1 to 1 and mixed linker comprising of 2-mIm and bIm (with 20% bIm incorporated to the framework). Interestingly, in the presence of mixed linker 2-mIm and bIm, the ratio of Co to Zn in the framework is reduced. While the ratio of Co and Zn in the synthesis solution is the same for both CoZn-ZIF-7-8 and $Co_{0.50}Zn_{0.50}$ZIF-8, NAA showed the amount of Co incorporated with respect to total metal is 36% for CoZn-ZIF-7-8 compared to 45% for the $Co_{0.50}Zn_{0.50}$ZIF-8.

As mentioned previously, both $Co_{0.50}Zn_{0.50}$ZIF-8 and ZIF-7-8 (with 20% bIm incorporation) retain the SOD topology of its ZIF parent (ZIF-8) with cubic unit cell in I-

43m space group. Therefore, it can be expected that the PXRD pattern of hybrid ZIF with mixed metal (Co to Zn ratio of 1 to 1) and mixed linker (with 20% bIm incorporation) to exhibit the same typical I-43m space group as shown in Figure III-8a. Electron micrograph shows well-developed CoZn-ZIF-7-8 crystals with the size of ~ 2 µm as exhibited in Figure III-8b. Elemental mapping and line scanning on the CoZn-ZIF-7-8 crystal with EDS-SEM presented in Figure III-8b display the uniform distribution of both Co and Zn throughout the crystal.

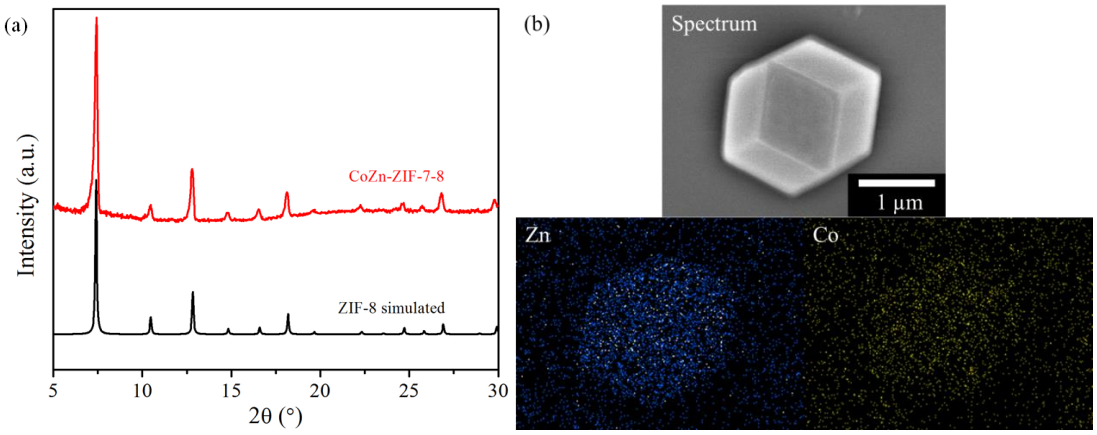

Figure III-8. (a) Powder x-ray diffraction (PXRD) pattern of CoZn-ZIF-7-8 with Co to Zn ratio of 1 to 1 and 20% bIm incorporated to the framework and (b) SEM-EDS elemental mapping of CoZn-ZIF-7-8 (Co to Zn ratio of 1 and 20% bIm).

From the previous nitrogen physisorption analyses on both CoZn-ZIF-8 and ZIF-7-8, mixing Co and Zn in the same framework does not alter the isotherm, while replacing 2-mIm with bIm leads to reduction of pore volume. Therefore, it can be anticipated that the CoZn-ZIF-7-8 isotherm to exhibit similar behavior as the ZIF-7-8 with 20% bIm

incorporation as shown in Figure III-9. The BET surface area of CoZn-ZIF-7-8 was determined to be 822.5 m^2/g, a comparable value to ZIF-7-8 with 20% bIm of 771.8 m^2/g. The CoZn-ZIF-7-8 also exhibits C=C stretching vibration from benzene ring (~1456 cm^{-1}) and C-H bending vibration of ortho-disubstituted benzene (~745 cm^{-1}) from bIm linker (Figure III-10a).[152-154] In addition, the IR-band corresponding to the M-N frequencies for CoZn-ZIF-7-8 (~ 422.3 cm^{-1}) appear between the Zn-N (~ 421.4 cm^{-1}) and Co-N (~ 425.2 cm^{-1}) indicating the incorporation of both Co and Zn in the framework (Figure III-10b).[36]

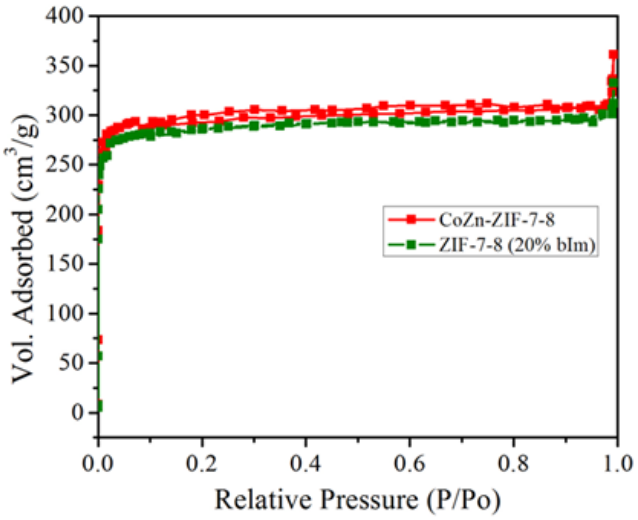

Figure III-9. Comparison of nitrogen physisorption on mixed metal and linker CoZn-ZIF-7-8 (Co to Zn ratio of 1 and 20% bIm) with ZIF-7-8 (20% bIm).

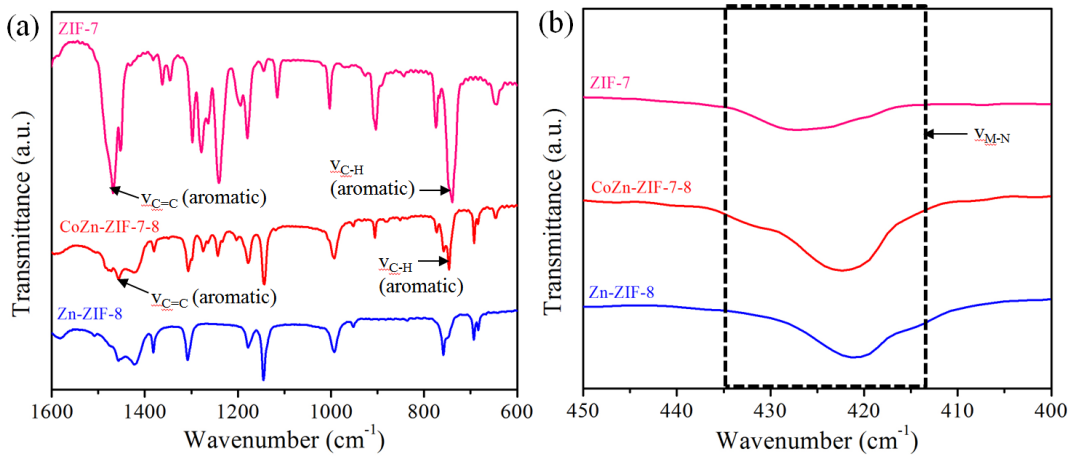

Figure III-10. FT-IR spectra comparing ZIF-7, Zn-ZIF-8, and CoZn-ZIF-7-8 from (a) 600 to 1600 cm-1 and (b) 400 to 450 cm-1. Note that ZIF-7 consists of Zn metal and pure bIm linker.

III.4. **Conclusions**

Mixed metal CoZnZIF-8 with various Co/Zn contents and mixed linker ZIF-7-8 with various bIm incorporation were rapidly synthesized using microwave irradiation method. In addition, the first example of one-step synthesis of mixed metal and linker CoZn-ZIF-7-8 was successfully obtained using the microwave irradiation. Other than the short synthesis time, crystallization using microwave irradiation produced higher yield, reduced the amount of linker and solvent, and eliminated the use of deprotonators when compared to conventional methods.[48, 50, 53-54, 100] Mixed metal CoZn-ZIF-8 retained the SOD topology from its ZIF parent for any Co to Zn ratio. Elemental mapping using Energy-dispersive X-ray spectroscopy (EDS) and electronic/geometric information obtained from X-ray absorption spectroscopy (XAS) confirmed the uniform distribution of tetrahedral Co and Zn metal centers within the same framework of the mixed-metal

ZIF. The metal to nitrogen (M-N) stretching frequencies on IR band were observed to be blue-shifted systematically as the Co/Zn ratio in mixed metal ZIFs increases.

CHAPTER IV

LINKER-DOPED ZEOLITIC-IMIDAZOLATE FRAMEWORKS AND THEIR ULTRATHIN MEMBRANES FOR TUNABLE GAS SEPARATIONS*

IV.1. **Introduction**

In general, hybrid ZIFs are required to maintain the topology/structure of their parent ZIFs (i.e., mono-metal and mono-linker) while varying the metal and/or linker ratio in the hybrid framework, thus enables tuning of their properties in a controlled manner. Intuitively, mixing isostructural ZIFs leads to formation of hybrid ZIFs while maintaining its topology.[41-44, 53] For example, both of the mixed-metal CoZn-ZIF-8 and CdZn-ZIF-8 are isostructural ZIF-8 analogues, possessing the same SOD topology of their parent ZIFs: ZIF-8, ZIF-67 (Co-substituted ZIF-8),[46] and CdIF-1 (Cd-substituted ZIF-8).[155] The same applies for the mixed-linker ZIF-8-90 retaining its cubic structure regardless of the ratio of the linkers. Mixed-linker ZIF-8-90 is a combination of ZIF-8[29] and ZIF-90 (ZIF-8 with Ica linker),[71] both possessing the same SOD topology. This strategy to obtain isostructural hybrid ZIFs, however, limit the option of metal centers and linkers that can be mixed. Table IV-1 shows the short list of reported Zn-based SOD ZIFs with various imidazolate linkers that were *de novo* synthesized.

**This chapter was adapted with permission from Febrian Hillman and Hae-Kwon Jeong, ACS Appl. Mater. Interfaces, submitted 2019.*

Table IV-1. List of Zn-based SOD ZIFs bridged by various imidazolate linkers de novo synthesized.

Nomenclature	Composition	Type of linker	Crystal family
ZIF-8[64] (or MAF-4)	$Zn(2\text{-}mIm)_2$	2-methylimidazole	Cubic
ZIF-7[29]	$Zn(bIm)_2$	Benzimidazole	Hexagonal
ZIF-90[29]	$Zn(Ica)_2$	Imidazole-2-carboxaldehyde	Cubic
MAF-7[44]	$Zn(mtz)_2$	3-methyl-1,2,4-triazole	Cubic
SIM-1[156]	$Zn(mcIm)_2$	4-methyl-5-imidazolecarboxaldehyde	Cubic
-[32]	$Zn(cIm)_2$	2-chloroimidazole	Cubic
-[32]	$Zn(brIm)_2$	2-bromoimidazole	Cubic

Mixing non-isostructural ZIFs can often lead to crystal systems different from the parent, likely presenting a challenge in predicting and obtaining the desired property change on the hybrid frameworks. For example, Huang et al.[64] attempted to mix SOD ZIF-8 and ANA ZIF-4 ($Zn(2\text{-}eIm)_2$, 2-eIm = 2-ethylimidazole). They reported that a precursor synthesis solution containing an equal molar mixture of 2-mIm and 2-eIm yielded crystals with a physical mixture of ZIF-8 and a new phase with RHO topology. No hybrid crystals were obtained possessing either of the parent's SOD or ANA topology. Furthermore, Schoenmakers[90] also reported that substituting Zn^{2+} ions in ZIF-8 framework with Cu^{2+} ions led to structural change due to the disruption of originally tetrahedral coordination of Zn^{2+} in ZIF-8 by the Cu^{2+} with octahedral coordination preference. Both 2-eIm linker and Cu^{2+} ions can be seen as "unsuitable" linker and ions for the formation of the SOD cubic structure of ZIF-8. Despite the unsuitability of Cu^{2+} nature, Schejn et al.[93] have successfully incorporated small amount of copper (known as copper doping) into ZIF-8 while preserving the cubic $I\bar{4}3m$ space group. Yang et al.[95] have also reported copper

doping into ZIF-67. Although copper ions are only doped at a small concentration into ZIF-8 or ZIF-67, both reports have shown that the copper-doped framework increases the catalytic activity and improves various gases uptake capacities. While Huang et al.[64] have attempted to incorporate 2-eIm linker to ZIF-8 at a relatively high concentration, there is no follow-up work on the attempt to incorporate the "unsuitable" 2-eIm linker at a smaller concentration (hereafter termed linker-doping) to obtain hybrid ZIFs (i.e., doped ZIFs) while retaining the parent ZIF structures.

Here, we report, for the first time, the doping of "unsuitable" secondary linkers to ZIF-8 so as to obtain mixed-linker hybrid ZIFs while preserving its SOD cubic structure. Two secondary linkers were investigated for this study: 2-ethylimidazole (2-eIm) and 2-phenylimidazole (2-phIm). A microwave-assisted technique was utilized to rapidly synthesize eIm-doped (referred as eIm/ZIF-8) and phIm-doped (referred as phIm/ZIF-8) ZIF-8 analogues in the $I\bar{4}3m$ space group. Resulting hybrid ZIFs were thoroughly characterized using a battery of techniques including XRD, ^{1}H-NMR, ATR-FT-IR, N_2 adsorption, and SEM. Gas adsorption studies revealed the linker-doping strategy affected the "gate-opening" behavior of parent ZIF-8. Finally, we have also prepared polycrystalline eIm/ZIF-8 membranes on α-Al_2O_3 supports using microwave-assisted seeding[33] and secondary growth methods.[30] Two effects were observed from the doping of 2-eIm on ZIF-8 membranes: 1) the incorporation of 2-eIm led to formation of thinner membranes than mono-linker ZIF-8 membranes; 2) the eIm/ZIF-8 membranes showed an

improved propylene and propane permeance at the expense of propylene/propane separation factor as compared to ZIF-8 membranes.

IV.2. **Experimental**

IV.2.1. ***Materials***

Zinc nitrate hexahydrate ($Zn(NO_3)_2 \bullet 6H_2O$, 98%, Sigma-Aldrich, hereafter ZnN) was used as a metal source. 2-methylimidazole ($C_4H_5N_2$, 97%, Sigma-Aldrich, hereafter 2-mIm), 2-ethylimidazole ($C_5H_8N_2$, 98%, Sigma-Aldrich, hereafter 2-eIm), and 2-phenylimidazole ($C_9H_8N_2$, 98%, Sigma-Aldrich, hereafter 2-phIm) were used as linker sources. Sodium formate (HCOONa, 99%, Sigma-Aldrich) was used as a deprotonating agent. Methanol (99.8%, Alfa Aesar) was used as a solvent. Acetic acid-d4 (CD_3CO_2D, 99.5 atom % D, Sigma-Aldrich) was used as a reference for ^{1}H-NMR analyses. All materials were used as purchased without further purification.

IV.2.2. ***Microwave synthesis of ZIF-8, eIm/ZIF-8, and phIm/ZIF-8***

For the synthesis of eIm/ZIF-8, a solution of 4.44 mmol of ZnN in 15 mL of methanol was prepared as a metal solution. A separate solution of (17.8 - x) mmol of 2-mIm and x mmol of 2-eIm in 15 mL of methanol was prepared as a linker solution. The value of x was varied from 0 to 17.8 (x = 0 for pure ZIF-8). The metal solution was then poured into the linker solution while continuously stirring the linker solution for 1 min. The mixed solution was then transferred to a microwave-inert glass tube, immediately followed by microwave irradiation with the power of 100 W for 90 seconds. The solution was then allowed to cool to room temperature by keeping it under ambient conditions for

30 min followed by centrifugation at 8000 RPM for 20 min. The precipitates were collected and dispersed in 30 mL of methanol and washed three times with fresh methanol. The resulting powder was then dried in an oven at 60 °C for 2 days prior to characterization. For the synthesis of phIm/ZIF-8, the procedure is the same as eIm/ZIF-8 except that 2-phIm is used as the secondary linker.

IV.2.3. ***Preparation of porous α-Al_2O_3 substrates***

Disk-shaped alumina substrates (porosity = ~ 46 %, diameter = 22 mm, and thickness = 2 mm) with an average pore diameter of ~ 200 nm were prepared by a pressing and sintering method slightly modified from a previously reported method.[33] Briefly, α-Al_2O_3 power (CR6, Baikowski) was molded into a disk shape by uniaxial pressing and was sintered at 1100 °C for 2 h. Then one side of the sintered disks was polished using a sand paper (grid #1200) to reduce the surface roughness of the substrates, followed by sonication for 1 min in methanol. Subsequently the supports were dried in an oven at 120 °C for 1 h before usage.

IV.2.4. ***Preparation of eIm/ZIF-8 seed layers and membranes***

an eIm/ZIF-8 seed layer on an α-Al_2O_3 substrate was prepared using the microwave-assisted method previously reported by our group[33] with a slight modification. The secondary growth of the eIm/ZIF-8 seed layer was carried out using a method similarly reported by Pan et al[37] with some modification. Briefly, 9.19 mmol of ZnN was dissolved in 45 mL methanol (solution A). A separate solution of (31.6 - x) mmol of 2-mIm and x mmol of 2-eIm were dissolved in 30 mL methanol (solution B). The value of

x was varied from 1.6 to 4.7 mmol. An α-Al_2O_3 disk was immersed in the solution A for 1 h to saturate the substrate with the metal solution. The saturated substrate was then held vertically using a home-made Teflon holder and immediately inserted into the solution B in a microwave-inert glass tube, followed by microwave irradiation with the power of 100 W for 1.5 min. Finally, the tube was naturally cooled down for 30 min and the seeded support was washed in 30 ml of methanol under gentle rocking for 18 h and dried at 60 °C for 4 h. For the secondary growth, an aqueous growth solution was prepared by pouring a metal solution of 0.37 mmol of ZnN in 20 mL of DI water to a linker solution of (27.7 – x) mmol of 2-mIm and x mmol of 2-eIm in 20 mL water, followed by continuous mixing for 1 min. The value of x was varied from 1.4 to 4.2 mmol. The seeded support was immersed vertically in the aqueous growth solution and kept in an oven at 30 °C for 24 hr. The membrane was washed in fresh methanol under stirring for 2 days while replenished with fresh methanol every 12 hours. The sample was dried at room temperature for 24 hr before further characterization. For comparison, mono-linker ZIF-8 membranes were prepared using microwave-assisted seeding and secondary growth as previously reported.[30, 33]

IV.2.5. ***Characterizations***

X-ray diffraction (XRD) was performed at room temperature on a Rigaku Miniflex II powder X-ray diffractometer using Cu-Kα radiation (λ = 1.5406 Å) which was scanned with a step size of 0.02°. Scanning electron micrographs were collected using a JEOL JSM-7500F operating at 5 keV acceleration voltage and 15 mm working distance. Infra-

red spectra were collected using a Nicolet IS5 from Thermo Scientific, equipped with a single reflection diamond attenuated total reflectance (ATR) attachment (ID5). Gas (N_2, CO_2, and CH_4) adsorption measurements were conducted using an ASAP 2010 (Micromeritics). Prior to adsorption measurements, the samples were further activated at 150 °C under vacuum for 24 h. Thermal analyses were performed in a Mettler-Toledo TGA/DSC 1 at a rate of 5 °C min^{-1} with an argon flow of 20 mL min^{-1}. Composition analyses of the linker ratio in linker-doped eIm/ZIF-8 and phIm/ZIF-8 powder and eIm/ZIF-8 membranes were determined through solution proton nuclear magnetic resonance (^{1}H-NMR) spectra taken from a Bruker Avance III (500 MHz system). For powder samples, ~ 5 mg of a sample was dissolved in 600 μL of deuterated acetic acid-d4. The acidic solution was then used for the ^{1}H-NMR analysis to determine the mIm-to-eIm and mIm-to-phIm linker ratio from each powder sample. For membrane samples, a well activated eIm/ZIF-8 membrane was submersed in 800 μL of deuterated acetic acid-d4 for 2 days. The acetic acid-d4 solution containing 2-mIm and 2-eIm linkers was then used for the ^{1}H-NMR analysis to determine the mIm-to-eIm linker ratio from each membrane sample.

IV.2.6. ***Permeation measurements***

The gas separation performance of eIm/ZIF-8 membranes were performed using the Wicke-Kallenbach technique under atmospheric pressure at room temperature (298 K). The equal-molar mixture of propylene and propane was supplied to the feed side while the permeate side was swept by argon with the total flow rates of both sides maintained at

100 mL min^{-1}. The gas composition of the permeate side was analyzed using a gas chromatograph (Agilent GC 7890A equipped with a HP-PLOT/Q column).

IV.3. **Results and analysis**

IV.3.1. ***Synthesis and analysis of eIm/ZIF-8 and phIm/ZIF-8 powder***

Two linker-doped ZIF-8 analogues with dopant linkers of 2-ethylimidazole (2-eIm) and 2-phenylimidazole (2-phIm) were obtained rapidly under ~ 90 seconds using the microwave-assisted synthesis. The amount of doped linker in the precursor solution was varied from 0, 5, 10, 15, 20, 50, and 100 %. However, the eIm/ZIF-8 was successfully synthesized up to 50% of 2-eIm, whereas the phIm/ZIF-8 can only be obtained up to 20% of 2-phIm in the precursor solution. The amount of a dopant linker that is actually incorporated in the framework was found much less than that in the starting precursor solution, which will be discussed later in more detail. Interestingly, the eIm/ZIF-8 can be synthesized with higher dopant incorporation than the phIm/ZIF-8. It is presumed that the bulkier phenyl group in the 2-position of 2-phIm linker as compared to the ethyl group of 2-eIm linker might likely distort the tetrahedral $Zn(L)_2$ (L: linker) units more significantly, thereby less incorporation while maintaining a SOD structure. In a recent report,[157] 2-phIm linker has been incorporated into ZIF-8 framework through solvent assisted linker exchange approach (known as SALE[65], two-step synthesis). Despite the long exchange process of 168 hours, only ~ 10% of 2-mIm has been successfully substituted with 2-phIm linker,[157] showing the "unsuitability" of 2-phIm linker in the SOD cubic structure of ZIF-8.

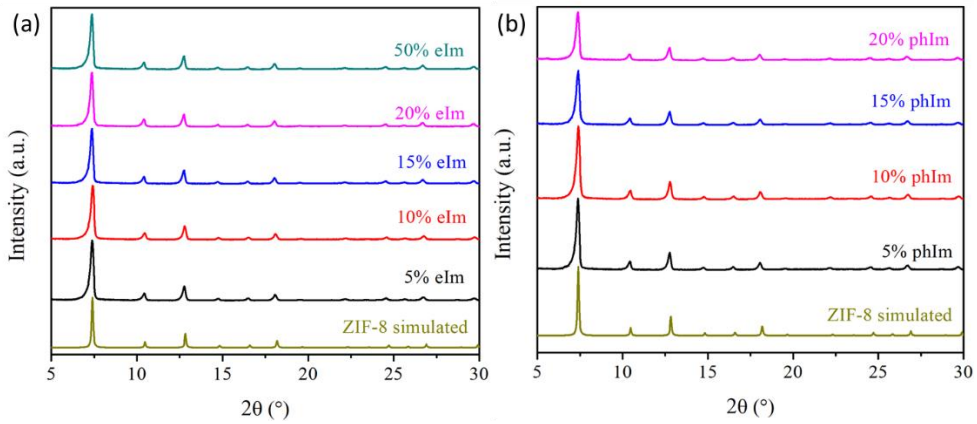

Figure IV-1. Powder X-ray diffraction (XRD) patterns of (a) eIm/ZIF-8 with various 2-eIm concentrations, and (b) phIm/ZIF-8 with various 2-phIm concentrations. Both 2-eIm and 2-phIm concentrations are in the precursor solution.

Figure IV-1 presents powder X-ray diffraction (XRD) patterns of the linker-doped eIm/ZIF-8 and phIm/ZIF-8 particles with various amounts of the secondary linkers in the precursor solutions. All of the synthesized eIm/ZIF-8 and phIm/ZIF-8 particles show phase pure crystalline structures and retain the cubic unit cell in the $I\bar{4}3m$ space group of ZIF-8. Unlike the common hybrid approach by Huang et al.,[64] the linker-doping strategy can, in principle, successfully incorporate any dopant imidazolate linker while maintaining the parent structure. The amount of a dopant linker incorporated is, however, likely dependent upon the type of a dopant (i.e., size and pKa). Figure IV-2 and Figure IV-3 present scanning electron micrographs, showing the particle sizes and morphologies of eIm/ZIF-8 and phIm/ZIF-8 powders at different dopant linker incorporations in comparison with those of ZIF-8. All crystals exhibit the typical rhombic dodecahedral morphology similar to that of ZIF-8 particles. Interestingly, the size of crystals increases

with more 2-eIm incorporation which is less pronounced with 2-phIm. The presence of dopant linkers may hamper the rate of nucleation, thereby promoting the growth of larger crystals.

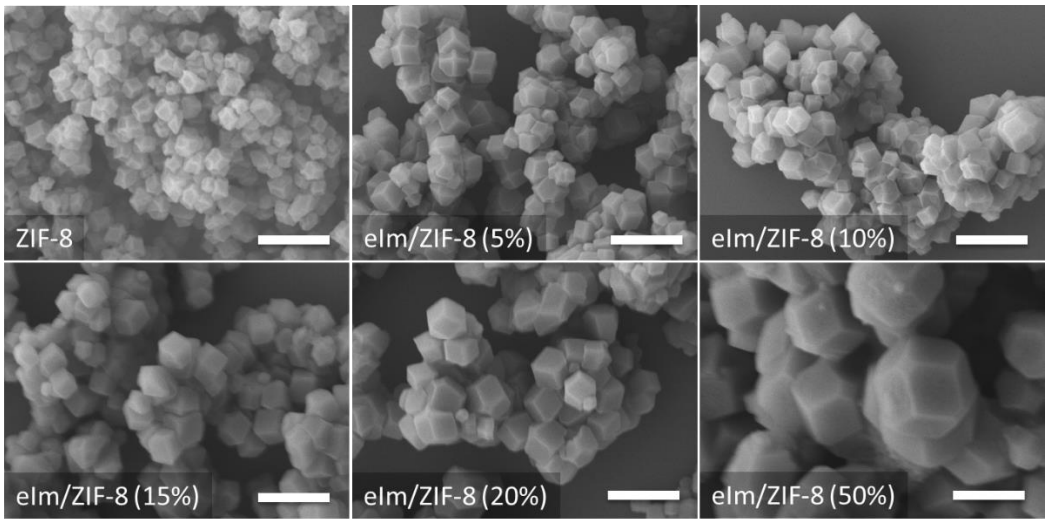

Figure IV-2. Scanning electron microscope (SEM) images of pristine ZIF-8 and eIm/ZIF-8 with various 2-eIm concentrations in the precursor solution as indicated within parentheses. All scale bars are 1 μm.

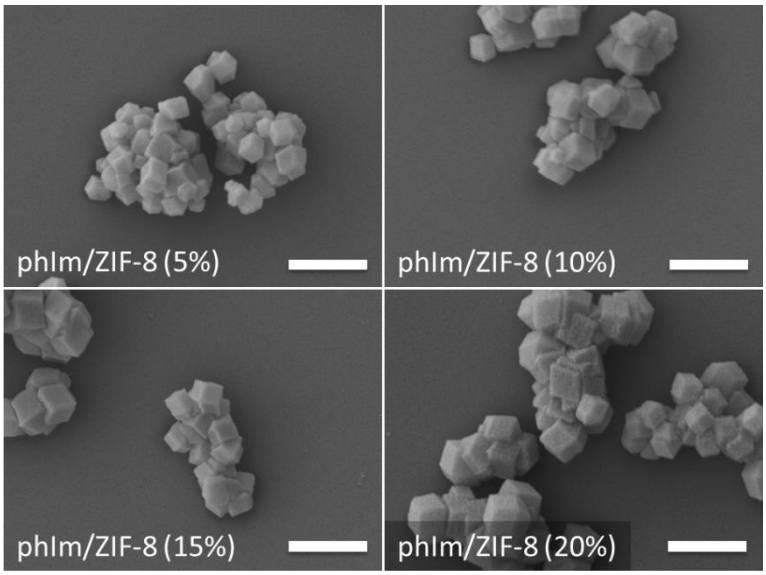

Figure IV-3. Scanning electron microscope (SEM) images of phIm/ZIF-8 with various 2-phIm concentrations in the precursor solution as indicated within parentheses. All scale bars are 1 μm.

The FT-IR spectra as shown in Figure IV-4 confirm the existence of dual linkers within the linker-doped ZIF-8 frameworks. The incorporation of 2-eIm into ZIF-8 adds the appearance of CH_2 in-plane rocking vibration signal (~ 1057 cm^{-1}) and asymmetric CH_2 vibration (~2970 cm^{-1})[158] to the IR spectra, in which their intensities increase with greater amount of 2-eIm used in the precursor solution (see Figure IV-4a). The phenyl ring gives additional IR signals from aromatic C-H stretching vibration (~3044 cm^{-1}) and in-plane C-H bending vibration (~1072 cm^{-1})[159] as shown in Figure IV-4b. The weak intensity from the aromatic phenyl ring may suggest the small incorporation of 2-phIm into ZIF-8 framework. Interestingly, the vibration from Zn to nitrogen (ν_{Zn-N}) bonding were found blue shifted with the incorporation of either 2-eIm or 2-phIm into the

framework, suggesting the increase in stiffness in the Zn—N bonding of the linker-doped ZIF-8 framework[36, 42] as shown in Figure IV-5.

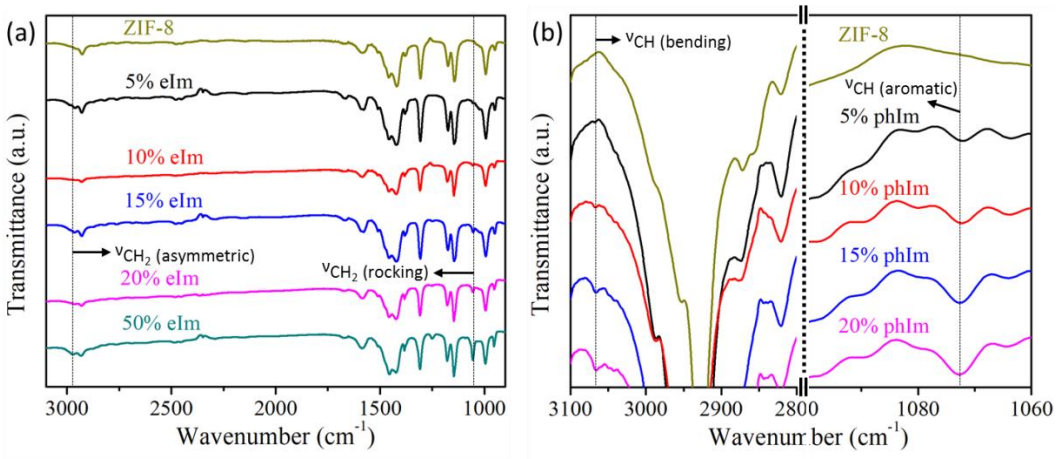

Figure IV-4. FT-IR spectrum for (a) eIm/ZIF-8 with the appearance of CH2 in-plane rocking vibration signal (~ 1057 cm-1) and asymmetric CH2 vibration (~2970 cm-1), and (b) phIm/ZIF-8 with the additional in-plane C-H bending vibration (~1072 cm-1) and aromatic C-H vibration (~3044 cm^{-1}).

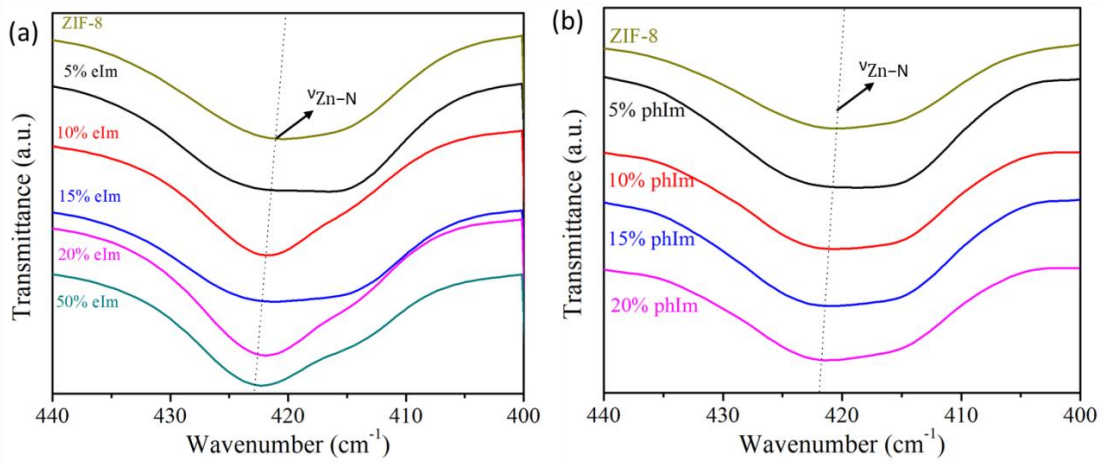

Figure IV-5. FT-IR spectrum showing blue shift on stretching vibrations of Zn-N with the incorporation of (a) 2-eIm linker and (b) 2-phIm linker into ZIF-8.

The actual dopant amounts in the frameworks were determined through solution ^{1}H-NMR as shown in Figure IV-6. For eIm/ZIF-8, the ethyl moiety from the 2-eIm linker gives two signals on the NMR spectra: a quadruplet from the –CH_2– and a triplet from the –CH_3– proton located at ~ 3.1 and ~ 1.4 ppm, respectively. The strong singlet peak at ~ 2.7 ppm belongs to the methyl moiety from the 2-mIm linker. For phIm/ZIF-8, the benzylic protons are all clustered into the multiplet in ~ 7.6 ppm region. Figure IV-7 shows the relationship between the fraction of doping linker used in the precursor solution versus the corresponding fraction that is actually incorporated in the framework of ZIF-8. Both 2-eIm and 2-phIm are incorporated into the framework at much lower fraction than they are present in precursor solution. The eIm/ZIF-8 samples synthesized with precursor solutions containing 5, 10, 15, 20, and 50% 2-eIm are determined to form doped hybrid ZIFs with 2-eIm concentration of approximately 2, 3, 5, 7, and 25%, respectively. The phIm/ZIF-8 powders obtained with precursor solutions containing 5, 10, 15, 20% 2-phIm are found with 2-phIm concentration in doped ZIFs of approximately 1, 2, 4, and 5%, respectively. The low incorporation of these secondary linkers can be expected as their bulkier nature than 2-mIm renders unfavorable incorporation into ZIF-8 crystals with SOD topology.

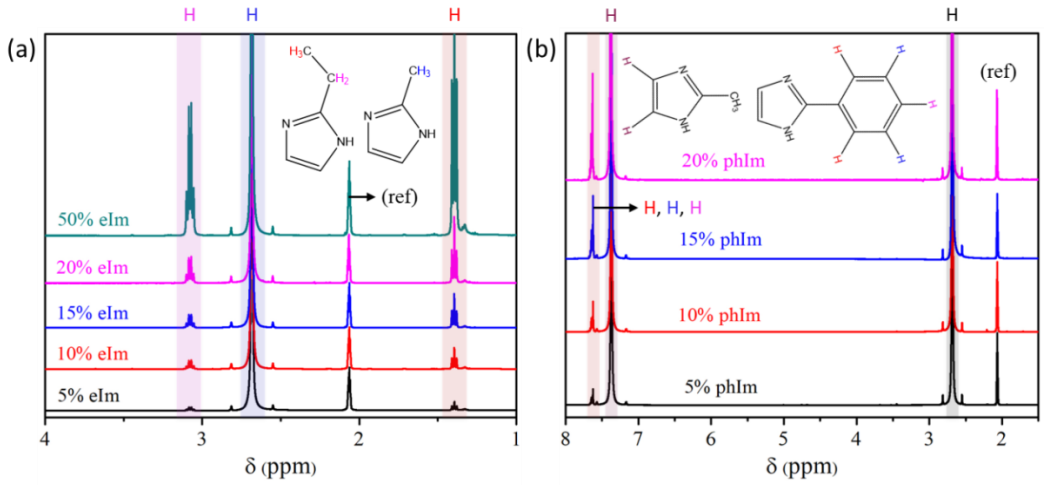

Figure IV-6. 1H-NMR spectrum of (a) eIm/ZIF-8 and (b) phIm/ZIF-8. The percentage of 2-eIm and 2-phIm as labeled indicates the concentration the precursor solution. (ref is acetic acid)

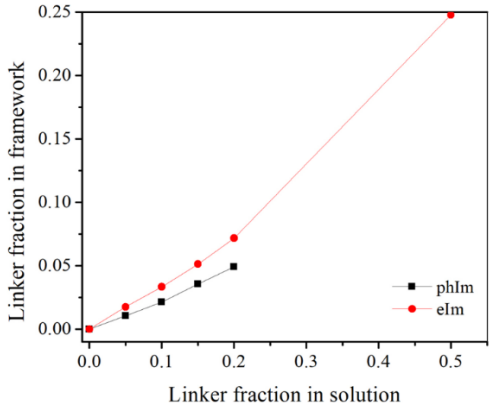

Figure IV-7. Relationship between the concentrations of secondary linker (2-eIm or 2-phIm) in the precursor solution vs. the actual amount incorporated in the ZIF-8 framework as determined through 1H-NMR.

Figure IV-8 and Figure IV-9 display the nitrogen physisorption isotherms for the eIm/ZIF-8 and phIm/ZIF-8 at different 2-eIm and 2-phIm concentrations. All the eIm/ZIF-8 and phIm/ZIF-8 samples show the typical type I isotherms, which are similar to those of

the parent ZIF-8. Nevertheless, both eIm/ZIF-8 and phIm/ZIF-8 show a decrease in the saturation volume as dopant concentrations increase likely due to the presence of bulkier dopants. This behavior is similar to the mixed-linker ZIF-7-8 where 2-mIm linker is replaced with bulkier benzimidazole linker.[53] Furthermore, the incorporation of either 2-eIm or 2-phIm linker to the ZIF-8 framework reduces both micropore volume and Brunauer-Emmet-Teller (BET) surface area as shown in Figure IV-10. ZIF-8 is known to be flexible through linker rotation, known as "gate-opening" behavior[108, 112] rendering sudden increase in nitrogen uptake into the micropores.[108] As a result, the adsorption isotherm of N_2 at 77 K on ZIF-8 displays two steps occurring at relative pressures (P/P_o) of ~ 0.002 and 0.02[108] as shown in Figure IV-8. Moggach et al.[160] have shown that ZIF-8 can realign its packing arrangement at high pressure (1.47 GPa) forming a new phase (ZIF-8HP)[108] different from its structure at ambient temperature and pressure (ZIF-8AP)[108] as illustrated in Figure IV-8. Later simulated studies[108] determined that the second step in N_2 adsorption isotherm at 77 K of ZIF-8 (P/P_o of ~ 0.02) corresponds to phase transition of ZIF-8 from ambient pressure to high pressure structure through "gate-opening"[108, 112] behavior. Interestingly, the doping of 2-eIm linker to the ZIF-8 framework increases the second step threshold "gate-opening" pressure from P/P_o of 0.02 (ZIF-8) to 0.05 (20% 2-eIm), and further 2-eIm incorporation (50% 2-eIm) leads to complete elimination of the gate-opening of ZIF-8. This is attributed to the fact that the bulkier ethyl group of 2-eIm adds constriction in the structure making the framework less flexible, thereby requiring higher pressure to allow "gate-opening" behavior. Similar observation is made for the

phIm/ZIF-8. The elimination of "gate-opening" of ZIF-8 has been previously observed as well when 2-mIm linker is substituted with bulkier benzimidazole linker.[53]

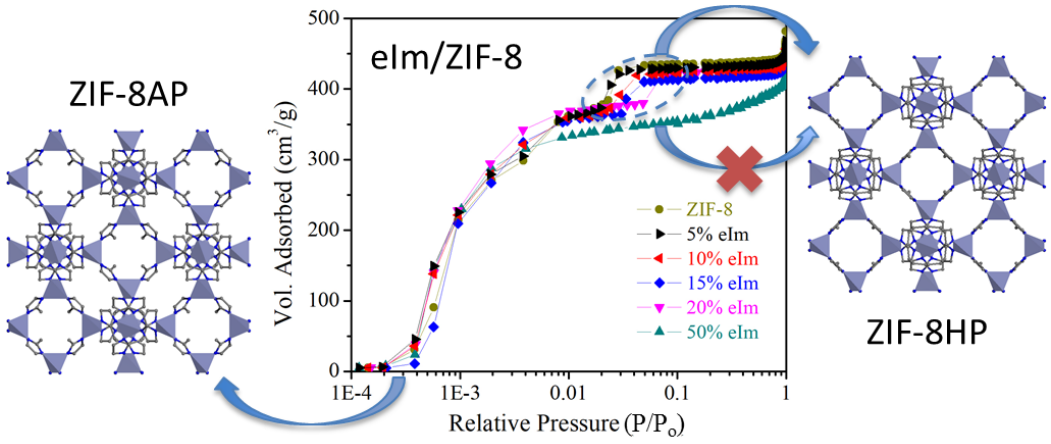

Figure IV-8. Nitrogen physisorption isotherms of eIm/ZIF-8 compared to ZIF-8 at 77 K along with Illustration of ZIF-8 structures at low relative pressure (ZIF-8AP) and high relative pressure (ZIF-8HP).

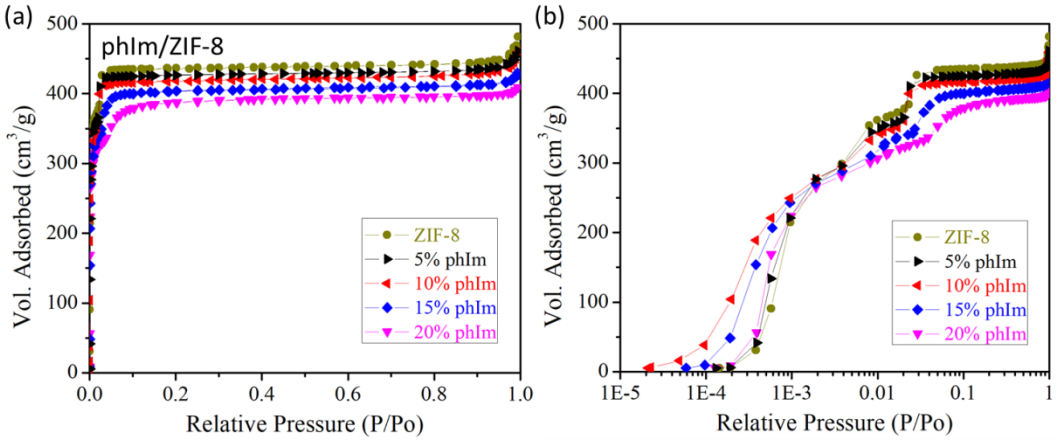

Figure IV-9. Nitrogen physisorption isotherms of phIm/ZIF-8 compared to ZIF-8 at 77 K on (a) linear scale and (b) log scale of the relative pressure (P/Po).

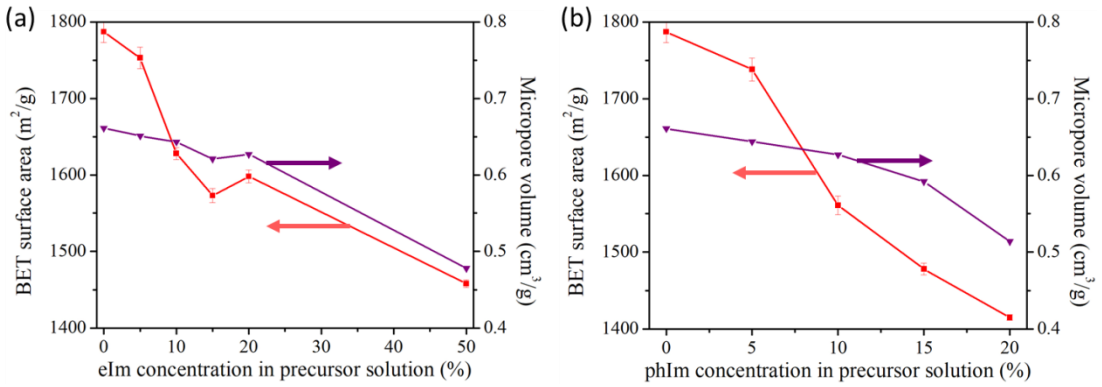

Figure IV-10. BET surface area and micropore volume of (a) eIm/ZIF-8 with various 2-eIm concentrations, and (b) phIm/ZIF-8 with various 2-phIm concentrations. Both doping linkers concentrations corresponds to the amount in precursor solution.

The adsorption isotherms of CO_2 and CH_4 for the linker-doped powders were also measured up to 1 bar at 273 K as shown in Figure IV-11. Both eIm/ZIF-8 and phIm/ZIF-8 exhibit slightly higher CO_2 sorption coefficients (34.8 and 32.5, respectively) as compared to the pristine ZIF-8 (30.9). At 1 bar, despite the lower surface areas, the maximum CO_2 uptakes for the both eIm/ZIF-8 (~37.7 cm^3/g) and phIm/ZIF-8 (~35.2 cm^3/g) were slightly higher as compared to the pristine ZIF-8 (~32.8 cm^3/g), suggesting an increase in CO_2 affinity upon doping. For the CH_4 adsorption isotherms, the linker-doped samples require higher initial uptake pressure of CH_4 as compared to ZIF-8. The ZIF-8 sample shows the first uptake of CH_4 as low as ~ 0.025 bar, whereas the phIm/ZIF-8 and eIm/ZIF-8 resist CH_4 uptake until ~ 0.11 and ~ 0.23 bar, respectively. Although all three samples exhibit different first uptake pressures, they share similar slope isotherms (~ 8.9), indicating the absence of preferred interaction between CH_4 molecules with any of the porous samples. The increase in initial CH_4 uptake threshold pressure may be

contributed solely to the framework constraint by the introduction of doping linker to the ZIF-8 structure, which is in an agreement with the higher second step threshold "gate-opening" pressure observed for the N_2 adsorption isotherms in Figure IV-8.

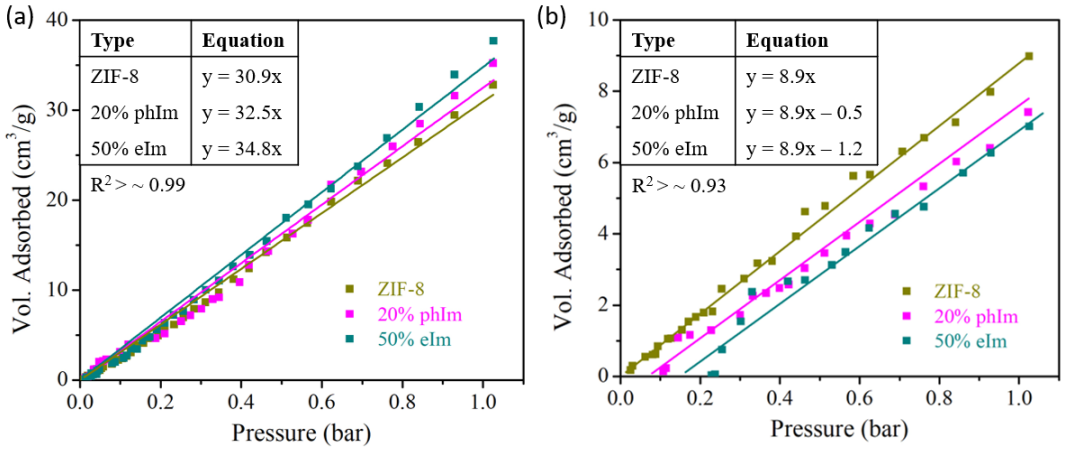

Figure IV-11. Adsorption isotherms of (a) CO2 and (b) CH4 at 273 K for ZIF-8, 50% 2-eIm, and 20% 2-phIm. Solid line indicates linear fit trend on the isotherms with equation shown in the table and average R2 value of ~ 0.99 and ~ 0.93 for CO2 and CH4, respectively. The slope of the linear fit line represents sorption coefficients of CO_2 and CH_4 on the ZIFs.

Finally, the thermal stability of the linker-doped ZIF-8 samples were analyzed with thermogravimetric analysis (TGA) up to 800 °C under inert argon gas flow at atmospheric condition as shown in Figure S6. Linker-doping is expected to introduce defects in the crystals which may reduce its thermal stability. Interestingly, the thermal stability of both eIm-doped and phIm-doped samples are comparable to the pristine ZIF-8 as shown in Figure IV-12. This suggests that linker-doping does not lead to formation of local defects.

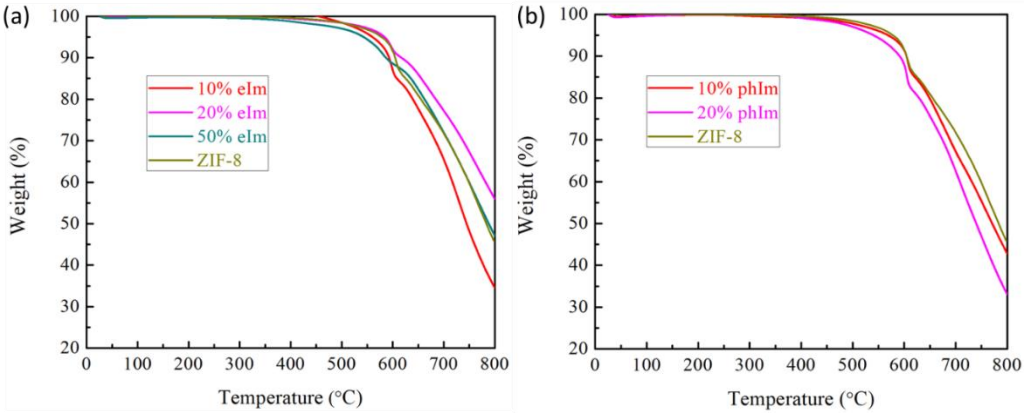

Figure IV-12. Thermogravimetric analysis of (a) eIm/ZIF-8 and (b) phIm/ZIF-8 with various amount of the doping linker.

IV.3.2. ***Synthesis and analysis of polycrystalline eIm/ZIF-8 membranes***

eIm/ZIF-8 membranes with various 2-eIm dopant concentrations were grown using the microwave-assisted seeding[33] and secondary growth method[30] and compared to pure ZIF-8 membranes. Briefly, eIm/ZIF-8 seed layers were deposited on α-Al_2O_3 substrates using the microwave assisted seeding approach, followed by secondary growth of the seed crystals in aqueous growth solutions to form continuous polycrystalline eIm/ZIF-8 membranes as described in the Experimental section. Three different 2-eIm concentrations were investigated to compare the effect of 2-eIm doping to ZIF-8 framework (5, 10, and 15% of 2-eIm in the seeding and growth solution). Figure IV-13 shows the XRD patterns of the eIm/ZIF-8 membranes with various 2-eIm concentrations, confirming that all eIm/ZIF-8 membranes retained the SOD cubic ZIF-8 structure.

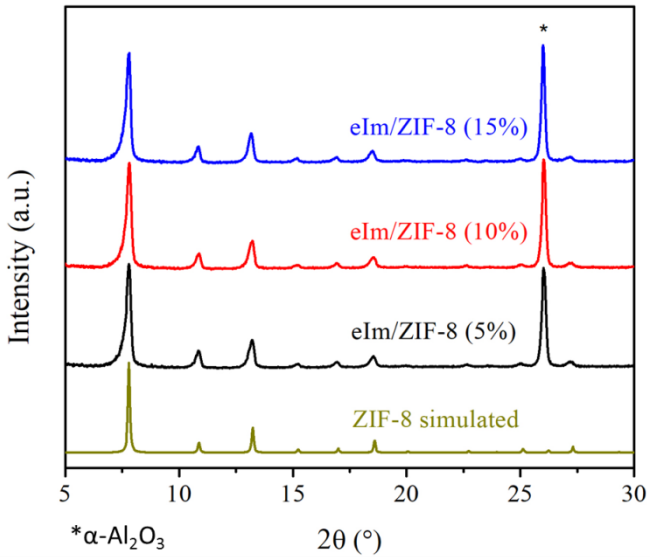

Figure IV-13. XRD patterns of eIm/ZIF-8 membranes compared with ZIF-8 simulated patterns. Percentage in parentheses corresponds to 2-eIm concentration in the seeding and growth solutions.

Figure IV-14 presents the SEM images of polycrystalline eIm/ZIF-8 membranes in comparison with ZIF-8 membranes. Regardless of dopant concentrations, well inter-grown continuous eIm/ZIF-8 membranes were formed on α-Al_2O_3 supports. The incorporation of 2-eIm led to a reduction in the grain size even for the smallest 2-eIm concentration (5%) investigated in this study. This change of grain size was also observed in our recent study[41] on the mixed-linker polycrystalline ZIF-7-8 membranes (hybrid ZIFs consisting Zn^{2+} metal nodes bridged by a mixture of 2-mIm and benzimidazole linkers), in which higher benzimidazole linker led to membranes with smaller crystal grains. Interestingly, the cross-sectional view showed that the higher the 2-eIm dopant concentration the lower the thickness of the membranes (as thin as ~ 750 nm). Ultrathin polycrystalline membranes are highly desirable for their high gas flux.[161] The

incorporation of a secondary linker such as 2-eIm to ZIF-8 structure may hamper the crystallization process by hindering the association of Zn^{2+} ions with imidazole linkers,[162] thus reducing the growth of crystals (i.e. smaller grains and thinner polycrystalline membranes).

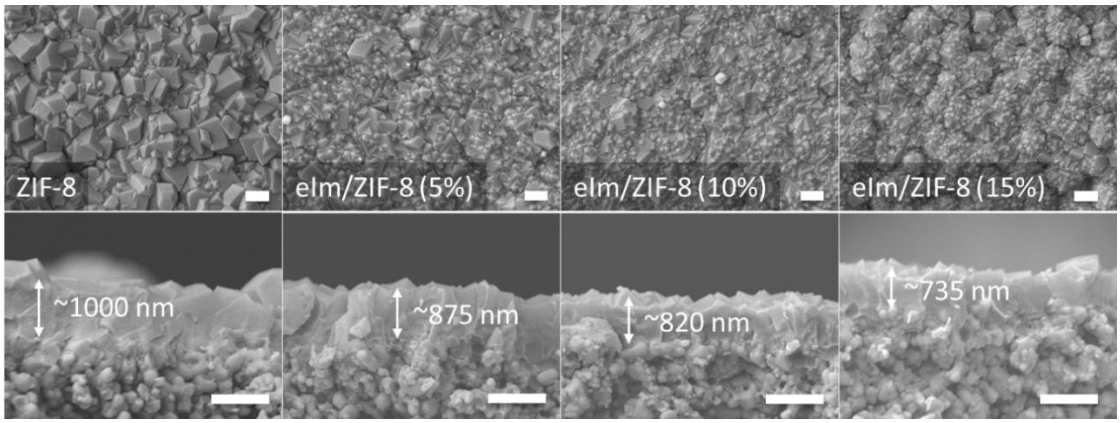

Figure IV-14. SEM images of ZIF-8 and eIm/ZIF-8 membranes with various 2-eIm concentrations on the top view (top row) and cross-sectional view (bottom row). Percentage in parentheses corresponds to 2-eIm concentration in the seeding and growth solutions.

The ATR-IR spectra as shown in Figure IV-15 confirm the presence of 2-eIm linkers in the doped ZIF-8 membranes. Similar to the powder samples, the eIm/ZIF-8 membranes also exhibit the CH_2 in-plane rocking vibration signal (~ 1057 cm^{-1}). Ultimately, the presence and actual amount of both 2-eIm and 2-mIm in the framework eIm/ZIF-8 membranes were determined using the solution ^{1}H-NMR as shown in Figure IV-16a. The doped ZIF-8 membranes prepared using seeding and growth solutions containing 5, 10, and 15 % 2-eIm are determined to form eIm/ZIF-8 membranes with 2-

eIm concentrations of approximately 0.3, 1.3, and 2.5 %, respectively as shown in Figure IV-16b. The doping amounts of 2-eIm in the membranes are much lower as compared to the eIm/ZIF-8 powder. This has been previously observed in our recent report[41] on the preparation of mixed-linker ZIF-7-8 membranes, where the amount of the secondary linker (benzimidazole) were incorporated at a lesser amount for the polycrystalline membrane fabrication than the mixed linker ZIF-7-8 powder synthesis.[42, 53]

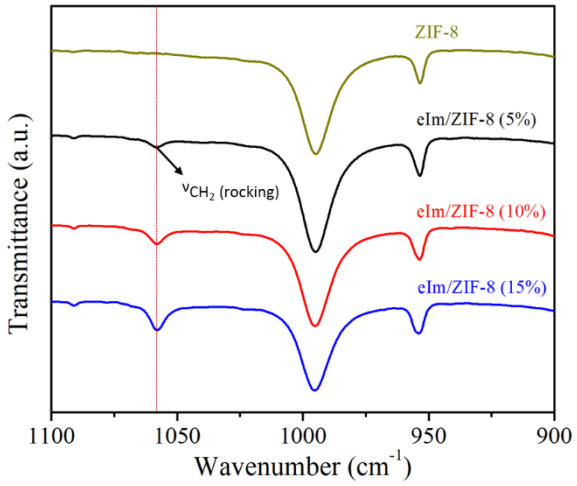

Figure IV-15. ATR-IR spectrum of ZIF-8 and eIm/ZIF-8 membranes with various 2-eIm concentrations in the seeding and growth solutions as indicated by percentage inside the parentheses.

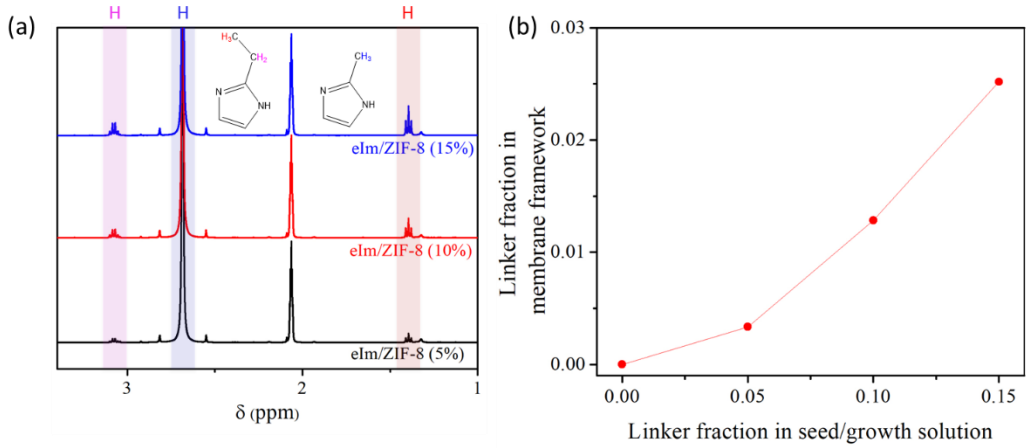

Figure IV-16. (a) 1H-NMR spectrum for eIm/ZIF-8 membranes with various 2-eIm concentrations in the seed/growth solution; (b) relationship between 2-eIm linker fraction in seed/growth solution vs. in the membrane framework.

To understand this in more detail, we compared the amount of 2-eIm incorporation in the framework by different synthesis approaches as summarized in Table IV-2, from which two observations can be made. First, the eIm/ZIF-8 seed crystals contain noticeably much lower 2-eIm concentration compared to other samples. Secondly, the 2-eIm incorporation in the framework for the powder collected from secondary growth solution is much higher (more than 3 times) than the eIm/ZIF-8 membranes grown on alumina support. . Based on this observation, it is speculated that the low 2-eIm concentration in the eIm/ZIF-8 membranes is dictated by the seed crystals despite having the secondary growth synthesis yielding eIm/ZIF-8 powder with higher 2-eIm concentration. This indicates the importance of linker composition in the nuclei of hybrid ZIFs as it controls the secondary linker incorporation during the crystal growth by retaining the same composition as the nuclei.

Table IV-2. Comparison of 2-eIm incorporation based on different synthesis approaches

Synthesis methods	In solution	In framework
Microwave synthesis (powder)	10 %	3.3 %
Microwave seeding (seed)	10 %	1.3 %
2^{nd} growth (powder)	10 %	5.6 %
2^{nd} growth (membrane)	10 %	1.3 %
Microwave synthesis (powder)	15 %	5.1 %
Microwave seeding (membrane)	15 %	2.1 %
2^{nd} growth (powder)	15 %	8.3 %
2^{nd} growth (membrane)	15 %	2.5 %

Finally, the gas separation performances of the membranes were compared and tested by performing binary gas permeation measurements with an equal-molar propylene/propane mixture using the Wicke-Kallenbach technique. Doping of 2-eIm linkers into ZIF-8 framework increases both propylene and propane permeances at the expense of reduction in separation factors as shown in Figure IV-17a. Despite the analyses performed on the doped eIm/ZIF-8 powders showing stiffer Zn-N bonding from FT-IR and N_2 adsorption isotherms showing increased restriction in linker rotation,[36, 42] the propylene/propane separation performances of eIm/ZIF-8 membranes display reduction in their separation factors. It is worth noting that the gas separation performances of polycrystalline membranes are affected not only by selective intracrystalline diffusion but also by nonselective intercrystalline diffusion which is mainly through the grain boundaries. Since the dopant concentrations in the membranes are less than ~ 2.5 %, significantly less than those in the powder samples, it is unlikely to observe improved intracrystalline separation due to the restricted linker rotation. Moreover, it is not

unreasonable to surmise that the linker doping, though small, compromised the quality of the grain boundaries, thereby reducing the separation performance of the membranes.

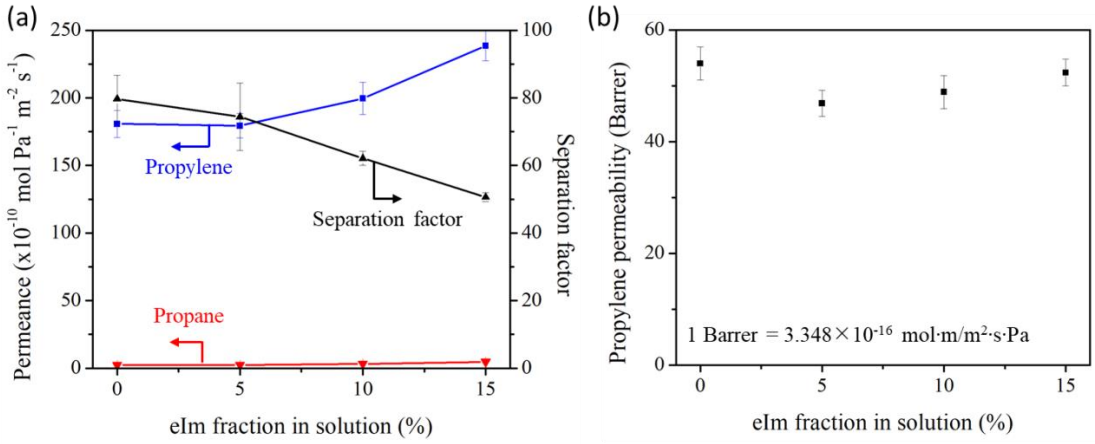

Figure IV-17. (a) Propylene and propane binary separation performances of eIm/ZIF-8 membranes in comparison with ZIF-8 membranes and (b) propylene permeabilities of eIm/ZIF-8 membranes as dopant content in solution increases.

For the increase in the propylene permeance, three attributes need to be considered: 1) enlargement of effective pore apertures, 2) reduction in membrane thickness, and 3) compromised grain boundary structures. Because the propylene permeabilities of all membranes (ZIF-8 and eIm/ZIF-8) are comparable as shown in Figure IV-17b, the 2-eIm concentration can be determined too low to modify the ZIF-8 membranes molecular sieving properties (i.e. effective pore apertures) as explained earlier. Therefore, the increase in the propylene permeance can be attributed solely to the reduction of membrane thickness and the enhancement of nonselective intercrystalline diffusion upon the doping of 2-eIm, decreasing the separation factor.

IV.4. **Conclusions**

For the first time, we successfully applied a linker doping strategy to incorporate two dopant linkers, 2-ethylimidazole (2-eIm) and 2-phenylimidazole (2-phIm), into ZIF-8 structure while maintaining its cubic SOD structure. It was found that only a limited amount of dopants can be incorporated due to the "unsuitability" of these dopant linkers to form SOD structures with Zn^{2+} metal center. The bulkiness and basicity of these dopants were also considered to affect the dopant incorporation in framework. As a result, the framework dopant concentrations were much less than those in the precursor solutions. The doping of both 2-eIm and 2-phIm into ZIF-8 increased the "stiffness" of Zn-N bonding, leading to constriction to the flexibility of ZIF-8 framework as displayed in the higher threshold "gate-opening" pressure of the doped ZIF-8 as compared to the undoped ZIF-8. The restriction also increased the initial CH_4 uptake threshold pressure on the eIm/ZIF-8. Furthermore, the bulkier moieties of ethyl and phenyl at the 2-position of the imidazole linker reduced the micropore volume of the doped ZIF-8. The first polycrystalline eIm/ZIF-8 membranes with various 2-eIm dopant concentrations were successfully prepared on α-Al_2O_3 substrates. Interestingly, the eIm-doping led to a noticeable reduction in the thickness of the polycrystalline membranes owing to hampered crystallization, thereby improving the permeance of propylene with decreased separation factor. The doping strategy presented here is expected to open up more options on the type of linkers that can be mixed into ZIFs, thereby controlling their properties (e.g. effective apertures, porosities, "gate-opening" behaviors, polarities, etc.).

CHAPTER V

SYNTHESIS OF MIXED METAL ZEOLITIC-IMIDAZOLATE FRAMEWORK MEMBRANES FOR PROPYLENE/PROPANE SEPARATION*

V.1. **Introduction**

The hybrid approach with mixed metals and/or linkers ZIFs were shown to be promising solution in tuning the molecular sieving properties (i.e. framework stiffness, gas adsorption) as discussed in Chapter III. Despite the potential of hybrid ZIFs (i.e., mixed metal and/or mixed linker ZIFs) for membrane-based gas separation applications, only a few groups reported successful synthesis of polycrystalline ZIF membranes consisting of mixed metal nodes and/or mixed linkers[36, 42, 127, 145]. Wang et al.[127] attempted to prepare polycrystalline mixed metal CoZn-ZIF-8 membranes for propylene/propane separation. However, poor membrane quality may have led to their contradicting separation performance when compared to computational studies.[63] In contrast, our group has recently prepared Co-ZIF-8[36] (formerly known as ZIF-67[46]) membranes, in which substitution of Zn^{2+} with Co^{2+} led to increase in the "stiffness" of metal—nitrogen bonding as discussed previously in Section 2. Computational studies by Krokidas et al.[63] showed that stiffer and slightly shorter Co-N bond restricts the flip-flopping motion of the 2-mIm linkers, reducing the effective aperture size. Thus, Co-ZIF-8 membranes showed the

**This chapter was adapted with permission from Febrian Hillman, John M. Zimmerman, Seung-Min Paek, Mohamed R. A. Hamid, Woo T. Lim, Hae-Kwon Jeong, J. Mater. Chem. A, 2017, 5, 6090-6099 and modified. Copyright 2017, The Royal Society of Chemistry.*

enhanced propylene/propane separation performances as compared to ZIF-8 membranes.[36] Zhang et al.[145] prepared mixed linker ZIF-9-67 (or Co-ZIF-7-8) membranes with Co^{2+} ions bridged by benzimidazolate and 2-methylimidazolate linkers and performed various single gas (H_2, N_2, CO, CH_4, CO_2) permeation measurements.

Here, we report preparation of high quality mixed metal CoZn-ZIF-8 membranes on α-Al2O3 supports using the microwave-seeding[33] and secondary method.[37] Contrary to the recent report by Wang et al.,[127] the membranes showed an improved propylene/propane binary gas separation performance with higher propylene/propane selectivity when compared to monometallic Zn-ZIF-8 membranes prepared similarly.

V.2. **Experimental**

V.2.1. ***Material***

Zinc nitrate hexahydrate ($Zn(NO_3)_2$•$6H_2O$, 98%, Sigma-Aldrich, hereafter ZnN) and cobalt nitrate hexahydrate ($Co(NO_3)_2$•$6H_2O$, 98%, Sigma-Aldrich, hereafter CoN) were used as metal sources. 2-methylimidazole ($C_4H_5N_2$, 97%, Sigma-Aldrich, hereafter 2-mIm) was used as linker sources. Sodium formate (HCOONa, 99%, Sigma-Aldrich) was used as a deprotonating agent. Methanol (99.8%, Alfa Aesar) was used as solvent. All chemicals were used as purchased without further purification.

V.2.2. ***Preparation of mixed metal CoZn-ZIF-8 seed layers and membranes***

CoZn-ZIF-8 seed layers on α-Al_2O_3 substrates were prepared using microwave-assisted method similar to previously reported by our group.[33] The secondary growth of

the CoZnZIF-8 seed layer was done using method similarly reported by Pan et al[37] with slight modification. Briefly, 4.08 mmol of ZnN and 4.08 mmol of CoN were dissolved in 40 mL methanol (solution A), and 31.6 mmol of 2-mIm and 1.84 mmol of sodium formate were dissolved in 30 mL methanol (solution B). A prepared α-Al2O3 disk was immersed in the solution A for 1 h to saturate the substrate with the metal solution. The saturated substrate was then held vertically using a home-made Teflon holder and immediately inserted into the solution B in a microwave-inert glass tube, followed by microwave irradiation with the power of 100 W for 1.5 min. Finally, the tube was naturally cooled down for 30 min and the prepared seeded support was washed in 30 ml of methanol under gentle rocking for 12 h and dried at room temperature for 24 h. For the secondary growth, solution of 0.185 mmol of ZnN and 0.185 mmol of CoN in 20 mL water were poured to solution of 27.7 mmol of 2-mIm in 20 mL water, followed by continuous mixing for 2 minutes. The growth solution was then transferred to a Teflon-lined steel autoclave with the seeded support held vertically inside the autoclave. The autoclave was then kept in an oven at 120 °C for 24 hour, and cooled by standing at ambient temperature for 2 hours. The membrane was washed in fresh methanol under stirring for 2 days. The sample was dried at room temperature for 24 hr before further characterization.

V.2.3. ***Preparation of monometallic Zn-ZIF-8 seed layers and membranes***

Monometallic Zn-ZIF-8 membranes were prepared similarly to CoZn-ZIF-8 membranes. Zn-ZIF-8 seed layers on α-Al2O3 substrates were prepared using microwave assisted method,33 follows with secondary growth using method similarly reported by

Pan et al37 with slight modification. Briefly, 8.16 mmol of ZNH was dissolved in 40 mL methanol (solution A), and 31.6 mmol of 2-mIm and 1.84 mmol of sodium formate were dissolved in 30 mL methanol (solution B). A prepared α-Al2O3 disk was immersed in the solution A for 1 h to saturate the substrate with the metal solution. The saturated substrate was then held vertically using a home-made Teflon holder and immediately inserted into the solution B in a microwave-inert glass tube, followed by microwave irradiation with the power of 100 W for 1.5 min. Finally, the tube was naturally cooled down for 30 min and the prepared seeded support was washed in 30 ml of methanol under gentle rocking for 12 h and dried at room temperature for 24 h. For the secondary growth, solution of 0.370 mmol of ZnN in 20 mL water were poured to solution of 27.7 mmol of 2-mIm in 20 mL water, followed by continuous mixing for 2 minutes. The growth solution was then transferred to a Teflon-lined steel autoclave with the seeded support held vertically inside the autoclave. The autoclave was kept in an oven at 120 °C for 24 hour, and cooled by standing at ambient temperature for 2 hours. The membrane was washed in fresh methanol under stirring for 2 days. Finally, the sample was dried at room temperature for 24 hr before further characterization.

V.2.4. ***Characterizations***

Powder X-ray diffraction (PXRD) was performed at room temperature on a Rigaku Miniflex II powder X-ray diffractometer using Cu-Kα radiation (λ = 1.5406 Å) which was scanned with a step size of 0.02°. Scanning electron micrographs were collected using a JEOL JSM-7500F operating at 5 keV acceleration voltage and 15 mm working distance.

The gas separation performance of CoZn-ZIF-8 membranes was tested using the Wicke-Kallenbach technique under atmospheric pressure. The 50:50 mixture of propylene and propane was supplied to a feed side while a permeate side was swept by argon with the total flow rates of both sides maintained at 100 ml/min. The gas composition of the permeate side was analyzed using a gas chromatography (Agilent GC 7890A equipped with HP-PLOT/Q column).

V.3. **Results and analysis**

CoZn-ZIF-8 with Co/Zn ratio of ~ 1 was grown to membranes using the microwave-seeding and secondary growth.[33,37] First, CoZn-ZIF-8 seed crystals were deposited on an α-Al_2O_3 substrate through microwave-assisted seeding method.[33] Second, the seed crystals were subjected to secondary growth to form a continuous CoZn-ZIF-8 membrane using an aqueous growth solution as described in experimental section. Figure V-1a shows the PXRD patterns of the seeded CoZn-ZIF-8 layer and the membrane after secondary growth, confirming the phase of both seed crystals and membrane is a SOD ZIF structure.

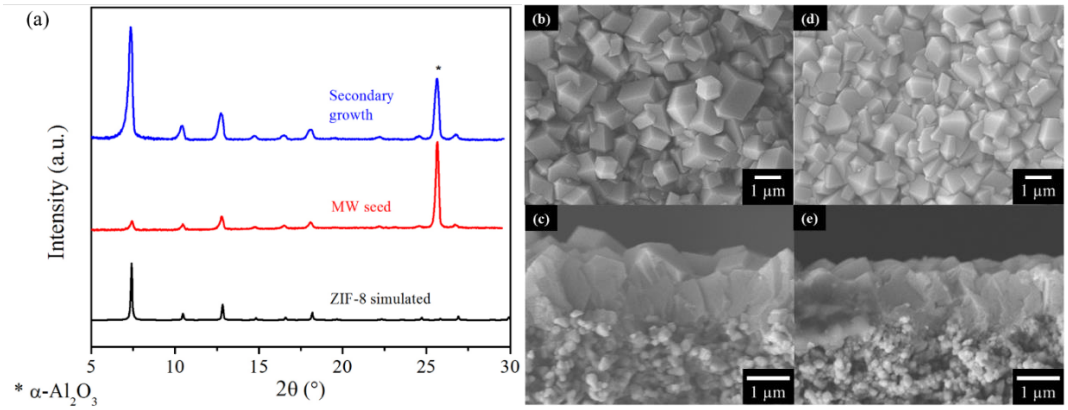

Figure V-1. (a) Powder x-ray diffraction (PXRD) pattern of $Co_{0.50}Zn_{0.50}$-ZIF-8 membrane with microwave seeding and after secondary growth; and SEM images of CoZn-ZIF-8 membrane with Co/Zn ~ 1: b) top view and c) cross section, and Zn-ZIF-8 membrane: d) top view and e) cross section.

Figure V-1(b-e) presents the SEM images of the seed crystal layer and the membrane after secondary growth (both top-view and cross-sectional view). From the top view, mixed metal CoZn-ZIF-8 crystals were shown to be well inter-grown, forming a continuous film on the α-Al_2O_3 substrate. The cross-section view displays the thickness of CoZn-ZIF-8 membrane to be ~ 1.2 µm. Line scanning on the cross section of the membrane using EDS-SEM confirms the presence of both Co and Zn for the CoZn-ZIF-8 membrane while pure Zn for the Zn-ZIF-8 membrane as shown in Figure V-2.

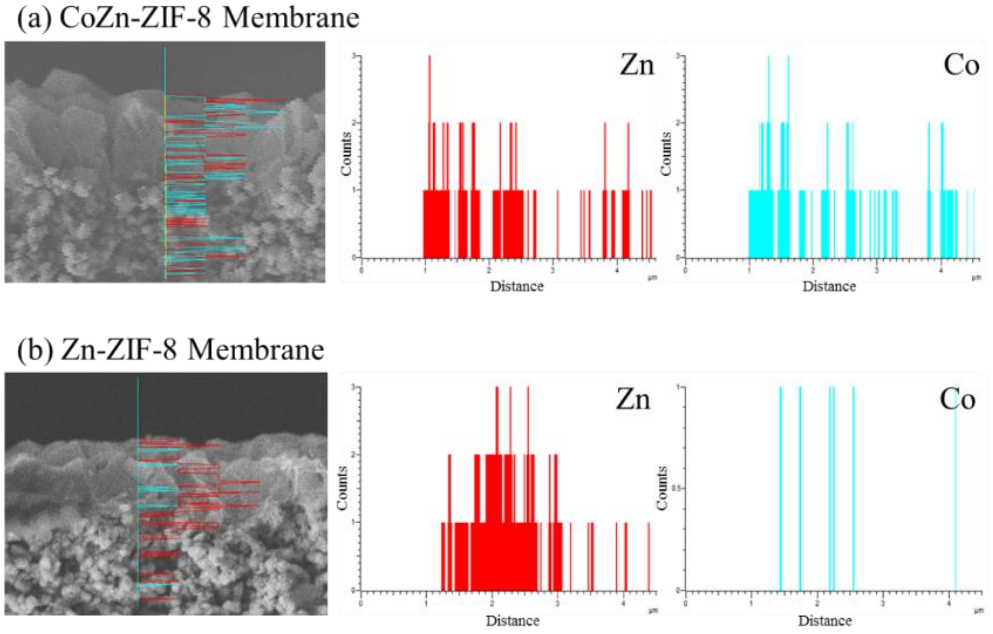

Figure V-2. SEM-EDS line scanning of (a) $Co_{0.50}Zn_{0.50}$-ZIF-8 membrane, and (b) Zn-ZIF-8 membrane for element Zn and Co.

The gas separation performance of the membranes was examined by performing binary gas permeation measurements with a propylene-propane mixture (50/50) using the Wicke-Kallenbach technique. The CoZn-ZIF-8 membranes showed an average propylene permeance of about ~ 203.6×10^{-10} mol Pa^{-1} m^{-2} s^{-1} with an average propylene/propane separation factor of ~ 120.2 (Figure V-3). This is a noticeable improvement in propylene-propane binary selectivity when compared to Zn-ZIF-8 membrane prepared with similar method which showed an average propylene permeance of ~ 213.9×10^{-10} mol Pa^{-1} m^{-2} s^{-1} and average propylene/propane separation factor of ~ 62.9. This result is contradictory to the findings by Wang et al.[127] where they showed a reduction in propylene-propane selectivity with increased Co to Zn ratio. However, our findings on the increased

selectivity with mixed Zn and Co in the frameworks may be supported by other studies. For example, Krokidas et al.[63] reported a computational study showing that Co-ZIF-8 has smaller aperture (3.31 Å) than Zn-ZIF-8 (3.42 Å) which hindered the diffusion of propane more so than that of propylene, leading to the enhanced propylene/propane selectivity. Therefore, it can be anticipated that the incorporation of Co in the framework of mixed metal CoZn-ZIF-8 may lead to smaller aperture than Zn-ZIF-8. Furthermore, as pointed out by Kwon et al.,[36] the increased stiffness of metal-nitrogen bonding upon incorporation of Co in the framework restricts the flipping motion in CoZn-ZIF-8, leading to the improvement of the separation factor by reducing the effective aperture size. It should, however, be noted that one cannot exclude the possibility of enhanced grain boundary structure upon the incorporation of Co, resulting in improved separation performance.

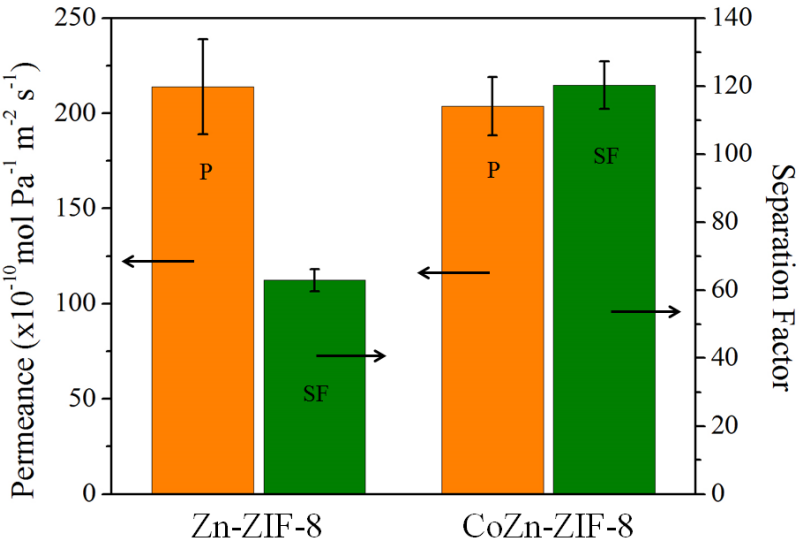

Figure V-3. Permeance and separation factor of propylene/propane binary mixture measured on Zn-ZIF-8 and CoZn-ZIF-8 membrane. P for permeance and SF for separation factor.

V.4. **Conclusions**

Mixed metal CoZn-ZIF-8 membranes with Co/Zn ~ 1 were successfully prepared and found to be more selective in separating binary gas mixture propylene propane with average separating factor of ~ 120.2 compared to monometallic Zn-ZIF-8 membranes with an average separating factor of ~ 62.9. The increased selectivity may be contributed from the smaller effective aperture of CoZn-ZIF-8 than Zn-ZIF-8 due to the increase in bond stiffness upon the incorporation of Co to the framework as shown from the blue shift of M-N on IR band. This work opens up an alternative synthesis method for hybrid ZIF both mixed metal and/or linker rapidly using microwave irradiation which could be an economically beneficial route for future industry scale up.

CHAPTER VI

RAPID ONE-POT MICROWAVE SYNTHESIS OF MIXED LINKER HYBRID ZEOLITIC-IMIDAZOLATE FRAMEWORK MEMBRANES WITH TUNABLE GAS SEPARATIONS*

VI.1. **Introduction**

The synthesis methods of polycrystalline ZIF membranes[30, 33-37, 121-122, 163-164] can generally be classified into either *in situ*[34-35, 165-166] or secondary (seeded) growth,[30, 33, 36-37, 42, 167] mostly in liquid phase. While the secondary growth allows the formation of thinner membranes with better grain boundary structures,[30, 33] the *in situ* methods lead to the formation of polycrystalline membranes in a simpler manner because they don't require additional seeding steps.[132, 135, 168-170] Besides, due to their unique labile coordination chemistry, ZIF films and membranes can be formed in vapor phases as well.[171-174] Despite these diverse synthesis methods reported, almost all of the current synthesis methods require lengthy and often complicated processes demanding several hours up to days to prepare well-intergrown polycrystalline ZIF membranes,[30, 33-37, 42, 121-122, 163-167, 171-172] potentially making them expensive. This issue stems from the fundamental limitation of crystallization processes by conventional heating, significantly impeding the scaling-up of ZIF membranes for commercial separation applications.

**This chapter was adapted with permission from Febrian Hillman, Jordan Brito, Hae-Kwon Jeong, ACS Appl. Mater. Interfaces, 2018, 10, 5586-5593. Copyright 2018, American Chemical Society.*

Microwave-assisted techniques have recently attracted substantial interests for the facile synthesis of MOF powders[58, 146, 151] and membranes[33, 42, 166, 175] due to its rapid and volumetric heating.[58, 146, 176-177] Jhung and co-worker[178] were the first to show the applicability of microwave synthesis for ZIF-8. Our group has reported the rapid microwave-assisted seeding of ZIF-8[33], MOF-5[175], and CoZn-ZIF-8.[42] To obtain the final well-intergrown polycrystalline membranes, however, hours of subsequent secondary growth steps were necessary. Caro and co-workers[163-164, 166] have adopted microwave-assisted approach for both *in situ* and secondary growth of polycrystalline ZIF-7[163-164] and ZIF-8[166] membranes, which require several hours to prepare well-intergrown high quality membranes. To drastically reduce the cost of ZIF membranes for their practical applications, it would be highly desirable to rapidly prepare high-quality ZIF membranes in a few minutes or less.

Despite several polycrystalline ZIF membranes reported, only ZIF-8[30, 33-35, 37, 124, 172, 179-182] and its structurally related ZIF-67[36, 42] (iso-structure of ZIF-8 with Co^{2+} centers) membranes showed impressive gas separation performance (i.e., propylene/propane separation). This rarity of high-performance ZIF membranes attests to the fundamental limitations of crystalline materials including ZIFs where the available aperture sizes are discrete. In other words, for ethylene/ethane separation, ZIFs with an effective aperture size of ~ 3.6 Å are desirable, yet no such reported ZIFs available. To overcome this materials challenge, researchers have introduced different metal nodes and linkers,[42, 53, 63] affecting the flip-flopping motion of linkers, thereby the effective aperture sizes (i.e.,

molecular sieving properties) of ZIFs. Furthermore, it has been shown that the effective apertures can be further finely tuned by mixing the metal nodes[42] and/or linkers[43] within the same ZIF frameworks, which can potentially extend the separation application of ZIF materials for many important gas mixtures.

Our group has recently prepared Co-ZIF-8[36] (formerly known as ZIF-67[46]) membranes, in which substitution of Zn^{2+} with Co^{2+} led to increase in the "stiffness" of metal—nitrogen bonding. Computational studies by Krokidas et al.[63] showed that stiffer and slightly shorter Co-N bond restricts the flip-flopping motion of the 2-mIm linkers, reducing the effective aperture size. Thus, Co-ZIF-8 membranes showed the enhanced propylene/propane separation performances as compared to ZIF-8 membranes.[36] Furthermore, Nair and co-worker[43, 53-54, 82] reported the introduction of mixed linkers in ZIF-8 led to continuous tuning of the framework functionality[43], porosity,[53-54] and pore size distribution.[53] For example, the authors showed that the hydrophobicity and gas transport diffusivity of ZIF-8 could be tuned by replacing 2-mIm linker with less bulky imidazole-2-carboxaldehyde (ICA) linker containing hydrophilic carbonyl group.[43]

Despite the potential of hybrid ZIFs (i.e., mixed metal and/or mixed linker ZIFs) for membrane-based gas separation applications, only a few groups reported successful synthesis of polycrystalline ZIF membranes consisting of mixed metal nodes and/or mixed linkers[36, 42, 127, 145]. Wang et al.[127] attempted to prepare polycrystalline mixed metal CoZn-ZIF-8 membranes for propylene/propane separation. However, poor membrane quality may have led to their contradicting separation performance when compared to

computational studies.[63] Recently, our group[42] prepared high quality mixed metal CoZn-ZIF-8 membranes showing improved separation factor in propylene/propane gas separations relative to ZIF-8 membranes. Zhang et al.[145] prepared mixed linker ZIF-9-67 (or Co-ZIF-7-8) membranes with Co^{2+} ions bridged by benzimidazolate and 2-methylimidazolate linkers and performed various single gas (H_2, N_2, CO, CH_4, CO_2) permeation measurements. To the best of our knowledge, there is no report on high quality polycrystalline hybrid ZIF membranes showing tunable gas separation capabilities through variation of mixing linker ratio.

Here we report a rapid microwave-assisted *in situ* synthesis of well-intergrown mixed linker ZIF-7-8 membranes in under ~ 90 seconds. ZIF-7-8 consists of Zn^{2+} metal nodes bridged by a mixture of benzimidazolate (bIm, ZIF-7 linker) and 2-methylimidazolate (2-mIm, ZIF-8 linker) linkers.[53] To the best of our knowledge, this is the fastest synthesis of any polycrystalline MOF membranes reported up to now. Furthermore, the gas separation performances (separation factor and permeance) of hybrid ZIF-7-8 membranes were systematically tuned by varying the bIm-to-mIm ratio incorporated into the framework. The unprecedentedly rapid synthesis of ZIF-7-8 membranes with tunable molecular sieving properties is an important step forward for their practical applications in separations of gas mixtures of interest.

VI.2. **Experimental**

VI.2.1. ***Materials***

Zinc nitrate hexahydrate ($Zn(NO_3)_2$•$6H_2O$, 98%, Sigma-Aldrich, hereafter ZnN) was used as metal sources. 2-methylimidazole ($C_4H_5N_2$, 97%, Sigma-Aldrich, hereafter HmIm) and benzimidazole ($C_7H_6N_2$, 98%, Sigma-Aldrich, hereafter HbIm) were used as linker sources. Methanol (99.8%, Alfa Aesar) and dimethylformamide (99.8%, Alfa Aesar, hereafter DMF) were used as solvents. Acetic acid-d4 (CD_3CO_2D, 99.5 atom % D, Sigma-Aldrich) was used as reference for ^{1}H-NMR analyses. All materials were used as purchased without further purification.

VI.2.2. ***Preparation of porous α-Al2O3 substrates***

Disk-shaped alumina substrates (porosity = ~ 46 %, diameter = 22 mm, and thickness = 2 mm) with an average pore diameter of ~200 nm were prepared by a pressing and sintering method slightly modified from a previously reported method.[33] Briefly, α-Al_2O_3 power (CR6, Baikowski) was molded into a disk shape by uniaxial pressing and was sintered at 1100 °C for 2 h. Then one side of the sintered disks was polished using a sand paper (grid #1200) to reduce the surface roughness of the substrates, followed by sonication for 1 min in methanol. Subsequently the supports were dried in an oven at 120 °C for 1 h before usage.

VI.2.3. ***Microwave synthesis of mixed linker ZIF-7-8 membranes***

A solution of 27.5 mmol of ZnN in 45 mL of methanol was prepared as a metal solution (solution A). A separate solution of (32.7 - x) mmol of HmIm and x mmol of

HbIm in 30 mL of DMF was prepared as a linker solution (solution B). The value of x was varied from 0 to 32.7. A prepared α-Al_2O_3 disk was immersed in the solution A for 1 h to saturate the substrate with the metal solution. The saturated substrate was then held vertically using a home-made Teflon holder and immediately inserted into the solution B in a microwave-inert glass tube, followed by microwave irradiation with the power of 100 W for 90 seconds. The temperature of the growth solution was measured post-microwave irradiation with IR gun to be ~ 78 to 83 °C. Finally, the tube was naturally cooled down for 30 min. The prepared membrane was washed in 35 ml of methanol under gentle rocking for 48 h with exchange of fresh methanol at 24 h mark. The washed membrane was dried at room temperature for 48 h.

VI.2.4. ***Characterizations***

X-ray diffraction (XRD) was performed at room temperature on a Rigaku Miniflex II powder X-ray diffractometer using Cu-Kα radiation (λ = 1.5406 Å) which was scanned with a step size of 0.02°. Scanning electron micrographs were collected using a JEOL JSM-7500F operating at 5 keV acceleration voltage and 15 mm working distance. Attenuated total reflection Infra-red (ATR-IR) spectra were collected using a NICOLET 6700 Series from Thermo Electron, equipped with a single reflection diamond attenuated total reflectance (ATR) attachment (Quest, Specac Inc.). Composition analyses of the linker ratios in the mixed linker ZIF-7-8 membranes were determined through solution proton nuclear magnetic resonance (^{1}H-NMR) spectra taken from a Varian Mercury 300 spectrometer (300 MHz system). NMR samples were prepared by submersion of well

activated ZIF-7-8 membranes in 800 μL of deuterated acetic acid-d4 for two days. The acidic solution dissolves the ZIF-7-8 membranes from the α-Al_2O_3 supports to Zn^{2+}, 2-methylimidazolate (2-mIm), and benzimidazolate (bIm). The acetic acid-d4 solution containing 2-mIm and bIm linkers were then used for the ^{1}H-NMR analysis to determine the bIm-to-mIm linker ratio from each membrane sample.

VI.2.5. ***Permeation measurements***

All permeation tests were performed using the Wicke-Kallenbach technique under atmospheric pressure at room temperature (298 K). For the single gas measurements of small gas molecules (H_2, CO_2, N_2, CH_4), both the feed and sweep gas (argon) flow rates were set to 100 mL/min. The gas composition of the permeate side was analyzed using a gas analyzer (QGA, Hiden Analytical). For the binary mixture measurements of propylene/propane, CO_2/CH_4, and H_2/CH_4, the total feed flow rate was kept at 100 mL/min with each gas at 50 mL/min (1:1 ratio). The permeate side was swept with argon. For the propylene/propane gas mixture, the gas composition of the permeate side was analyzed using a gas chromatography (Agilent GC 7890A equipped with HP-PLOT/Q column). For the CO_2/CH_4 and H_2/CH_4 gas mixtures, the gas composition of the permeate side was analyzed using a gas analyzer (QGA, Hiden Analytical).

VI.3. **Results and analysis**

Well-intergrown polycrystalline ZIF-7-8 membranes with various bIm-to-mIm linker ratios were prepared rapidly (~ 90 seconds) under microwave irradiation illustrated in Figure VI-1a. As illustrated in Figure VI-1b, we attempted to tune the effective aperture

sizes of hybrid ZIFs by systematically incorporate bIm in the frameworks. Three different linker ratios were investigated with bIm amount of 6%, 8%, and 11% in the precursor solution (not in the actual framework of ZIF-7-8 membranes). The actual amount of bIm incorporation in the framework of ZIF-7-8 membranes may differ from the original synthesis solution,[42, 53] which will be discussed later in detail. ATR-IR spectra as shown in Figure VI-2 confirmed the existence of both linkers in the framework. ZIF-7-8 membranes exhibit C=C stretching vibration from the aromatic benzene ring of bIm linker (~1456 cm^{-1}) and aliphatic C-H stretching bands of the methyl groups from 2-mIm linker (~1307 cm^{-1}) verifying the presence of dual linkers in the framework. Interestingly, the intensity from methyl group of 2-mIm linker signal (in particular C-H aliphatic stretching bands) becomes weaker with increasing bIm concentration, which indicates the incorporation of more bIm linker in the framework.

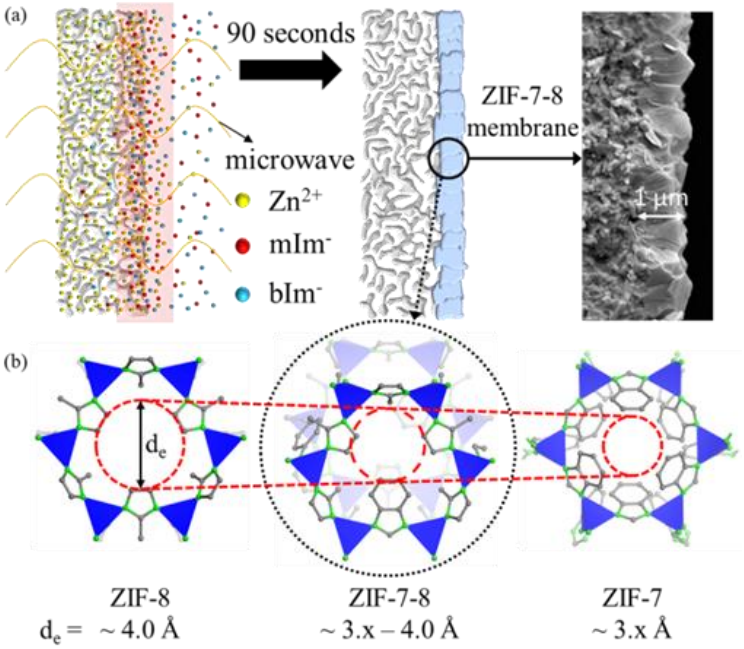

Figure VI-1. (a) Schematic illustration for the rapid microwave-assisted in situ synthesis of mixed linker ZIF-7-8 membranes and (b) comparison of effective pore aperture of ZIF-8, ZIF-7, and mixed linker ZIF-7-8. d_e = effective aperture size.

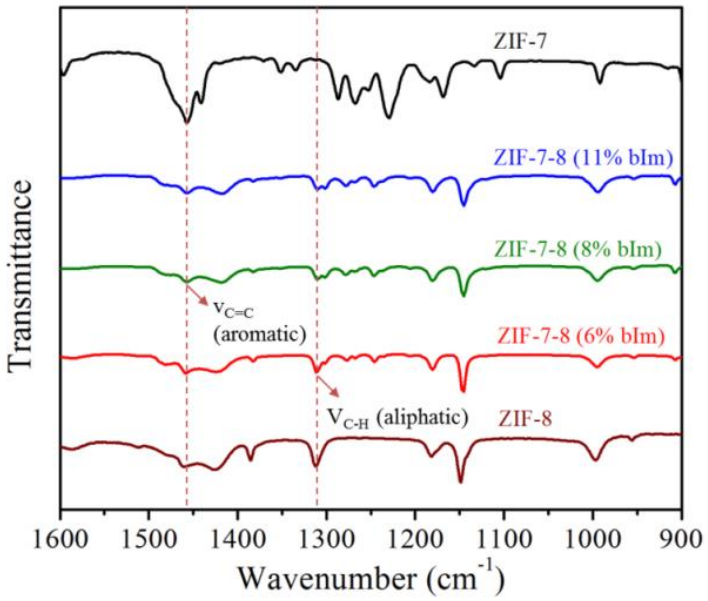

Figure VI-2. ATR-IR spectra of mixed linker ZIF-7-8 membranes at various linker ratios. Signal ~1456 cm^{-1} corresponds to the C=C stretching vibration from the aromatic benzene ring of bIm linker, and ~1307 cm^{-1} represents the C-H stretching bands of the methyl groups from 2-mIm linker.

As presented in Figure VI-3, the XRD patterns of all three ZIF-7-8 membranes with different linker ratio match well with ZIF-8, confirming the formation of phase pure highly crystalline SOD structures. Furthermore, the peak intensity appears stronger for ZIF-7-8 membranes with higher bIm concentration, which may suggest a thicker membrane formation. According to the past studies,[53] the mixed linker framework maintains the $I\bar{4}3m$ space group of ZIF-8 up to 35% bIm loading, and thereafter transitions to the $R\bar{3}$ space group of ZIF-7. Based on these observations, the mixed linker membranes are estimated containing less than 35% of bIm in the frameworks. Solution ^{1}H-NMR was used to quantify the actual bIm incorporation to the hybrid frameworks. The mixed linker

membranes prepared using precursor solutions containing 6%, 8%, and 11% bIm were determined to form hybrid membranes with bIm concentrations of approximately 11%, 15%, and 23%, respectively, which subsequently denoted as ZIF-7_{11}-8, ZIF-7_{15}-8, and ZIF-7_{23}-8, respectively.

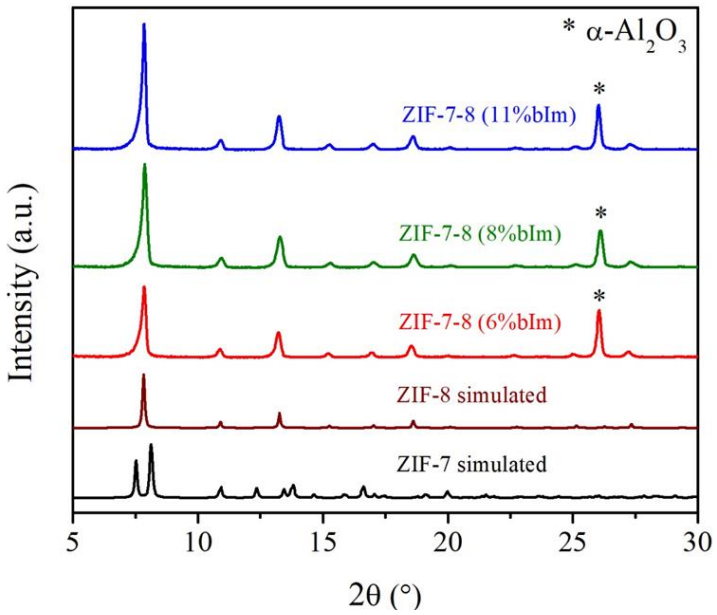

Figure VI-3. X-ray diffraction patterns of mixed linker ZIF-7-8 membranes at various bIm-to-mIm ratios compared with simulated ones of ZIF-7 and ZIF-8.

SEM images of ZIF-7-8 membranes presented in Figure VI-4 show well-intergrown ZIF-7-8 membranes formed on alumina substrates with no visible macroscopic defects. The microwave synthesis enabled rapid nucleation and growth of crystals forming thin films with thicknesses of around 1 - 2 μm. The ZIF-7-8 membranes with higher bIm concentration are slightly thicker, as implied by the stronger peak intensity in the XRD

patterns. The morphology of ZIF-7-8 membranes are similar to that of randomly oriented ZIF-8 membranes,[30, 33-34] agreeing with the XRD results. Interestingly, higher bIm linker (in particular for the ZIF-7_{23}-8) led to membranes with smaller crystal grains as shown on the top view of the SEM images (Figure VI-4e). This indicates that addition of HbIm linker in the precursor solution increases nucleation rate, thereby forming more uniform but smaller crystal grains[183] as illustrated in Figure VI-5. This behavior can be attributed due to difference in the acidities of various imidazole linkers,[162, 184] affecting the crystallization of ZIFs. Protonated bIm linker (i.e., HbIm) has a lower pKa value of 12.8[184] than the protonated 2-mIm (HmIm) of 14.2,[162, 184] allowing more dissociation of HbIm than HmIm. Therefore, addition of HbIm linker to the precursor solution promotes coordination reaction of zinc ions with the deprotonated imidazole linkers (i.e., bIm) for crystallization, which affects the formation of ZIF-7-8 membranes, consequently their morphologies and microstructures (see Figure VI-5a). Furthermore, the relatively high concentration of deprotonated bIm resulted in more incorporation of bIm in the framework relative to HbIm-to-HmIm ratio in the precursor solution (see Figure VI-5b).

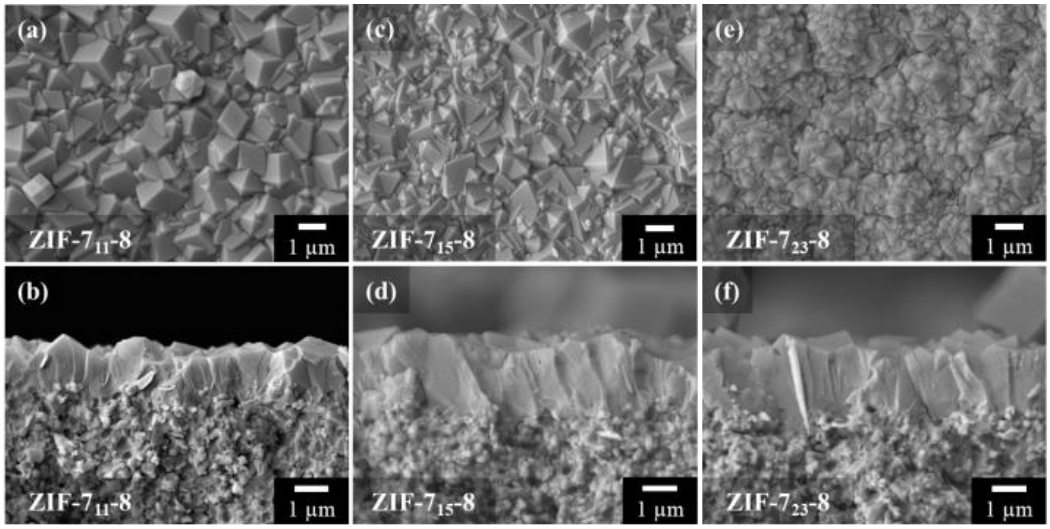

Figure VI-4. Scanning electron microscopy (SEM) images of (a-b) ZIF-7_{11}-8, (c-d) ZIF-7_{15}-8, (e-f) ZIF-7_{23}-8. Top and bottom rows are the surface views and cross-sectional views of the membranes, respectively.

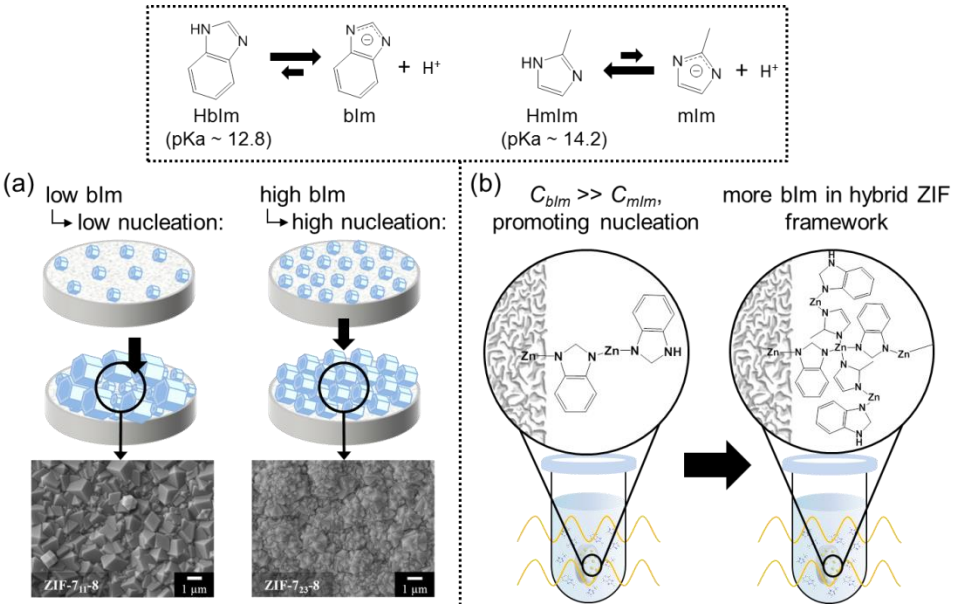

Figure VI-5. Illustration showing lower pKa value of HbIm than HmIm allows more dissociation of HbIm than HmIm leading to two effects: (a) amount of bIm in precursor solution can alter the nucleation rate, which affect the morphologies and microstructures of the ZIF-7-8 membranes. (b) The relatively high concentration of deprotonated bIm resulted in more incorporation of bIm in the framework relative to HbIm-to-HmIm ratio in the precursor solution.

It is worthy of mentioning here that it was not possible to obtain mono-linker ZIF-8 or ZIF-7 membranes one-pot under microwaves. In the case of ZIF-8, as shown in our previous reports,[33, 172] ZIF-8 films consist of ZIF-8 nanoparticles in the range of ~ 100 nm that are well distributed but not intergrown (see Figure VI-6). This strongly suggests the importance of HbIm linker for the rapid one-pot formation of well-intergrown ZIF membranes under microwaves. It is surmised that the promoted nucleation and growth in the presence of HbIm linkers may lead not only to the rapid formation of more nuclei but also to the promotion of intergrowth. Similar observations were made in the case of mono-linker ZIF-7, resulting in the formation of ZIF-7 films of non-uniform crystal size

distribution with the smaller one of ~ 300 nm, much larger than ZIF-8 crystals (~ 100 nm). Interestingly, Zhang et al.[145] also observed the similar difficulties of synthesizing mono-linker Co-ZIF membranes (i.e. Co-ZIF-7 and Co-ZIF-8) while they successfully prepared mixed linker Co-ZIF-7-8 membranes.

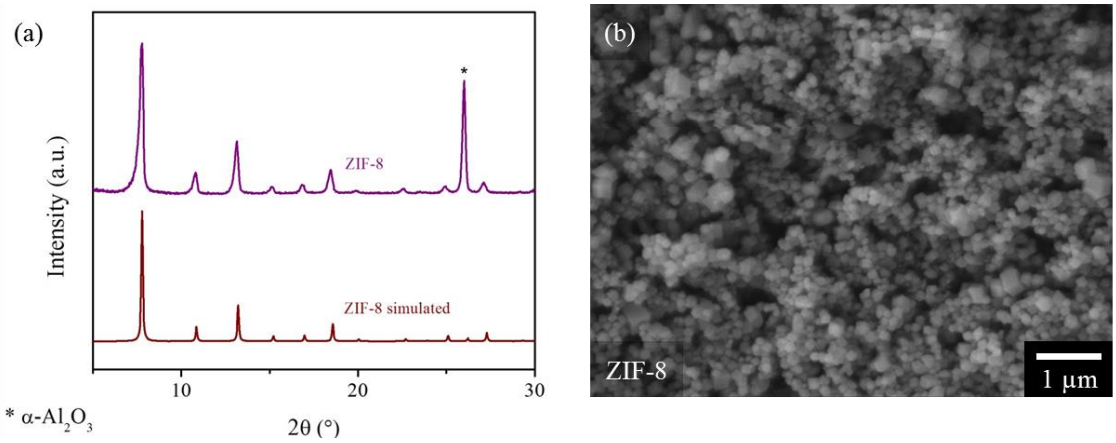

Figure VI-6. (a) XRD patterns and (b) scanning electron microscopy (SEM) images of ZIF-8 prepared using the microwave assisted method in this study.

To study the pore tunability of ZIF-7-8 membranes based on linker ratio variation, the prepared membranes were examined by performing binary gas permeation measurements using the Wicke-Kallenbach technique. Prior to gas permeation testing, it is worth noting the importance of careful activation mixed linker membranes. When mixed linker ZIF-7-8 membranes were activated at 120 °C for 4 hours, cracks were formed throughout the surface of membranes. The crack formation was likely due to the rapid removal of a large organic solvent, DMF (~ 5.5 Å), from the pore of the membranes as previously observed.[122] In order to avoid the crack formation, ZIF-7-8 membranes were

subjected to a controlled activation process as described under the Experimental section. The complete removal of DMF solvents from ZIF-7-8 membranes was confirmed through the absence of DMF signal in the ATR-IR spectra as shown in Figure VI-7.

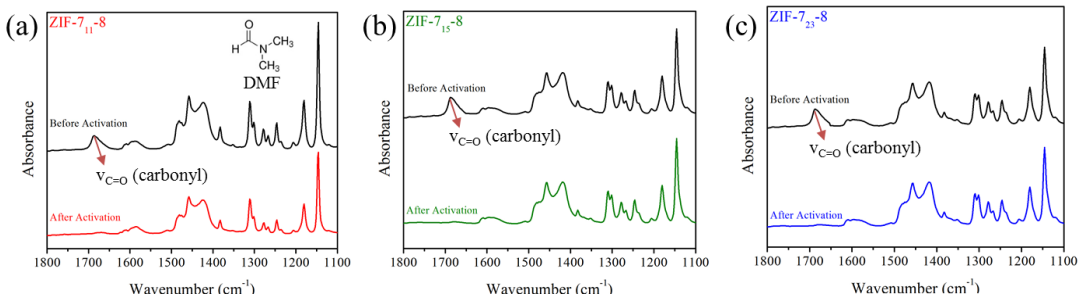

Figure VI-7. ATR-IR spectra comparing before and after activation of (a) ZIF-7$_{11}$-8, (b) ZIF-7$_{15}$-8, and (c) ZIF-7$_{23}$-8 membranes. IR spectra of activated ZIF-7-8 membranes showed the absence of C=O stretching vibration from the dimethylformamide solvent.

Activated ZIF-7-8 membranes were then tested for binary gas permeation performances with a propylene-propane mixture (50/50) as shown in Figure VI-8. Systematic reduction of propylene permeance can be clearly observed with increase of bulkier bIm incorporation, suggesting the reduction in the effective apertures of the ZIF-7-8 membranes.[43] The aperture restriction inhibit the movement of guest molecules through the membranes.[53-54] Interestingly, the propane molecule was not detectable possibly due to the limitation of our instrument. Consequently, single gas permeation measurements were performed using smaller gases such as H_2, CO_2, N_2, and CH_4. The quality of rapidly synthesized ZIF-7-8 membranes were assessed by comparing with

previously reported high-quality ZIF-8 membranes prepared through microwave-assisted seeding and secondary growth (labeled as ZIF-8(SG)).[33]

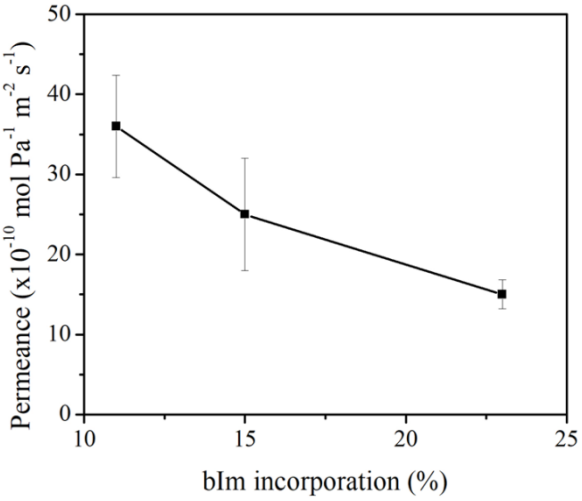

Figure VI-8. Propylene permeance from the binary gas mixture of propylene-propane (50/50) of ZIF-7-8 membranes with varying bIm incorporation to the framework.

The permeances of these small gas molecules (H_2, CO_2, N_2, and CH_4) were reduced while the ideal selectivities were improved with increasing bIm-to-mIm ratios (reduction in pore opening) as shown in Figure VI-9. The permselectivity constitutes of sorption selectivity (thermodynamic partitioning) and diffusion selectivity (kinetic mobility).[62] The sorption selectivity can be derived from adsorption isotherms of the guest molecule on ZIFs, in which Henry's solubility constant may be obtained as a sorption coefficient. The CO_2 and CH_4 isotherms on ZIF-7 and ZIF-8 have been reported previously.[185-186] The Henry's constants of CO_2 and CH_4 at 298 K for ZIF-7 were estimated by Wu et al.[186] as ~ 2.16×10^{-3} and ~ 2.64×10^{-2}, respectively, and for ZIF-8 as ~ 8.0×10^{-4} and ~ 3.4×10^{-4},

respectively. The CO_2/CH_4 sorption selectivities of ZIF-7 and ZIF-8 at 298 K were then evaluated to be ~ 12.22 and ~ 2.35, respectively. This shows the improvement of CO_2/CH_4 ideal selectivity in ZIF-7-8 membranes (Figure VI-9b) may not only be attributed to the reduction in pore opening (diffusive selectivity), but also higher CO_2/CH_4 sorption selectivity of ZIF-7 over ZIF-8.

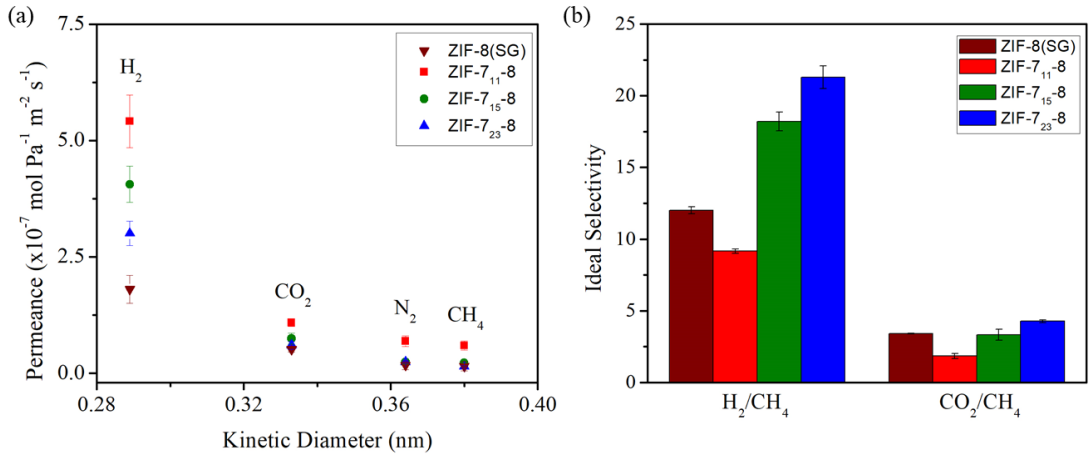

Figure VI-9. (a) Single gas permeances of various gases on the mixed linker ZIF-7-8 and ZIF-8(SG) membranes at 298 K and 1 bar as a function of the kinetic diameter. (b) Ideal selectivity of H_2/CH_4 and CO_2/CH_4 on ZIF-7-8 and ZIF-8(SG) membranes. ZIF-8(SG) membranes were prepared through microwave seeding followed by secondary growth as reported elsewhere.[33]

Finally, binary gas permeation measurements with H_2/CH_4 and CO_2/CH_4 equimolar mixtures were performed on mixed linker ZIF-7-8 membranes. As shown in Figure VI-10, both H_2 and CO_2 separation factors increased systematically as more bIm was incorporated, strongly suggesting the continuous tunability of molecular sieving

properties of hybrid ZIF membranes through variation of bIm-to-mIm ratio in the mixed linker membranes. The separation factor of CO_2/CH_4 for the ZIF-7_{11}-8 (low bIm incorporation) is comparable to the Knudsen selectivity $\alpha_{CO_2/CH_4} = \sqrt{m_{CO_2}/m_{CH_4}} = 1.66$. Interestingly, reduction in H_2/CH_4 separation factor of ZIF-7-8 membranes was observed when compared to the ideal selectivity from single gas permeation tests. This is possibly due to the hindrance on the diffusion of highly mobile H_2 molecules[117] through the reduced apertures of ZIF-7-8 membranes by the slower and larger CH_4 molecules. When compared to the mono-linker ZIF membranes (ZIF-7[163-164] and ZIF-8[30, 140, 166-167, 187-191]), the mixed linker ZIF-7-8 membranes prepared through the rapid microwave process still exhibit comparative performance for both H_2/CH_4 and CO_2/CH_4 gas separations as shown in Figure VI-11. This suggests the fast microwave in situ synthesis yielded good quality ZIF-7-8 membranes.

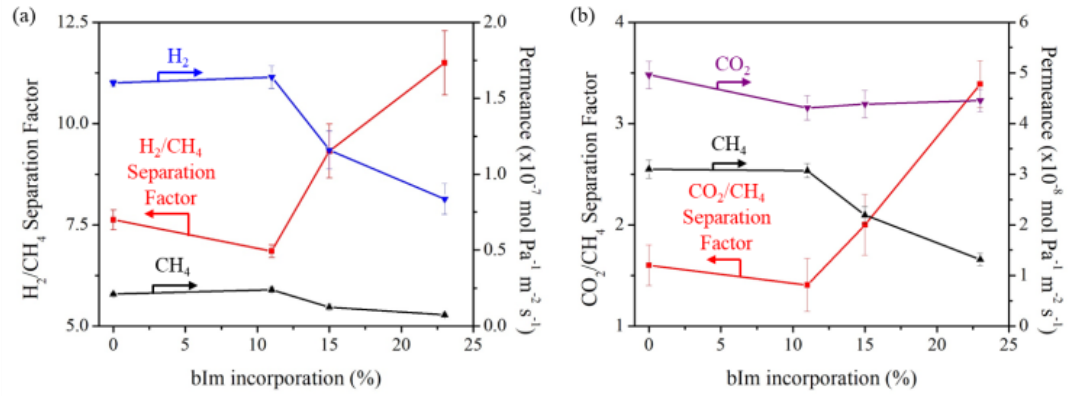

Figure VI-10. Binary testing of (a) H_2/CH_4 and (b) CO_2/CH_4 for ZIF-7-8 membranes with varying bIm incorporation.

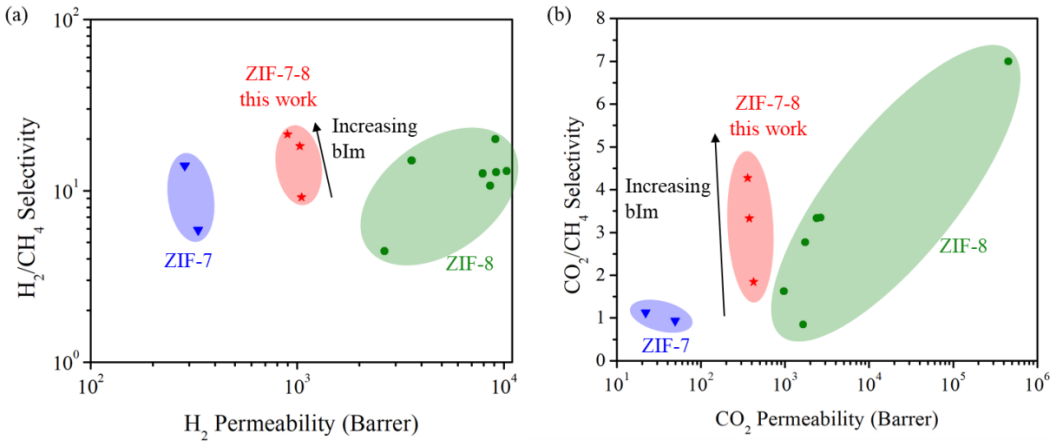

Figure VI-11. Comparison of (a) H_2/CH_4 and (b) CO_2/CH_4 separation performance for mixed linker ZIF-7-8 membranes with the parent ZIF membranes (ZIF-7[163-164] and ZIF-8[30, 140, 166-167, 187-191]). 1 Barrer = 3.348×10^{-16} mol m m^{-2} s^{-1} Pa^{-1}

VI.4. **Conclusions**

In this report, well-intergrown hybrid ZIF membranes with 2-methylimidazolate (mIm) and benzimidazolate (bIm) linkers (termed ZIF-7-8 membranes) were synthesized *in situ* under rapid microwave heating in less than ~ 90 seconds. To the best of our knowledge, this is the fastest preparation of polycrystalline MOF membranes. The presence of HbIm linker in the synthesis solution was found critical to obtain high-quality ZIF membranes one pot under microwaves. Permeation tests of hybrid ZIF membranes showed the systematic tuning in the separation performances. This is attributed to the fact that an increase of bulky benzimidazolate linker incorporation reduces the effective aperture size of the hybrid framework, consequently improving the separation factor at the expense of reduction in permeance. The unprecedented rapid one-pot synthesis of well-

intergrown ZIF-7-8 membranes with tunable molecular sieving properties is an important step forward for their practical applications in the separation of gas mixtures of interest.

CHAPTER VII

CONCLUSION

VII.1. **Conclusions**

In this dissertation, we successfully developed three synthesis techniques for various hybrid ZIFs crystals by utilizing the microwave irradiation. The microwave-assisted approach significantly shortens synthesis time and produces a higher yield as compared to traditional synthesis. Furthermore, for the first time, we were able to obtain hybrid ZIFs with mixed metals and mixed linkers (i.e. CoZn-ZIF-7-8) through one-step microwave. Some doped ZIFs, such as eim/ZIF-8 and phIm/ZIF-8, were also successfully obtained through one-step microwave-assisted synthesis, which were previously failed through conventional approach.[64] Furthermore, we successfully fabricated a high quality mixed metal CoZn-ZIF-8 polycrystalline membrane showing improved propylene/propane separation performance. We were able to adopt the microwave technique to significantly reduce the synthesis of mixed linker ZIF-7-8 membranes through one-pot method to under 90 seconds.

The hybrid ZIFs reported here showed interesting tunable framework properties. For example, the "stiffness" of metal-nitrogen bond can be improved continuously as more Co is incorporated in the framework of the mixed metal CoZn-ZIF-8. As a result, the effective pore apertures can be finely tuned by varying the Co to Zn ratio. Thus, the

fabricated mixed metal CoZn-ZIF-8 membranes showed an improved separation factor performance when compared to the pristine Zn-ZIF-8 membranes owing to the incorporation of Co that reduces the effective pore apertures of the mixed metal framework. The eIm/ZIF-8 and phIm/ZIF-8 synthesized through the linker-doping strategy displayed alteration in their framework properties. IR spectra showed that M-N bonding vibration were blue-shifted with incorporation of dopant linker. Furthermore, the doping of 2-eIm introduce constriction in the framework flexibility. For example, the nitrogen physisorption isotherms for eIm/ZIF-8 showed an increase in threshold pressure to initiate the "gate-opening" motion owing to a bulkier dopant 2-eIm linker than the original 2-mIm linker. Furthermore, the eIm/ZIF-8 also displayed an increase in the initial uptake pressure for the CH_4 gas adsorption isotherms.

The fabricated hybrid linker ZIF polycrystalline membranes also displayed tunable framework properties and membrane morphology. For example, the permeation tests of ZIF-7-8 membranes showed the systematic tuning in the separation performance attributed to the fact that an increase in bulky benzimidazole linker incorporation reduces the effective aperture size of the hybrid framework. Consequently, the separation factor is improved at the expense of reduction in permeance.

It is worth noting that aside from the tunable framework properties, the hybrid approach affects the morphology of the crystal formation. This can be expected as different metal salts and imidazolate linkers would have varying properties (e.g. pH, size, preferred coordination for metal center, etc.). As a result, the crystal sizes and distribution

could be altered with the presence of secondary metals and/or linkers. The morphology of the polycrystalline membranes have also been shown to be affected significantly due to presence of secondary linker. For example, the membrane thickness were shown to be reduced with incorporation of eIm dopant into the framework, increasing membrane productivity. Furthermore, both mixed linker ZIF-7-8 membranes and linker-doped eIm/ZIF-8 membranes displayed a smaller crystal grain with crystal intergrown as compared to the pristine ZIF-8 membranes. These crystal intergrown may cause increased in the grain boundaries which could jeopardize the separation performance of these polycrystalline hybrid ZIF membranes.

VII.2. **Perspective in using hybrid ZIF deriving from ZIF-8 for gas separations**

The SOD cage consists of eight six-member ring (6-MR) and six four-member ring (4-MR). Gas diffusion through ZIF-8 involves molecular jumping from one SOD cage to another which is mainly governed by the pore apertures of 6-MR. As illustrated in Figure VII-1a, the effective diameter of these pore apertures is influenced by the distance between the closest CH group hydrogens of two neighboring linkers.[111, 126] Thus, the three alternating imidazolate linkers with the C4 and C5 pointing toward the center of 6-MR mainly contributed to the effective pore apertures. However, this should not exclude the importance in modification of C2 position as it has been shown to modify the effective pore apertures of the 6-MR as well.[43] This brings attention to the importance in location of secondary M/L within the 6-MR. For example, there are multiple combination to arrange the location of three secondary M/L within the 6-MR as illustrated in Figure 3c

and d. It is not surprising that series distribution (Figure VII-1d) would have different effective pore apertures than alternating placement (Figure VII-1c) of the secondary M/L. While it is not an easy task to control the location of these secondary linkers, steric hindrance could be inferred as the main influence that guide their location. Krokidas et al.[192] have performed density functional theory (DFT) calculations showing non-uniform linker distribution reveals higher energies as compared to random ones. On the other hand, Goodwin and co-worker[92] have found evidence of compositional inhomogeneity in mixed metal CdZn-ZIF-8 (dual metal Cd^{2+} and Zn^{2+} of ZIF-8), which affect the framework aperture characteristics. They integrated non-negative matrix factorization (NMF) analysis with infrared spectroscopy data and identified the tendency of homometallic clustering.[92]

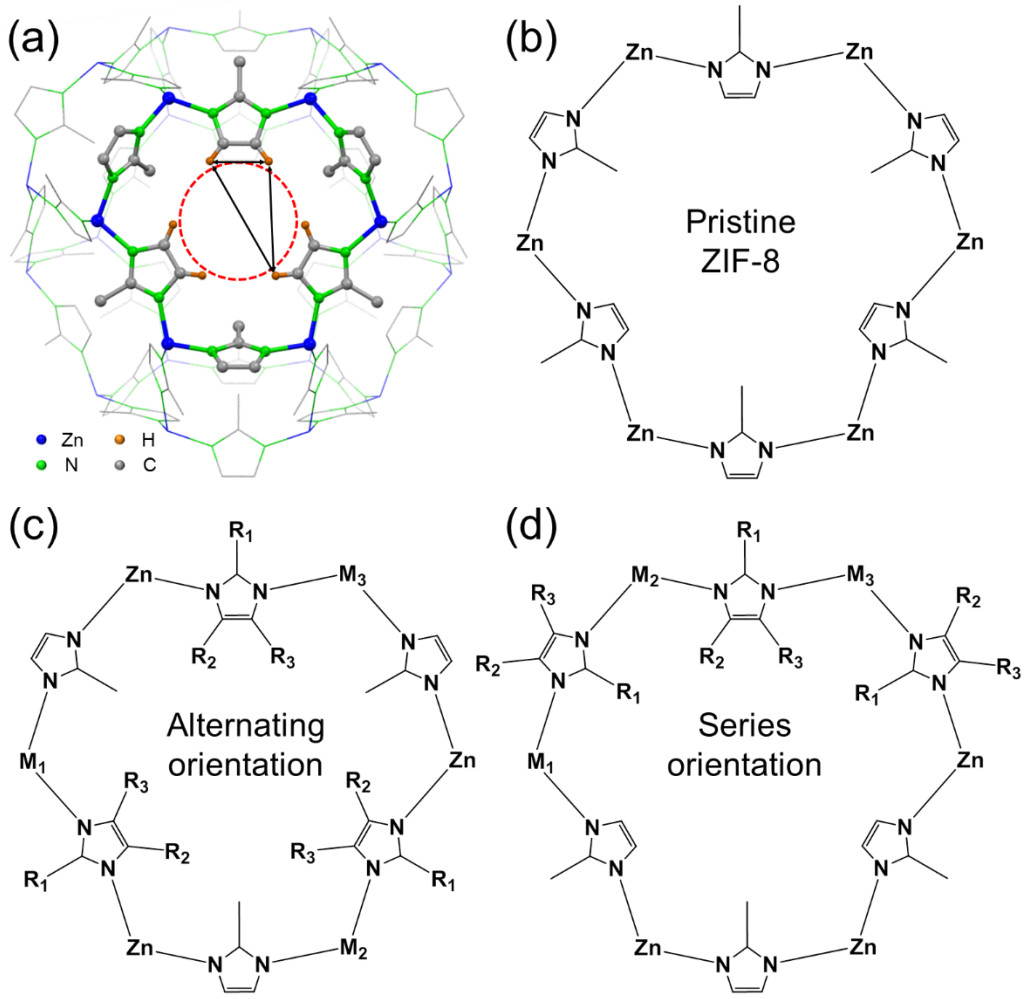

Figure VII-1. (a) Effective pore aperture diameter of 6-MR in ZIF-8 (i.e. red circular dotted line) is influenced by the distance between the closest CH group hydrogens of two neighboring linkers (i.e. black arrow lines);[126] and illustration of 6-MR in SOD cage of (b) pristine ZIF-8, and hybrid ZIF-8 with (c) alternating and (d) series orientation of secondary M/L.

The distribution of secondary linker is even more crucial in modifying the gas diffusivity through the hybrid frameworks. A successful modification can be expected with at least one secondary linker in all eight 6-MR of the SOD cage, and preferably with

linker placement where the C4 and C5 of the secondary linker is pointing toward the center of 6-MR. For example, substitution of 2-mIm linker in ZIF-8 with bulkier bIm linker is expected to reduce the pore aperture of the framework.[41, 53] However, at least one mIm linker need to be replaced from all eight 6-MR available in the SOD cage to have a reduction pore apertures that effectively improve the selectivity of the hybrid framework.[192] 6-MR in absence of bIm linker can be considered as defective windows of the SOD cage where mixture of penetrants can diffuse through these windows non-selectively. Furthermore, it is desirable for the bIm linker to have its benzene ring pointing toward the center of 6-MR to adequately reduce the effective pore apertures of the SOD cage.

The critical requirement of modifying gas diffusivity through mixed linker approach could explain the unexpectedly moderate improvement in separation factor of various binary gas mixtures through the mixed linker ZIF-7-8 membranes recently reported by our group.[41] Although considerable amount of bIm linker (up to 23%) were successfully incorporated in the mixed linker membranes,[41] it may not be enough to modify all eight 6-MR in the hybrid SOD cages. Krokidas et al.[192] recently reported a further analysis through computational studies in the effect of linker distribution and ratio of ZIF-7-8 on penetrants diffusivity through the hybrid frameworks. Considering that there are two cages in one unit cell of ZIF-8 and a total of 24 linkers in one SOD cage,[29] a minimum of 33% bIm linker replacement is necessary to incorporate at least one bIm linker in all eight 6-MR and modify the penetrants diffusivity through the hybrid

frameworks. Diffusivity study clearly shows that below the 33% replacement threshold the separation performance is ruined severely by the presence of at least one all-mIm 6-MR apertures (ZIF-8-alike apertures), which keep the overall diffusivity ratio of penetrants at low levels.[192]

Aside from M/L distribution in the hybrid frameworks, there are more points that need to be considered from the effect of mixing M/L in fabricating hybrid ZIF polycrystalline membranes for gas separations. First, it is reasonable to surmise that incorporation of foreign M/L, with different sizes, can introduce distortion in the hybrid frameworks,[53] which yields more defects[193-194] (i.e. linker vacancy, metal center vacancy, and dangling linker) compromising the separation performance and stability of the membranes.

Secondly, secondary M/L introduce new crystallization rate (nucleation and growth),[41-42, 53, 195] impacting the morphology and microstructure of the membranes. For example, the presence of protonated bIm linker, with lower pKa value than protonated mIm linker, increases both crystal growth and nucleation rate, thereby forming thicker mixed linker ZIF-7-8 membranes with smaller crystal grains than pristine ZIF-8 ones.[41] Furthermore, different metal centers with various sizes and bonding stability with the imidazolate linker could also impact the crystallization rate,[42, 195] which may impose morphological change in the fabrication of mixed metal ZIF membranes. While the thickness of the membranes certainly contributes to the gas permeances through the membranes, the size of the crystal grains may also affect the gas separation performance.

The formation of polycrystalline membranes consist of overgrown crystal grains into each other, in which small crystal grains present more grain boundaries that can be a weakness point for defect formation.[196-198] It is worth noting that varying the M/L ratio could essentially affect the crystallization rate. Therefore, a synthesis procedure that works for one M/L ratio to fabricate well-intergrown hybrid ZIF membranes may not work for other M/L ratio.

Thirdly, the variation in M/L ratio among the hybrid crystal grains throughout the polycrystalline layer may influence the effective diffusion through the membranes as illustrated in Figure VII-2. Berens et al.[199] recently reported evidences for a distribution over ethane diffusivities among ZIF-7-8 crystals synthesized from the same batch. Therefore, it is not unlikely for the possibility in variation of M/L ratio among the seed crystals which are continuously grown into uneven distribution of hybrid crystal grains throughout the polycrystalline layer as illustrated in Figure VII-2. Differences in M/L ratio among the crystal grains poses uneven gas transport throughout the hybrid ZIF polycrystalline membranes affecting their gas separation performance.

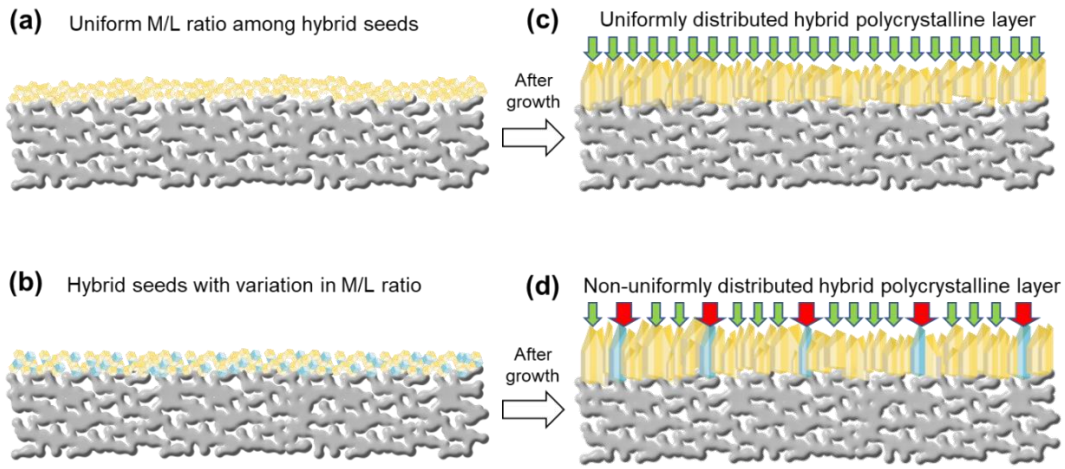

Figure VII-2. Illustration of hybrid crystal seeds on ceramic support with (a) uniform and (b) non-uniform M/L ratio represented by yellow and blue crystals, respectively; follow by continuous growth into (c) uniformly and (d) non-uniformly distributed hybrid polycrystalline layer with uniform M/L ratio, whereas red arrows represent non-uniform gas transport through hybrid polycrystalline layer with non-uniform M/L ratio among the crystal grains.

Fourthly, the distribution of secondary M/L within the hybrid crystal grain can affect the framework properties as well. For example, mixed linker ZIF with random linker distribution throughout the hybrid crystals have different adsorption properties than the same mixed linker ZIF with unique yolk-shell structure[85] (as previously mentioned in "General synthesis approach for hybrid ZIFs" section). Interestingly, our group have shown the outer-shell modification can be a mean to alter the effective thickness of polycrystalline ZIF membranes, which can alter their gas separation performance.[200]

REFERENCES

(1) Lin, J. Y. S. Molecular sieves for gas separation. *Science* **2016,** *353* (6295), 121-122.

(2) Lively, R. P.; Sholl, D. S. From water to organics in membrane separations. *Nat Mater* **2017,** *16* (3), 276-279.

(3) Sholl, D. S.; Lively, R. P. Seven Chemical Separations to Change the World. *Nature* **2016,** *532*, 435-437.

(4) Humphrey, J. L.; Keller II, G. E. *Separation Process Technology*, McGraw-Hill: **1997**.

(5) *Materials for Separation Technologies: Energy and Emission Reduction Opportunities*; Oak Ridge National Laboratory: Oak Ridge, TN, **2005**.

(6) Melillo, J. T., Richmond; Yohe, Gary *Climate Change Impacts in the United States: The Third National Climate Assessment*; **2014**.

(7) Stocker, T. F. Q., D., Plattner, G-.K.; Tignor, M.; Allen, S.K.; Boschung, J.; Nauels, A.; Xia, Y.; Bex, V.; Midgley, P. M. *Climate Change 2013: The Physical Science Basis*; Cambridge, United Kindom and New York, USA, **2013**.

(8) Lutz, W.; Muttarak, R. Forecasting societies' adaptive capacities through a demographic metabolism model. *Nature Clim. Change* **2017,** *7* (3), 177-184.

(9) Freemantle, M. Advanced organic and inorganic materials being developed for separtions offer cost benefits for environmental and energy-related processes. *Chem. Eng. News* **2005,** *83* (40), 49-57.

(10) Robeson, L. M. Correlation of separation factor versus permeability for polymeric membranes. *Journal of Membrane Science* **1991,** *62* (2), 165-185.

(11) Robeson, L. M. The upper bound revisited. *Journal of Membrane Science* **2008,** *320* (1–2), 390-400.

(12) Dechnik, J.; Gascon, J.; Doonan, C. J.; Janiak, C.; Sumby, C. J. Mixed-Matrix Membranes. *Angewandte Chemie International Edition* **2017,** *56* (32), 9292-9310.

(13) Suleman, M. S.; Lau, K. K.; Yeong, Y. F. Plasticization and Swelling in Polymeric Membranes in CO2 Removal from Natural Gas. *Chemical Engineering & Technology* **2016,** *39* (9), 1604-1616.

(14) Wessling, M.; Schoeman, S.; van der Boomgaard, T.; Smolders, C. A. Plasticization of gas separation membranes. *Gas Separation & Purification* **1991,** *5* (4), 222-228.

(15) Petropoulos, J. H. Plasticization effects on the gas permeability and permselectivity of polymer membranes. *Journal of Membrane Science* **1992,** *75* (1), 47-59.

(16) Caro, J.; Noack, M. Zeolite membranes – Recent developments and progress. *Microporous and Mesoporous Materials* **2008,** *115* (3), 215-233.

(17) Kang, Z.; Fan, L.; Sun, D. Recent advances and challenges of metal-organic framework membranes for gas separation. *J. Mater. Chem. A* **2017,** *5* (21), 10073-10091.

(18) Koros, W. J. Some opportunities & challenges for our membrane community to consider—with an emphasis on gas separations. *Membrane Science and Technology* **2006,** *26* (4), 0001-05.

(19) Burrows, A. D. Mixed-component metal-organic frameworks (MC-MOFs): enhancing functionality through solid solution formation and surface modifications. *CrystEngComm* **2011,** *13* (11), 3623-3642.

(20) Dhakshinamoorthy, A.; Asiri, A. M.; Garcia, H. Mixed-metal or mixed-linker metal organic frameworks as heterogeneous catalysts. *Catalysis Science & Technology* **2016,** *6* (14), 5238-5261.

(21) Goh, P. S.; Ismail, A. F.; Sanip, S. M.; Ng, B. C.; Aziz, M. Recent advances of inorganic fillers in mixed matrix membrane for gas separation. *Separation and Purification Technology* **2011,** *81* (3), 243-264.

(22) Bastani, D.; Esmaeili, N.; Asadollahi, M. Polymeric mixed matrix membranes containing zeolites as a filler for gas separation applications: A review. *Journal of Industrial and Engineering Chemistry* **2013,** *19* (2), 375-393.

(23) Jusoh, N.; Yeong, Y. F.; Chew, T. L.; Lau, K. K.; Shariff, A. M. Current Development and Challenges of Mixed Matrix Membranes for CO2/CH4 Separation. *Separation & Purification Reviews* **2016,** *45* (4), 321-344.

(24) Chung, T.-S.; Jiang, L. Y.; Li, Y.; Kulprathipanja, S. Mixed matrix membranes (MMMs) comprising organic polymers with dispersed inorganic fillers for gas separation. *Progress in Polymer Science* **2007,** *32* (4), 483-507.

(25) Vinh-Thang, H.; Kaliaguine, S. Predictive Models for Mixed-Matrix Membrane Performance: A Review. *Chem. Rev.* **2013,** *113* (7), 4980-5028.

(26) Aroon, M. A.; Ismail, A. F.; Matsuura, T.; Montazer-Rahmati, M. M. Performance studies of mixed matrix membranes for gas separation: A review. *Separation and Purification Technology* **2010,** *75* (3), 229-242.

(27) Galizia, M.; Chi, W. S.; Smith, Z. P.; Merkel, T. C.; Baker, R. W.; Freeman, B. D. 50th Anniversary Perspective: Polymers and Mixed Matrix Membranes for Gas and Vapor Separation: A Review and Prospective Opportunities. *Macromolecules* **2017,** *50* (20), 7809-7843.

(28) Dong, G.; Li, H.; Chen, V. Challenges and opportunities for mixed-matrix membranes for gas separation. *J. Mater. Chem. A* **2013,** *1* (15), 4610-4630.

(29) Park, K. S.; Ni, Z.; Cote, A. P.; Choi, J. Y.; Huang, R.; Uribe-Romo, F. J.; Chae, H. K.; O'Keeffe, M.; Yaghi, O. M. Exceptional chemical and thermal stability of zeolitic imidazolate frameworks. *Proc. Natl. Acad. Sci. U. S. A.* **2006,** *103* (27), 10186-10191.

(30) Pan, Y.; Lai, Z. Sharp separation of C2/C3 hydrocarbon mixtures by zeolitic imidazolate framework-8 (ZIF-8) membranes synthesized in aqueous solutions. *Chem. Comm.* **2011,** *47* (37), 10275-10277.

(31) Zhang, C.; Lively, R. P.; Zhang, K.; Johnson, J. R.; Karvan, O.; Koros, W. J. Unexpected Molecular Sieving Properties of Zeolitic Imidazolate Framework-8. *The Journal of Physical Chemistry Letters* **2012,** *3* (16), 2130-2134.

(32) Li, K.; Olson, D. H.; Seidel, J.; Emge, T. J.; Gong, H.; Zeng, H.; Li, J. Zeolitic Imidazolate Frameworks for Kinetic Separation of Propane and Propene. *J. Am. Chem. Soc.* **2009,** *131* (30), 10368-10369.

(33) Kwon, H. T.; Jeong, H.-K. Highly propylene-selective supported zeolite-imidazolate framework (ZIF-8) membranes synthesized by rapid microwave-assisted seeding and secondary growth. *Chem. Comm.* **2013,** *49* (37), 3854-3856.

(34) Kwon, H. T.; Jeong, H.-K. In Situ Synthesis of Thin Zeolitic–Imidazolate Framework ZIF-8 Membranes Exhibiting Exceptionally High Propylene/Propane Separation. *J. Am. Chem. Soc.* **2013,** *135* (29), 10763-10768.

(35) Kwon, H. T.; Jeong, H.-K. Improving propylene/propane separation performance of Zeolitic-Imidazolate framework ZIF-8 Membranes. *Chem. Eng. Sci.* **2015,** *124*, 20-26.

(36) Kwon, H. T.; Jeong, H.-K.; Lee, A. S.; An, H. S.; Lee, J. S. Heteroepitaxially Grown Zeolitic Imidazolate Framework Membranes with Unprecedented Propylene/Propane Separation Performances. *J. Am. Chem. Soc.* **2015,** *137* (38), 12304-12311.

(37) Pan, Y.; Li, T.; Lestari, G.; Lai, Z. Effective separation of propylene/propane binary mixtures by ZIF-8 membranes. *Journal of Membrane Science* **2012,** *390–391*, 93-98.

(38) Zhou, H.-C.; Long, J. R.; Yaghi, O. M. Introduction to Metal–Organic Frameworks. *Chem. Rev.* **2012,** *112* (2), 673-674.

(39) Li, J.-R.; Kuppler, R. J.; Zhou, H.-C. Selective gas adsorption and separation in metal-organic frameworks. *Chem. Soc. Rev.* **2009,** *38* (5), 1477-1504.

(40) James, S. L. Metal-organic frameworks. *Chem. Soc. Rev.* **2003,** *32* (5), 276-288.

(41) Hillman, F.; Brito, J.; Jeong, H.-K. Rapid One-Pot Microwave Synthesis of Mixed-Linker Hybrid Zeolitic-Imidazolate Framework Membranes for Tunable Gas Separations. *ACS Applied Materials & Interfaces* **2018,** *10* (6), 5586-5593.

(42) Hillman, F.; Zimmerman, J. M.; Paek, S.-M.; Hamid, M. R. A.; Lim, W. T.; Jeong, H.-K. Rapid microwave-assisted synthesis of hybrid zeolitic-imidazolate frameworks with mixed metals and mixed linkers. *J. Mater. Chem. A* **2017,** *5* (13), 6090-6099.

(43) Eum, K.; Jayachandrababu, K. C.; Rashidi, F.; Zhang, K.; Leisen, J.; Graham, S.; Lively, R. P.; Chance, R. R.; Sholl, D. S.; Jones, C. W.; Nair, S. Highly Tunable Molecular Sieving and Adsorption Properties of Mixed-Linker Zeolitic Imidazolate Frameworks. *J. Am. Chem. Soc.* **2015,** *137* (12), 4191-4197.

(44) Zhang, J.-P.; Zhu, A.-X.; Lin, R.-B.; Qi, X.-L.; Chen, X.-M. Pore Surface Tailored SOD-Type Metal-Organic Zeolites. *Advanced Materials* **2011,** *23* (10), 1268-1271.

(45) Banerjee, R.; Furukawa, H.; Britt, D.; Knobler, C.; O'Keeffe, M.; Yaghi, O. M. Control of Pore Size and Functionality in Isoreticular Zeolitic Imidazolate Frameworks and their Carbon Dioxide Selective Capture Properties. *J. Am. Chem. Soc.* **2009,** *131* (11), 3875-3877.

(46) Banerjee, R.; Phan, A.; Wang, B.; Knobler, C.; Furukawa, H.; O'Keeffe, M.; Yaghi, O. M. High-Throughput Synthesis of Zeolitic Imidazolate Frameworks and Application to CO2 Capture. *Science* **2008,** *319* (5865), 939-943.

(47) Phan, A.; Doonan, C. J.; Uribe-Romo, F. J.; Knobler, C. B.; O'Keeffe, M.; Yaghi, O. M. Synthesis, Structure, and Carbon Dioxide Capture Properties of Zeolitic Imidazolate Frameworks. *Acc. Chem. Res.* **2010,** *43* (1), 58-67.

(48) Kaur, G.; Rai, R. K.; Tyagi, D.; Yao, X.; Li, P.-Z.; Yang, X.-C.; Zhao, Y.; Xu, Q.; Singh, S. K. Room-temperature synthesis of bimetallic Co-Zn based zeolitic imidazolate

frameworks in water for enhanced CO2 and H2 uptakes. *J. Mater. Chem. A* **2016,** *4*, 14932-14938.

(49) Chen, Y.-Z.; Wang, C.; Wu, Z.-Y.; Xiong, Y.; Xu, Q.; Yu, S.-H.; Jiang, H.-L. From Bimetallic Metal-Organic Framework to Porous Carbon: High Surface Area and Multicomponent Active Dopants for Excellent Electrocatalysis. *Advanced Materials* **2015,** *27* (34), 5010-5016.

(50) Roshan, R. K.; Babu, R.; Jeong, H.-M.; Hwang, G.-Y.; Jeong, G.-S.; Kim, M.-I.; Kim, D.; Park, D.-W. A solid solution zeolitic imidazolate framework as a room temperature efficient catalyst for the chemical fixation of CO2. *Green Chem.* **2016,** *18* (23), 6349-6356.

(51) Wu, T.; Bu, X.; Zhang, J.; Feng, P. New Zeolitic Imidazolate Frameworks: From Unprecedented Assembly of Cubic Clusters to Ordered Cooperative Organization of Complementary Ligands. *Chem. Mater.* **2008,** *20* (24), 7377-7382.

(52) Kahr, J.; Mowat, J. P. S.; Slawin, A. M. Z.; Morris, R. E.; Fairen-Jimenez, D.; Wright, P. A. Synthetic control of framework zinc purinate crystallisation and properties of a large pore, decorated, mixed-linker RHO-type ZIF. *Chem. Comm.* **2012,** *48* (53), 6690-6692.

(53) Thompson, J. A.; Blad, C. R.; Brunelli, N. A.; Lydon, M. E.; Lively, R. P.; Jones, C. W.; Nair, S. Hybrid Zeolitic Imidazolate Frameworks: Controlling Framework Porosity and Functionality by Mixed-Linker Synthesis. *Chem. Mater.* **2012,** *24* (10), 1930-1936.

(54) Thompson, J. A.; Brunelli, N. A.; Lively, R. P.; Johnson, J. R.; Jones, C. W.; Nair, S. Tunable CO2 Adsorbents by Mixed-Linker Synthesis and Postsynthetic Modification of Zeolitic Imidazolate Frameworks. *The Journal of Physical Chemistry C* **2013,** *117* (16), 8198-8207.

(55) Huang, L.; Xue, M.; Song, Q.; Chen, S.; Pan, Y.; Qiu, S. Carbon dioxide selective adsorption within a highly stable mixed-ligand Zeolitic Imidazolate Framework. *Inorg. Chem. Commun.* **2014,** *46*, 9-12.

(56) Liao, Y.-T.; Dutta, S.; Chien, C.-H.; Hu, C.-C.; Shieh, F.-K.; Lin, C.-H.; Wu, K. C.-W. Synthesis of Mixed-Ligand Zeolitic Imidazolate Framework (ZIF-8-90) for CO2 Adsorption. *Journal of Inorganic and Organometallic Polymers and Materials* **2015,** *25* (2), 251-258.

(57) Rashidi, F.; Blad, C. R.; Jones, C. W.; Nair, S. Synthesis, characterization, and tunable adsorption and diffusion properties of hybrid ZIF-7-90 frameworks. *AIChE J.* **2016,** *62* (2), 525-537.

(58) Khan, N. A.; Jhung, S. H. Synthesis of metal-organic frameworks (MOFs) with microwave or ultrasound: Rapid reaction, phase-selectivity, and size reduction. *Coord. Chem. Rev.* **2015,** *285*, 11-23.

(59) Hobday, C. L.; Bennett, T. D.; Fairen-Jimenez, D.; Graham, A. J.; Morrison, C. A.; Allan, D. R.; Düren, T.; Moggach, S. A. Tuning the Swing Effect by Chemical

Functionalization of Zeolitic Imidazolate Frameworks. *J. Am. Chem. Soc.* **2018,** *140* (1), 382-387.

(60) Lee, Y.-R.; Jang, M.-S.; Cho, H.-Y.; Kwon, H.-J.; Kim, S.; Ahn, W.-S. ZIF-8: A comparison of synthesis methods. *Chemical Engineering Journal* **2015,** *271*, 276-280.

(61) Pan, Y.; Liu, Y.; Zeng, G.; Zhao, L.; Lai, Z. Rapid synthesis of zeolitic imidazolate framework-8 (ZIF-8) nanocrystals in an aqueous system. *Chem. Comm.* **2011,** *47* (7), 2071-2073.

(62) Koros, W. J.; Zhang, C. Materials for next-generation molecularly selective synthetic membranes. *Nat Mater* **2017,** *16* (3), 289-297.

(63) Krokidas, P.; Castier, M.; Moncho, S.; Sredojevic, D. N.; Brothers, E. N.; Kwon, H. T.; Jeong, H.-K.; Lee, J. S.; Economou, I. G. ZIF-67 Framework: A Promising New Candidate for Propylene/Propane Separation. Experimental Data and Molecular Simulations. *The Journal of Physical Chemistry C* **2016,** *120* (15), 8116-8124.

(64) Huang, X.-C.; Lin, Y.-Y.; Zhang, J.-P.; Chen, X.-M. Ligand-Directed Strategy for Zeolite-Type Metal–Organic Frameworks: Zinc(II) Imidazolates with Unusual Zeolitic Topologies. *Angewandte Chemie International Edition* **2006,** *45* (10), 1557-1559.

(65) Karagiaridi, O.; Bury, W.; Sarjeant, A. A.; Stern, C. L.; Farha, O. K.; Hupp, J. T. Synthesis and characterization of isostructural cadmium zeolitic imidazolate frameworks via solvent-assisted linker exchange. *Chem. Sci.* **2012,** *3* (11), 3256-3260.

(66) Karagiaridi, O.; Lalonde, M. B.; Bury, W.; Sarjeant, A. A.; Farha, O. K.; Hupp, J. T. Opening ZIF-8: A Catalytically Active Zeolitic Imidazolate Framework of Sodalite Topology with Unsubstituted Linkers. *J. Am. Chem. Soc.* **2012,** *134* (45), 18790-18796.

(67) Zhang, C.; Koros, W. J. Tailoring the Transport Properties of Zeolitic Imidazolate Frameworks by Post-Synthetic Thermal Modification. *ACS Applied Materials & Interfaces* **2015,** *7* (42), 23407-23411.

(68) Liu, X.; Li, Y.; Ban, Y.; Peng, Y.; Jin, H.; Bux, H.; Xu, L.; Caro, J.; Yang, W. Improvement of hydrothermal stability of zeolitic imidazolate frameworks. *Chem. Comm.* **2013,** *49* (80), 9140-9142.

(69) Fei, H.; Cahill, J. F.; Prather, K. A.; Cohen, S. M. Tandem Postsynthetic Metal Ion and Ligand Exchange in Zeolitic Imidazolate Frameworks. *Inorg. Chem.* **2013,** *52* (7), 4011-4016.

(70) Ban, Y.; Peng, Y.; Zhang, Y.; Jin, H.; Jiao, W.; Guo, A.; Wang, P.; Li, Y.; Yang, W. Dual-ligand zeolitic imidazolate framework crystals and oriented films derived from metastable mono-ligand ZIF-108. *Microporous and Mesoporous Materials* **2016,** *219,* 190-198.

(71) Morris, W.; Doonan, C. J.; Furukawa, H.; Banerjee, R.; Yaghi, O. M. Crystals as Molecules: Postsynthesis Covalent Functionalization of Zeolitic Imidazolate Frameworks. *J. Am. Chem. Soc.* **2008,** *130* (38), 12626-12627.

(72) Liu, C.; Liu, Q.; Huang, A. A superhydrophobic zeolitic imidazolate framework (ZIF-90) with high steam stability for efficient recovery of bioalcohols. *Chem. Comm.* **2016,** *52* (16), 3400-3402.

(73) Bernt, S.; Feyand, M.; Modrow, A.; Wack, J.; Senker, J.; Stock, N. [Zn(C3H3N2)(C3H2N2–N=N–C6H5)], a Mixed-Linker ZIF Containing a Photo-switchable Phenylazo Group. *Eur. J. Inorg. Chem.* **2011,** *2011* (35), 5378-5383.

(74) Wang, F.; Fu, H.-R.; Kang, Y.; Zhang, J. A new approach towards zeolitic tetrazolate-imidazolate frameworks (ZTIFs) with uncoordinated N-heteroatom sites for high CO2 uptake. *Chem. Comm.* **2014,** *50* (81), 12065-12068.

(75) Nguyen, N. T. T.; Furukawa, H.; Gándara, F.; Nguyen, H. T.; Cordova, K. E.; Yaghi, O. M. Selective Capture of Carbon Dioxide under Humid Conditions by Hydrophobic Chabazite-Type Zeolitic Imidazolate Frameworks. *Angewandte Chemie International Edition* **2014,** *53* (40), 10645-10648.

(76) Wang, F.; Liu, Z.-S.; Yang, H.; Tan, Y.-X.; Zhang, J. Hybrid Zeolitic Imidazolate Frameworks with Catalytically Active TO4 Building Blocks. *Angewandte Chemie International Edition* **2011,** *50* (2), 450-453.

(77) Erkartal, M.; Erkilic, U.; Tam, B.; Usta, H.; Yazaydin, O.; Hupp, J. T.; Farha, O. K.; Sen, U. From 2-methylimidazole to 1,2,3-triazole: a topological transformation of ZIF-8 and ZIF-67 by post-synthetic modification. *Chem. Comm.* **2017,** *53* (12), 2028-2031.

(78) Sheng, L.; Yang, F.; Wang, C.; Yu, J.; Zhang, L.; Pan, Y. Comparison of the hydrothermal stability of ZIF-8 nanocrystals and polycrystalline membranes derived from zinc salt variations. *Materials Letters* **2017,** *197* (Supplement C), 184-187.

(79) Ramu, G.; Lee, M.; Jeong, H.-K. Effects of zinc salts on the microstructure and performance of zeolitic-imidazolate framework ZIF-8 membranes for propylene/propane separation. *Microporous and Mesoporous Materials* **2018,** *259* (Supplement C), 155-162.

(80) Pan, Y.; Xue, M.; Chen, M.; Fang, Q.; Zhu, L.; Valtchev, V.; Qiu, S. ZIF-derived in situ nitrogen decorated porous carbons for CO2 capture. *Inorganic Chemistry Frontiers* **2016,** *3* (9), 1112-1118.

(81) Wang, F.; Hou, D.-C.; Yang, H.; Kang, Y.; Zhang, J. Tetrahedral tetrazolate frameworks for high CO2 and H2 uptake. *Dalton Transactions* **2014,** *43* (8), 3210-3214.

(82) Thompson, J. A.; Vaughn, J. T.; Brunelli, N. A.; Koros, W. J.; Jones, C. W.; Nair, S. Mixed-linker zeolitic imidazolate framework mixed-matrix membranes for aggressive CO2 separation from natural gas. *Microporous and Mesoporous Materials* **2014,** *192*, 43-51.

(83) Bae, T.-H.; Lee, J. S.; Qiu, W.; Koros, W. J.; Jones, C. W.; Nair, S. A High-Performance Gas-Separation Membrane Containing Submicrometer-Sized Metal–Organic Framework Crystals. *Angewandte Chemie International Edition* **2010,** *49* (51), 9863-9866.

(84) Burnett, B. J.; Barron, P. M.; Hu, C.; Choe, W. Stepwise Synthesis of Metal–Organic Frameworks: Replacement of Structural Organic Linkers. *J. Am. Chem. Soc.* **2011,** *133* (26), 9984-9987.

(85) Jayachandrababu, K. C.; Sholl, D. S.; Nair, S. Structural and Mechanistic Differences in Mixed-Linker Zeolitic Imidazolate Framework Synthesis by Solvent Assisted Linker Exchange and de Novo Routes. *J. Am. Chem. Soc.* **2017,** *139* (16), 5906-5915.

(86) Brozek, C. K.; Dincă, M. Ti3+-, V2+/3+-, Cr2+/3+-, Mn2+-, and Fe2+-Substituted MOF-5 and Redox Reactivity in Cr- and Fe-MOF-5. *J. Am. Chem. Soc.* **2013,** *135* (34), 12886-12891.

(87) Lammert, M.; Bernt, S.; Vermoortele, F.; De Vos, D. E.; Stock, N. Single- and Mixed-Linker Cr-MIL-101 Derivatives: A High-Throughput Investigation. *Inorg. Chem.* **2013,** *52* (15), 8521-8528.

(88) Park, K. S. Design, synthesis and control of topology and properties of zeolitic imidazolate frameworks and metal-organic frameworks based on pyrazolate. Dissertation Thesis, University of California Los Angeles, 2007.

(89) Lalonde, M.; Bury, W.; Karagiaridi, O.; Brown, Z.; Hupp, J. T.; Farha, O. K. Transmetalation: routes to metal exchange within metal-organic frameworks. *J. Mater. Chem. A* **2013,** *1* (18), 5453-5468.

(90) Schoenmakers, J. Post-synthetic modification of zeolitic imidazolate framework-8 (ZIF-8) via cation exchange. Master Thesis, Universiteit Utrecht, 2016.

(91) Sun, J.; Semenchenko, L.; Lim, W. T.; Ballesteros Rivas, M. F.; Varela-Guerrero, V.; Jeong, H.-K. Facile synthesis of Cd-substituted zeolitic-imidazolate framework Cd-ZIF-8 and mixed-metal CdZn-ZIF-8. *Microporous and Mesoporous Materials* **2018,** *264*, 35-42.

(92) Sapnik, A. F.; Geddes, H. S.; Reynolds, E. M.; Yeung, H. H. M.; Goodwin, A. L. Compositional inhomogeneity and tuneable thermal expansion in mixed-metal ZIF-8 analogues. *Chem. Comm.* **2018,** *54* (69), 9651-9654.

(93) Schejn, A.; Aboulaich, A.; Balan, L.; Falk, V.; Lalevee, J.; Medjahdi, G.; Aranda, L.; Mozet, K.; Schneider, R. Cu2+-doped zeolitic imidazolate frameworks (ZIF-8): efficient and stable catalysts for cycloadditions and condensation reactions. *Catalysis Science & Technology* **2015,** *5* (3), 1829-1839.

(94) Ban, Y.; Li, Y.; Peng, Y.; Jin, H.; Jiao, W.; Liu, X.; Yang, W. Metal-substituted zeolitic imidazolate framework ZIF-108: gas-sorption and membrane-separation properties. *Chemistry (Easton)* **2014,** *20* (36), 11402-9.

(95) Yang, H.; He, X.-W.; Wang, F.; Kang, Y.; Zhang, J. Doping copper into ZIF-67 for enhancing gas uptake capacity and visible-light-driven photocatalytic degradation of organic dye. *J. Mater. Chem.* **2012,** *22* (41), 21849-21851.

(96) Zhang, J.; Wu, T.; Zhou, C.; Chen, S.; Feng, P.; Bu, X. Zeolitic Boron Imidazolate Frameworks. *Angewandte Chemie International Edition* **2009,** *48* (14), 2542-2545.

(97) Wu, T.; Zhang, J.; Zhou, C.; Wang, L.; Bu, X.; Feng, P. Zeolite RHO-Type Net with the Lightest Elements. *J. Am. Chem. Soc.* **2009,** *131* (17), 6111-6113.

(98) Nguyen, N. T. T.; Lo, T. N. H.; Kim, J.; Nguyen, H. T. D.; Le, T. B.; Cordova, K. E.; Furukawa, H. Mixed-Metal Zeolitic Imidazolate Frameworks and their Selective Capture of Wet Carbon Dioxide over Methane. *Inorg. Chem.* **2016,** *55* (12), 6201-6207.

(99) Lu, Y.; Zhou, Q.; Chen, L.; Zhan, W.; Xie, Z.; Kuang, Q.; Zheng, L. Templated synthesis of diluted magnetic semiconductors using transition metal ion-doped metal-organic frameworks: the case of Co-doped ZnO. *CrystEngComm* **2016,** *18* (22), 4121-4126.

(100) Sámano-Alonso, C.; Hernández-Obregón, J.; Cabrera, R.; Díaz-Góngora, J. A. I.; Reguera, E. Tuning the adsorption potential. Separation of aromatic hydrocarbons by cobalt and zinc zeolitic imidazolate frameworks. *Colloids and Surfaces A: Physicochemical and Engineering Aspects* **2016,** *506*, 50-55.

(101) Zhou, K.; Mousavi, B.; Luo, Z.; Phatanasri, S.; Chaemchuen, S.; Verpoort, F. Characterization and properties of Zn/Co zeolitic imidazolate frameworks vs. ZIF-8 and ZIF-67. *J. Mater. Chem. A* **2017,** *5* (3), 952-957.

(102) Irving, H.; Williams, R. J. P. The stability of transition-metal complexes. *J. Chem. Soc.* **1953,** *0* (0), 3192-3210.

(103) Zhang, L.; Hu, Y. H. Strong Effects of Higher-Valent Cations on the Structure of the Zeolitic Zn(2-methylimidazole)2 Framework (ZIF-8). *The Journal of Physical Chemistry C* **2011,** *115* (16), 7967-7971.

(104) Wu, W.; Xie, J.; Xie, D. Two copper complexes with imidazole ligands: Syntheses, crystal structures and fluorescence. *Russian Journal of Inorganic Chemistry* **2010,** *55* (3), 384-389.

(105) Eilbeck, W. J.; Holmes, F.; Underhill, A. E. Cobalt(II), nickel(II), and copper(II) complexes of imidazole and thiazole. *Journal of the Chemical Society A: Inorganic, Physical, Theoretical* **1967,** (0), 757-761.

(106) Zheng, B.; Wang, L. L.; Du, L.; Huang, K.-W.; Du, H. ZIF-8 gate tuning via terminal group modification: A computational study. *Chem. Phys. Lett.* **2016,** *658*, 270-275.

(107) Aguado, S.; Bergeret, G.; Titus, M. P.; Moizan, V.; Nieto-Draghi, C.; Bats, N.; Farrusseng, D. Guest-induced gate-opening of a zeolite imidazolate framework. *New Journal of Chemistry* **2011,** *35* (3), 546-550.

(108) Fairen-Jimenez, D.; Moggach, S. A.; Wharmby, M. T.; Wright, P. A.; Parsons, S.; Düren, T. Opening the Gate: Framework Flexibility in ZIF-8 Explored by Experiments and Simulations. *J. Am. Chem. Soc.* **2011,** *133* (23), 8900-8902.

(109) van den Bergh, J.; Gucuyener, C.; Pidko, E. A.; Hensen, E. J.; Gascon, J.; Kapteijn, F. Understanding the anomalous alkane selectivity of ZIF-7 in the separation of light alkane/alkene mixtures. *Chemistry (Easton)* **2011,** *17* (32), 8832-40.

(110) Zhang, L.; Hu, Z.; Jiang, J. Sorption-Induced Structural Transition of Zeolitic Imidazolate Framework-8: A Hybrid Molecular Simulation Study. *J. Am. Chem. Soc.* **2013,** *135* (9), 3722-3728.

(111) Kolokolov, D. I.; Stepanov, A. G.; Jobic, H. Mobility of the 2-Methylimidazolate Linkers in ZIF-8 Probed by 2H NMR: Saloon Doors for the Guests. *The Journal of Physical Chemistry C* **2015,** *119* (49), 27512-27520.

(112) Casco, M. E.; Cheng, Y. Q.; Daemen, L. L.; Fairen-Jimenez, D.; Ramos-Fernandez, E. V.; Ramirez-Cuesta, A. J.; Silvestre-Albero, J. Gate-opening effect in ZIF-8: the first experimental proof using inelastic neutron scattering. *Chem. Comm.* **2016,** *52* (18), 3639-3642.

(113) Huang, X.; Zhang, J.; Chen, X. [Zn(bim)2] · (H2O)1.67: A metal-organic open-framework with sodalite topology. *Chinese Science Bulletin* **2003,** *48* (15), 1531-1534.

(114) Wu, H.-P.; Janiak, C.; Uehlin, L.; Klufers, P.; Mayer, P. 2,2[prime or minute]-Bi-1,6-naphthyridine metal complexes: a new ligand and a novel 2 [times] 2 inclined interpenetration of (4,4) nets or formation of helicoidal chains[dagger]. *Chem. Comm.* **1998,** (23), 2637-2638.

(115) Nik, O. G.; Chen, X. Y.; Kaliaguine, S. Functionalized metal organic framework-polyimide mixed matrix membranes for CO2/CH4 separation. *Journal of Membrane Science* **2012,** *413*, 48-61.

(116) Chen, X. Y.; Vinh-Thang, H.; Rodrigue, D.; Kaliaguine, S. Amine-Functionalized MIL-53 Metal–Organic Framework in Polyimide Mixed Matrix Membranes for CO2/CH4 Separation. *Ind. Eng. Chem. Res.* **2012,** *51* (19), 6895-6906.

(117) Huang, A.; Caro, J. Covalent Post-Functionalization of Zeolitic Imidazolate Framework ZIF-90 Membrane for Enhanced Hydrogen Selectivity. *Angewandte Chemie International Edition* **2011,** *50* (21), 4979-4982.

(118) Huang, A.; Wang, N.; Kong, C.; Caro, J. Organosilica-Functionalized Zeolitic Imidazolate Framework ZIF-90 Membrane with High Gas-Separation Performance. *Angewandte Chemie International Edition* **2012,** *51* (42), 10551-10555.

(119) Huang, A.; Dou, W.; Caro, J. Steam-Stable Zeolitic Imidazolate Framework ZIF-90 Membrane with Hydrogen Selectivity through Covalent Functionalization. *J. Am. Chem. Soc.* **2010,** *132* (44), 15562-15564.

(120) Huang, A.; Bux, H.; Steinbach, F.; Caro, J. Molecular-Sieve Membrane with Hydrogen Permselectivity: ZIF-22 in LTA Topology Prepared with 3-Aminopropyltriethoxysilane as Covalent Linker. *Angewandte Chemie International Edition* **2010,** *49* (29), 4958-4961.

(121) Huang, A.; Chen, Y.; Wang, N.; Hu, Z.; Jiang, J.; Caro, J. A highly permeable and selective zeolitic imidazolate framework ZIF-95 membrane for H2/CO2 separation. *Chem. Comm.* **2012,** *48* (89), 10981-10983.

(122) Dong, X.; Huang, K.; Liu, S.; Ren, R.; Jin, W.; Lin, Y. S. Synthesis of zeolitic imidazolate framework-78 molecular-sieve membrane: defect formation and elimination. *J. Mater. Chem.* **2012,** *22* (36), 19222-19227.

(123) Ban, Y.; Li, Y.; Liu, X.; Peng, Y.; Yang, W. Solvothermal synthesis of mixed-ligand metal–organic framework ZIF-78 with controllable size and morphology. *Microporous and Mesoporous Materials* **2013,** *173*, 29-36.

(124) Hara, N.; Yoshimune, M.; Negishi, H.; Haraya, K.; Hara, S.; Yamaguchi, T. Effect of Temperature on Synthesis of ZIF-8 Membranes for Propylene/propane Separation by Counter Diffusion Method. *Journal of the Japan Petroleum Institute* **2015,** *58* (4), 237-244.

(125) Hara, N.; Yoshimune, M.; Negishi, H.; Haraya, K.; Hara, S.; Yamaguchi, T. Effect of Solution Concentration on Structure and Permeation Properties of ZIF-8 Membranes for Propylene/Propane Separation. *Journal of Chemical Engineering of Japan* **2016,** *49* (2), 97-103.

(126) Krokidas, P.; Castier, M.; Moncho, S.; Brothers, E.; Economou, I. G. Molecular Simulation Studies of the Diffusion of Methane, Ethane, Propane, and Propylene in ZIF-8. *The Journal of Physical Chemistry C* **2015,** *119* (48), 27028-27037.

(127) Wang, C.; Yang, F.; Sheng, L.; Yu, J.; Yao, k.; Zhang, L.; Pan, Y. Zinc-Substituted ZIF-67 Nanocrystals and Polycrystalline Membranes for Propylene/Propane Separation. *Chem. Comm.* **2016,** *52*, 12578-12581.

(128) An, H.; Park, S.; Kwon, H. T.; Jeong, H.-K.; Lee, J. S. A new superior competitor for exceptional propylene/propane separations: ZIF-67 containing mixed matrix membranes. *Journal of Membrane Science* **2017,** *526* (Supplement C), 367-376.

(129) Davis, M. E. Ordered porous materials for emerging applications. *Nature* **2002,** *417* (6891), 813-821.

(130) Chen, B.; Yang, Z.; Zhu, Y.; Xia, Y. Zeolitic imidazolate framework materials: recent progress in synthesis and applications. *J. Mater. Chem. A* **2014,** *2* (40), 16811-16831.

(131) Yao, J.; Wang, H. Zeolitic imidazolate framework composite membranes and thin films: synthesis and applications. *Chem. Soc. Rev.* **2014,** *43* (13), 4470-4493.

(132) Caro, J.; Noack, M.; Kölsch, P.; Schäfer, R. Zeolite membranes – state of their development and perspective. *Microporous and Mesoporous Materials* **2000,** *38* (1), 3-24.

(133) Kreno, L. E.; Leong, K.; Farha, O. K.; Allendorf, M.; Van Duyne, R. P.; Hupp, J. T. Metal–Organic Framework Materials as Chemical Sensors. *Chem. Rev.* **2012,** *112* (2), 1105-1125.

(134) Lee, J.; Farha, O. K.; Roberts, J.; Scheidt, K. A.; Nguyen, S. T.; Hupp, J. T. Metal-organic framework materials as catalysts. *Chem. Soc. Rev.* **2009,** *38* (5), 1450-1459.

(135) Tavolaro, A.; Drioli, E. Zeolite Membranes. *Advanced Materials* **1999,** *11* (12), 975-996.

(136) Shah, M.; McCarthy, M. C.; Sachdeva, S.; Lee, A. K.; Jeong, H.-K. Current Status of Metal–Organic Framework Membranes for Gas Separations: Promises and Challenges. *Ind. Eng. Chem. Res.* **2012,** *51* (5), 2179-2199.

(137) Mottillo, C.; Friscic, T. Carbon dioxide sensitivity of zeolitic imidazolate frameworks. *Angew. Chem. Int. Ed. Engl.* **2014,** *53* (29), 7471-4.

(138) Cravillon, J.; Münzer, S.; Lohmeier, S.-J.; Feldhoff, A.; Huber, K.; Wiebcke, M. Rapid Room-Temperature Synthesis and Characterization of Nanocrystals of a Prototypical Zeolitic Imidazolate Framework. *Chem. Mater.* **2009,** *21* (8), 1410-1412.

(139) Zhang, C.; Koros, W. J. Zeolitic Imidazolate Framework-Enabled Membranes: Challenges and Opportunities. *The Journal of Physical Chemistry Letters* **2015,** *6* (19), 3841-3849.

(140) McCarthy, M. C.; Varela-Guerrero, V.; Barnett, G. V.; Jeong, H.-K. Synthesis of Zeolitic Imidazolate Framework Films and Membranes with Controlled Microstructures. *Langmuir* **2010,** *26* (18), 14636-14641.

(141) Keskin, S.; van Heest, T. M.; Sholl, D. S. Can Metal–Organic Framework Materials Play a Useful Role in Large-Scale Carbon Dioxide Separations? *ChemSusChem* **2010,** *3* (8), 879-891.

(142) Caskey, S. R.; Wong-Foy, A. G.; Matzger, A. J. Dramatic Tuning of Carbon Dioxide Uptake via Metal Substitution in a Coordination Polymer with Cylindrical Pores. *J. Am. Chem. Soc.* **2008,** *130* (33), 10870-10871.

(143) Zhu, X.-W.; Zhou, X.-P.; Li, D. Exceptionally water stable heterometallic gyroidal MOFs: tuning the porosity and hydrophobicity by doping metal ions. *Chem. Comm.* **2016,** *52* (39), 6513-6516.

(144) Botas, J. A.; Calleja, G.; Sánchez-Sánchez, M.; Orcajo, M. G. Cobalt Doping of the MOF-5 Framework and Its Effect on Gas-Adsorption Properties. *Langmuir* **2010,** *26* (8), 5300-5303.

(145) Zhang, C.; Xiao, Y.; Liu, D.; Yang, Q.; Zhong, C. A hybrid zeolitic imidazolate framework membrane by mixed-linker synthesis for efficient CO2 capture. *Chem. Comm.* **2013,** *49* (6), 600-602.

(146) Ni, Z.; Masel, R. I. Rapid Production of Metal−Organic Frameworks via Microwave-Assisted Solvothermal Synthesis. *J. Am. Chem. Soc.* **2006,** *128* (38), 12394-12395.

(147) Venna, S. R.; Jasinski, J. B.; Carreon, M. A. Structural Evolution of Zeolitic Imidazolate Framework-8. *J. Am. Chem. Soc.* **2010,** *132* (51), 18030-18033.

(148) Feng, X.; Carreon, M. A. Kinetics of transformation on ZIF-67 crystals. *Journal of Crystal Growth* **2015,** *418*, 158-162.

(149) Zhao, Y.; Liu, M.; Fan, B.; Chen, Y.; Lv, W.; Lu, N.; Li, R. Pd nanoparticles supported on ZIF-8 as an efficient heterogeneous catalyst for the selective hydrogenation of cinnamaldehyde. *Catalysis Communications* **2014,** *57*, 119-123.

(150) Qian, J.; Sun, F.; Qin, L. Hydrothermal synthesis of zeolitic imidazolate framework-67 (ZIF-67) nanocrystals. *Materials Letters* **2012,** *82*, 220-223.

(151) Bao, Q.; Lou, Y.; Xing, T.; Chen, J. Rapid synthesis of zeolitic imidazolate framework-8 (ZIF-8) in aqueous solution via microwave irradiation. *Inorg. Chem. Commun.* **2013,** *37*, 170-173.

(152) Chang, Z.; Pu, H.; Wan, D.; Liu, L.; Yuan, J.; Yang, Z. Chemical oxidative degradation of Polybenzimidazole in simulated environment of fuel cells. *Polymer Degradation and Stability* **2009,** *94* (8), 1206-1212.

(153) Yang, T.; Xiao, Y.; Chung, T.-S. Poly-/metal-benzimidazole nano-composite membranes for hydrogen purification. *Energy Environ. Sci.* **2011,** *4* (10), 4171-4180.

(154) Tu, M.; Wiktor, C.; Rosler, C.; Fischer, R. A. Rapid room temperature syntheses of zeolitic-imidazolate framework (ZIF) nanocrystals. *Chem. Comm.* **2014,** *50* (87), 13258-13260.

(155) Tian, Y.-Q.; Yao, S.-Y.; Gu, D.; Cui, K.-H.; Guo, D.-W.; Zhang, G.; Chen, Z.-X.; Zhao, D.-Y. Cadmium Imidazolate Frameworks with Polymorphism, High Thermal Stability, and a Large Surface Area. *Chemistry – A European Journal* **2010,** *16* (4), 1137-1141.

(156) Aguado, S.; Canivet, J.; Farrusseng, D. Facile shaping of an imidazolate-based MOF on ceramic beads for adsorption and catalytic applications. *Chem. Comm.* **2010,** *46* (42), 7999-8001.

(157) Tsai, C.-W.; Niemantsverdriet, J. W.; Langner, E. H. G. Enhanced CO2 adsorption in nano-ZIF-8 modified by solvent assisted ligand exchange. *Microporous and Mesoporous Materials* **2018,** *262*, 98-105.

(158) Arivazhagan, M.; Manivel, S.; Jeyavijayan, S.; Meenakshi, R. Vibrational spectroscopic (FTIR and FT-Raman), first-order hyperpolarizablity, HOMO, LUMO, NBO, Mulliken charge analyses of 2-ethylimidazole based on Hartree–Fock and DFT

calculations. *Spectrochimica Acta Part A: Molecular and Biomolecular Spectroscopy* **2015,** *134*, 493-501.

(159) Güllüoğlu, M. T.; Erdogdu, Y.; Karpagam, J.; Sundaraganesan, N.; Yurdakul, Ş. DFT, FT-Raman, FT-IR and FT-NMR studies of 4-phenylimidazole. *J. Mol. Struct.* **2011,** *990* (1), 14-20.

(160) Moggach, S. A.; Bennett, T. D.; Cheetham, A. K. The Effect of Pressure on ZIF-8: Increasing Pore Size with Pressure and the Formation of a High-Pressure Phase at 1.47 GPa. *Angewandte Chemie International Edition* **2009,** *48* (38), 7087-7089.

(161) Joo, L. M.; Taek, K. H.; Hae-Kwon, J. High-Flux Zeolitic Imidazolate Framework Membranes for Propylene/Propane Separation by Postsynthetic Linker Exchange. *Angewandte Chemie International Edition* **2018,** *57* (1), 156-161.

(162) Cravillon, J.; Nayuk, R.; Springer, S.; Feldhoff, A.; Huber, K.; Wiebcke, M. Controlling Zeolitic Imidazolate Framework Nano- and Microcrystal Formation: Insight into Crystal Growth by Time-Resolved In Situ Static Light Scattering. *Chem. Mater.* **2011,** *23* (8), 2130-2141.

(163) Li, Y.; Liang, F.; Bux, H.; Yang, W.; Caro, J. Zeolitic imidazolate framework ZIF-7 based molecular sieve membrane for hydrogen separation. *Journal of Membrane Science* **2010,** *354* (1–2), 48-54.

(164) Li, Y.-S.; Liang, F.-Y.; Bux, H.; Feldhoff, A.; Yang, W.-S.; Caro, J. Molecular Sieve Membrane: Supported Metal–Organic Framework with High Hydrogen Selectivity. *Angewandte Chemie* **2010,** *122* (3), 558-561.

(165) Bux, H.; Chmelik, C.; Krishna, R.; Caro, J. Ethene/ethane separation by the MOF membrane ZIF-8: Molecular correlation of permeation, adsorption, diffusion. *Journal of Membrane Science* **2011,** *369* (1), 284-289.

(166) Bux, H.; Liang, F.; Li, Y.; Cravillon, J.; Wiebcke, M.; Caro, J. Zeolitic Imidazolate Framework Membrane with Molecular Sieving Properties by Microwave-Assisted Solvothermal Synthesis. *J. Am. Chem. Soc.* **2009,** *131* (44), 16000-16001.

(167) Bux, H.; Feldhoff, A.; Cravillon, J.; Wiebcke, M.; Li, Y.-S.; Caro, J. Oriented Zeolitic Imidazolate Framework-8 Membrane with Sharp H2/C3H8 Molecular Sieve Separation. *Chem. Mater.* **2011,** *23* (8), 2262-2269.

(168) Li, J.-R.; Sculley, J.; Zhou, H.-C. Metal–Organic Frameworks for Separations. *Chem. Rev.* **2012,** *112* (2), 869-932.

(169) Qiu, S.; Xue, M.; Zhu, G. Metal-organic framework membranes: from synthesis to separation application. *Chem. Soc. Rev.* **2014,** *43* (16), 6116-6140.

(170) Rangnekar, N.; Mittal, N.; Elyassi, B.; Caro, J.; Tsapatsis, M. Zeolite membranes - a review and comparison with MOFs. *Chem. Soc. Rev.* **2015,** *44* (20), 7128-7154.

(171) Li, W.; Su, P.; Li, Z.; Xu, Z.; Wang, F.; Ou, H.; Zhang, J.; Zhang, G.; Zeng, E. Ultrathin metal–organic framework membrane production by gel–vapour deposition. *Nature Communications* **2017,** *8* (1), 406.

(172) Kwon, H. T.; Jeong, H.-K.; Lee, A. S.; An, H. S.; Lee, T.; Jang, E.; Lee, J. S.; Choi, J. Defect-induced ripening of zeolitic-imidazolate framework ZIF-8 and its implication to vapor-phase membrane synthesis. *Chem. Comm.* **2016,** *52* (78), 11669-11672.

(173) Stassen, I.; Campagnol, N.; Fransaer, J.; Vereecken, P.; De Vos, D.; Ameloot, R. Solvent-free synthesis of supported ZIF-8 films and patterns through transformation of deposited zinc oxide precursors. *CrystEngComm* **2013,** *15* (45), 9308-9311.

(174) Stassen, I.; Styles, M.; Grenci, G.; Gorp, H. V.; Vanderlinden, W.; Feyter, S. D.; Falcaro, P.; Vos, D. D.; Vereecken, P.; Ameloot, R. Chemical vapour deposition of zeolitic imidazolate framework thin films. *Nat Mater* **2016,** *15* (3), 304-310.

(175) Yoo, Y.; Lai, Z.; Jeong, H.-K. Fabrication of MOF-5 membranes using microwave-induced rapid seeding and solvothermal secondary growth. *Microporous and Mesoporous Materials* **2009,** *123* (1), 100-106.

(176) Gokulakrishnan, R.; Jeong, H.-K. Recent Progress on Metal-Organic Framework Membranes for Gas Separations: Conventional Synthesis vs. Microwave-Assisted Synthesis. *Membrane Journal* **2017,** *27,* 1-42.

(177) Hayes, B. L. *Microwave Synthesis: Chemistry at the Speed of Light*, Cem Corp: 2002.

(178) Park, J. H.; Park, S. H.; Jhung, S. H. Microwave-Syntheses of Zeolitic Imidazolate Framework Material, ZIF-8. *Journal of the Korean Chemical Society* **2009,** *53* (5), 553-559.

(179) Brown, A. J.; Brunelli, N. A.; Eum, K.; Rashidi, F.; Johnson, J. R.; Koros, W. J.; Jones, C. W.; Nair, S. Interfacial microfluidic processing of metal-organic framework hollow fiber membranes. *Science* **2014,** *345* (6192), 72-75.

(180) Eum, K.; Rownaghi, A.; Choi, D.; Bhave, R. R.; Jones, C. W.; Nair, S. Fluidic Processing of High-Performance ZIF-8 Membranes on Polymeric Hollow Fibers: Mechanistic Insights and Microstructure Control. *Advanced Functional Materials* **2016,** *26* (28), 5011-5018.

(181) Eum, K.; Ma, C.; Rownaghi, A.; Jones, C. W.; Nair, S. ZIF-8 Membranes via Interfacial Microfluidic Processing in Polymeric Hollow Fibers: Efficient Propylene Separation at Elevated Pressures. *ACS Applied Materials & Interfaces* **2016,** *8* (38), 25337-25342.

(182) Hara, N.; Yoshimune, M.; Negishi, H.; Haraya, K.; Hara, S.; Yamaguchi, T. Diffusive separation of propylene/propane with ZIF-8 membranes. *Journal of Membrane Science* **2014,** *450*, 215-223.

(183) Tsai, C.-W.; Langner, E. H. G. The effect of synthesis temperature on the particle size of nano-ZIF-8. *Microporous and Mesoporous Materials* **2016,** *221*, 8-13.

(184) Walba, H.; Isensee, R. W. Acidity Constants of Some Arylimidazoles and Their Cations. *The Journal of Organic Chemistry* **1961,** *26* (8), 2789-2791.

(185) McEwen, J.; Hayman, J.-D.; Ozgur Yazaydin, A. A comparative study of CO2, CH4 and N2 adsorption in ZIF-8, Zeolite-13X and BPL activated carbon. *Chem. Phys.* **2013,** *412* (Supplement C), 72-76.

(186) Wu, X.; Niknam Shahrak, M.; Yuan, B.; Deng, S. Synthesis and characterization of zeolitic imidazolate framework ZIF-7 for CO2 and CH4 separation. *Microporous and Mesoporous Materials* **2014,** *190* (Supplement C), 189-196.

(187) Ge, L.; Zhou, W.; Du, A.; Zhu, Z. Porous Polyethersulfone-Supported Zeolitic Imidazolate Framework Membranes for Hydrogen Separation. *The Journal of Physical Chemistry C* **2012,** *116* (24), 13264-13270.

(188) Pan, Y.; Wang, B.; Lai, Z. Synthesis of ceramic hollow fiber supported zeolitic imidazolate framework-8 (ZIF-8) membranes with high hydrogen permeability. *Journal of Membrane Science* **2012,** *421* (Supplement C), 292-298.

(189) Venna, S. R.; Carreon, M. A. Highly Permeable Zeolite Imidazolate Framework-8 Membranes for CO2/CH4 Separation. *J. Am. Chem. Soc.* **2010,** *132* (1), 76-78.

(190) Hertäg, L.; Bux, H.; Caro, J.; Chmelik, C.; Remsungnen, T.; Knauth, M.; Fritzsche, S. Diffusion of CH4 and H2 in ZIF-8. *Journal of Membrane Science* **2011,** *377* (1), 36-41.

(191) Lai, L. S.; Yeong, Y. F.; Lau, K. K.; Shariff, A. M. CO2 and CH4 permeation through zeolitic imidazolate framework (ZIF)-8 membrane synthesized via in situ layer-by-layer growth: an experimental and modeling study. *RSC Advances* **2015,** *5* (96), 79098-79106.

(192) Krokidas, P.; Moncho, S.; Brothers, E. N.; Castier, M.; Jeong, H.-K.; Economou, I. G. On the Efficient Separation of Gas Mixtures with the Mixed-Linker Zeolitic-Imidazolate Framework-7-8. *ACS Applied Materials & Interfaces* **2018**.

(193) Zhang, C.; Han, C.; Sholl, D. S.; Schmidt, J. R. Computational Characterization of Defects in Metal-Organic Frameworks: Spontaneous and Water-Induced Point Defects in ZIF-8. *J. Phys. Chem. Lett.* **2016,** *7* (3), 459-64.

(194) Fang, Z.; Bueken, B.; De Vos, D. E.; Fischer, R. A. Defect-Engineered Metal–Organic Frameworks. *Angewandte Chemie International Edition* **2015,** *54* (25), 7234-7254.

(195) Saliba, D.; Ammar, M.; Rammal, M.; Al-Ghoul, M.; Hmadeh, M. Crystal Growth of ZIF-8, ZIF-67, and Their Mixed-Metal Derivatives. *J. Am. Chem. Soc.* **2018,** *140* (5), 1812-1823.

(196) Gleiter, H. Grain boundaries as point defect sources or sinks—Diffusional creep. *Acta Metallurgica* **1979,** *27* (2), 187-192.

(197) Uberuaga, B. P.; Vernon, L. J.; Martinez, E.; Voter, A. F. The relationship between grain boundary structure, defect mobility, and grain boundary sink efficiency. *Sci. Rep.* **2015,** *5*, 9095.

(198) Gupta, T. K.; Carlson, W. G. A grain-boundary defect model for instability/stability of a ZnO varistor. *Journal of Materials Science* **1985,** *20* (10), 3487-3500.

(199) Berens, S.; Chmelik, C.; Hillman, F.; Kärger, J.; Jeong, H.-K.; Vasenkov, S. Ethane diffusion in mixed linker zeolitic imidazolate framework-7-8 by pulsed field gradient NMR in combination with single crystal IR microscopy. *Phys. Chem. Chem. Phys.* **2018,** *20* (37), 23967-23975.

(200) Lee, M. J.; Kwon, H. T.; Jeong, H.-K. High-Flux Zeolitic Imidazolate Framework Membranes for Propylene/Propane Separation by Postsynthetic Linker Exchange. *Angewandte Chemie International Edition* **2018,** *57* (1), 156-161.